

REPORT DOCUMENTATION PAGE

AFRL-SR-BL-TR-01-

Public reporting burden for this collection of information is estimated to average 1 hour per response, including the time for reviewing instructions, gathering existing data needed, and completing and reviewing this collection of information. Send comments regarding this burden estimate or any other aspect of this burden to Department of Defense, Washington Headquarters Services, Directorate for Information Operations and Reports (0704-0188) 4302. Respondents should be aware that notwithstanding any other provision of law, no person shall be subject to any penalty for failing to provide information if it does not have a valid OMB control number. PLEASE DO NOT RETURN YOUR FORM TO THE ABOVE ADDRESS.

0576

1. REPORT DATE (DD-MM-YYYY) 01-10-2001		2. REPORT TYPE Final Technical		3. DATES COVERED Jun 1998 - Sep 2001	
4. TITLE AND SUBTITLE (DEPSCoR-98) STUDIES OF THE TIME DEPENDENT REACTANT TEMPERATURES AND CONCENTRATIONS IN RF NITRIDE DEPOSITION PLASMA USING CARS				5a. CONTRACT NUMBER	
				5b. GRANT NUMBER F49620-98-1-0455	
				5c. PROGRAM ELEMENT NUMBER	
6. AUTHOR(S) Rodriguez, Rene, G, Ph.D.				5d. PROJECT NUMBER 3484/BS	
				5e. TASK NUMBER	
				5f. WORK UNIT NUMBER	
7. PERFORMING ORGANIZATION NAME(S) AND ADDRESS(ES) Idaho State University Office of Sponsored Programs 921 South 8th Ave. Pocatello, ID 83209-8046				8. PERFORMING ORGANIZATION REPORT NUMBER CFDA #12.630	
9. SPONSORING / MONITORING AGENCY NAME(S) AND ADDRESS(ES) AFOSR/NE 110 Duncan Ave., Room B115 Bolling AFB, DC 20332-8050				10. SPONSOR/MONITOR'S ACRONYM(S) AFOSR	
				11. SPONSOR/MONITOR'S REPORT NUMBER(S) 98-NE-146	
12. DISTRIBUTION / AVAILABILITY STATEMENT <div style="text-align: right;">AIR FORCE OFFICE OF SCIENTIFIC RESEARCH (AFOSR) NOTICE OF TRANSMITTAL DTIC. THIS TECHNICAL REPORT HAS BEEN REVIEWED AND IS APPROVED FOR PUBLIC RELEASE LAW AFR 190-12. DISTRIBUTION IS UNLIMITED.</div>					
13. SUPPLEMENTARY NOTES					
14. ABSTRACT A radiofrequency pulsed plasma enhanced chemical vapor deposition reactor for silicon nitride production was designed, tested, and used to investigate the relationship of the reactor conditions to the depletion of and temperature of gas phase reactants in the rf plasma and to the properties of the deposited silicon nitride thin films and nano-particles. Correlations were found to exist between the depletion of silane and the uniformity of the thin films and particle sizes or also the atomic composition of the thin films and particles. Two methods were implemented to measure the depletion of silane gas in the plasma. Coherent anti-Stokes Raman scattering (CARS) spectroscopy for thin film depositions, and pulsed sampling mass spectrometry (PSMS) for nano-particle depositions. The PSMS instrument represents a new method for sampling pulsed plasmas by mass spectrometry. Insight into the relative roles of gas and surface chemical processes was gained by this work.					
15. SUBJECT TERMS silicon nitride, thin films, nano-particles, CARS spectroscopy, rf-PECVD, mass spectrometry					
16. SECURITY CLASSIFICATION OF:			17. LIMITATION OF ABSTRACT	18. NUMBER OF PAGES 155	19a. NAME OF RESPONSIBLE PERSON Rodriguez, Rene, G.
a. REPORT	b. ABSTRACT	c. THIS PAGE			19b. TELEPHONE NUMBER (include area code) 208 282-2613

20011126 066

**Studies of the Time Dependent Reactant Temperatures and Concentrations
in RF Nitride Deposition Plasmas Using CARS**

by

**Prof. Rene Rodriguez
Dept. of Chemistry
Idaho State University**

**A Final Technical Report
Submitted in partial fulfillment of the Guidelines
required regarding this proposal with Control # 98-NE-146
Sept 29, 2001**

ACKNOWLEDGMENTS

I would like to thank the Department of Defense for funding this project. Also thanks goes to Terry Gardner at American Microsystems Inc. for help in installing the gas control systems and for donating safety equipment related to that installation. Royce Martin and Miles Whiting of the Electronics and Machining Services Departments at Idaho State University were very helpful during the three year duration of the project constructing electronic interfaces and building the reaction chambers. Much of the work and results are due to the efforts of graduate students Shane Steidley and BarJean Phillips and to the dedication of our capable technician Lisa Lau.

TABLE OF CONTENTS

1. List of Figures	01
2. List of Tables	03
3. Abstract	04
4. Introduction	
Background	06
Studies Executed	10
5. Methodology	
Construction of the rf-PPECVD Reactor and Supporting Equipment	15
Instrumentation for Spectroscopic Monitoring of Reactants in a Pulsed Plasma	23
Instrumentation for Analysis of the Silicon Nitride Thin Films and Particles	28
Particulars of the Studies Accomplished in This Work	31
6. Results	
Thin Film Studies #1 - #6	39
Particle Studies #7 - #11	58
7. Conclusions	69
8. Executive Summary	73
9. Appendices	
Appendix A - Drawings of the Plasma Chamber	74
Appendix B - Standard Operating Procedure for the Radio Frequency Pulsed Plasma Enhanced Chemical Vapor Deposition System	97
Appendix C - Calculations of the Speed of the Gas Exiting the Holes in the Radial Showerhead	122
Appendix D - Manuscript of Journal Article Currently Being Submitted	124
Appendix E - Supporting Data	142
10. References	155

LIST OF FIGURES

Figure 1.	Overview Sketch of Plasma Electrode Arrangement.....	16
Figure 2.	Overall Layout for the CARS Experiments.....	25
Figure 3.	Block Diagram of the Mass Spectrometer System.....	27
Figure 4.	Typical Pulsed Sampling Mass Spectroscopy Spectra Taken Before the Plasma and During a Pulsed Plasma.....	37
Figure 5.	CARS Spectra of ν_1 of SiH_4 , Preplasma and at Various Delay Times.....	40
Figure 6.	CARS Determined Silane Depletions for rf Pulse Widths at Specific Delay Times after the Pulse.....	42
Figure 7.	CARS Determined Silane Concentrations as a Function of Power at Specific Delays for 2 and 5 ms Pulse Widths.....	42
Figure 8.	Schematic of Reactant Flow and Depletion as a Function of rf Pulse Width.....	43
Figure 9a.	Visual Summary of Silicon Nitride Thin Films Deposited on Si Wafers.....	50
Figure 9b.	Visual Summary of Silicon Nitride Thin Films Deposited on Si Wafers.....	51
Figure 10a.	Contour Diagram of Thin Film Thickness Deposited from the Square Showerhead at 40W and 10 ms rf Pulse.....	52
Figure 10b.	Contour Diagram of Thin Film Thickness Deposited from the Radial Showerhead at 30W and 5 ms rf Pulse.....	52
Figure 10c.	Contour Diagram of Thin Film Thickness Deposited from the Square Showerhead at 30 W and 5 ms rf Pulse.....	53
Figure 11.	CARS Determined Depletion of Silane as a Function of Temperature at Several Delay Times after the Pulse.....	57

LIST OF FIGURES (CONTINUED)

Figure 12. Argon Calibration Curves Obtained from Pulsed Sampling Mass Spectrometry.....	59
Figure 13. Silane Calibration Curves Obtained from Pulsed Sampling Mass Spectrometry with Variation in the Signal Amplifier.....	60
Figure 14. Pulsed Sampling MS Determined Silane Depletion as a Function of Continuous rf Power.....	62
Figure 15a. SEM Micrograph of Silicon Nitride Particles Showing Agglomerates.....	64
Figure 15b. SEM Micrograph of Silicon Nitride Particles Showing Cases without Significant Agglomeration.....	65

LIST OF TABLES

Table 1. Thermocouple Values vs. the Actual Temperature at the Top Center of the Lower Electrode.....	18
Table 2. Thin Film Parameters and Silane Depletion as a Function of rf Peak Power.....	45
Table 3. Thin Film Properties and Silane Depletion as a Function of rf Pulse Width.....	46
Table 4. Thin Film Parameters and Silane Depletion as a Function of Showerhead Type at 175°C for 10Hz Pulsed Plasma and 75min Depositions.....	49
Table 5. Thin Film Parameters and Silane Depletion as a Function of Substrate Temperatures for 5 ms rf puls at 30W Peak Power.....	55
Table 6. Comparison of CARS and Pulsed Sampling MS Determined Silane Depletions in a 25 Watt Plasma.....	61
Table 7. Effect of rf Power on Silane Depletion and Silicon Nitride Particle Size and Composition.....	63
Table 8. The Importance of rf Pulse Width on Silane Depletion and Silicon Nitride Particle Size and Composition.....	67
Table 9. The effect of Reactant Flow Composition on Silane Depletion and Silicon Nitride Particle Size and Composition.....	68

ABSTRACT

A radiofrequency pulsed plasma enhanced chemical vapor deposition (rf-PPECVD) reactor for silicon nitride production was designed, tested, and used to investigate the relationship of the reactor conditions to the depletion of and temperature of gas phase reactants in the rf plasma and to the properties of the deposited silicon nitride thin films and nano-particles. Correlations were found to exist between the depletion of silane and the uniformity of the thin films and particles sizes or also the atomic composition of the thin films and particles.

Two methods were implemented to measure the depletion of silane gas in the plasma. Coherent anti-Stokes Raman scattering (CARS) spectroscopy for thin film depositions, and pulsed sampling mass spectrometry (PSMS) for nano-particle deposits. The PSMS instrument represents a new method for sampling pulsed plasmas by mass spectrometry. It was tested and developed during these studies. CARS spectroscopy was used to determine that the change in the temperature of the silane gas, due to a pulsed plasma, was negligible, at least for the conditions used to make the thin films.

For these investigations, flow rates of the reactant gases were most often held at 10 sccm silane, 20 sccm nitrogen, and 20 sccm ammonia. Peak powers between 25 and 80 watts and pulse widths between 2 and 10 ms in a 10Hz plasma were used for the thin films. For the particles, the pulse-on and pulse-off times were much longer. The times were typically between 200 ms and 2 s.

The reactant depletion and film properties both changed when alterations in the rf power or changes in the length of the rf pulse were made. When the substrate temperature was altered, however, only the film properties changed. And if the showerhead was changed, the silane

depletion varied and the atomic composition stayed relatively constant. But at the same time, the relative ratio of SiH and NH bonds changed and the stress on the wafer due to the film was also different. This suggests that the film had a different formulation even though the atomic percentage of Si in the film did not change much. In the case of the particles, changes in the peak power affected both the atomic composition and particle size as did changes in the pulse width. For the particle depositions, reactant flow rates were also altered and at a low percentage of silane flow a much narrower and smaller distribution of nano-particle sizes, with minimal agglomeration was observed.

Taken as a whole, these studies provided insight into the relative importance or role that gas phase chemistry plays the one that surface chemistry plays during an rf-PPECVD of silicon nitride thin films or particles. Certainly, both CARS and PSMS spectra, correlated with thin film and surface properties, suggest that the chemical process in the gas phase and the chemistry on the surface are both affected by changes in the reactor processes.

INTRODUCTION

Background

Nitride materials have many uses such as coating materials in electronic circuit processing, as hard, high melting ceramics, and as a hard material for coating tools. Additionally SiN has been used as a passivation coating, a gate dielectric material, a diffusion barrier, and interlevel metal isolator.^{1,2} SiN and TiN have excellent high temperature structural properties, like high strength and low weight that would make them excellent candidates for many applications such as engine parts. Materials formed from nanometer-sized units often show improved ductility or superplasticity. Chemical homogeneity with minimal defects is improved by starting with particles in the tens of nanometers range that are very pure.³

Nitride films and nano-sized particles are produced in a few different ways. Radio frequency pulsed plasma enhanced chemical vapor deposition, rf-PPECVD, is a relatively low temperature method. The plasma enhancement allows the use of much lower substrate temperatures. The rf-PPECVD process produces a product which is not generally stoichiometric silicon nitride but is more properly described as a polysilazane (SiN_xH_y). That is hydrogen is often part of the matrix and often various amounts of oxygen will be present as well. Many researchers have studied the composition, physical properties, and electrical properties of the films and particles as a function of rf power, rf frequency, flow rate, reactant flow composition, substrate temperature, and the presence of inert gases. They have made a sizable contribution to the understanding of the effect of the plasma condition parameters on the particles and film material. But a relatively small amount of work has been done to examine why these deposition conditions affect the resulting nitride particles and films in the manner suggested by these studies. In-situ

probing of the reactants and/or products in the plasma has been accomplished to a limited extent, mostly by mass spectrometric studies.²

It is expected that a great deal of insight into the depositions could be gained by in-situ measurement of the time dependence of the molecular temperatures and the depletion of the reactant gases directly in the plasma region. Measurement of the temperature of the reactant gases in the plasma could suggest explanations for why the SiH/NH ratio of silicon nitride films change with increasing rf power.⁴ If the temperature of the gases in the plasma increase with increasing plasma "on-time", then this may cause the Si/N or SiH/NH ratio of the deposited material to change due to differences in thermal breakdown of the gases. This would mean that temperatures would need to increase to more than a thousand degrees centigrade. The addition of inert gases like argon or helium have been observed to affect the deposition rate and stress characteristics of the thin films produced with them present in the reactant gases.⁵ This could also be related to the ability of the electrons to reach a higher energies in a helium containing plasma and/or the possibility that the electrons could exchange energy more readily with the helium atoms. The excited helium atoms could then more effectively couple the energy to the reactant gases, heating them up and allowing more thermal degradation to occur. Measurements of the temperatures in a rf-PPECVD plasma for depositing particles may help explain why the surface morphology of nano-sized particles is a smoothed surface which appears to have been due to melting after agglomeration.⁶

There is interest also in the temperature of the substrate on which the nitride thin films and particles are deposited. Some studies indicate that the temperature of the substrate affects the amount of oxygen which is incorporated into the films and particles. A surface oxygen layer is

known to be present in all silicon nitride powders, and the type of contacting atmosphere during ageing has been found to affect the amount of oxygen present in the particles.⁷ In other studies, the particles were annealed after they were formed, before they were exposed to air, and the amount of oxygen present in the silicon nitride particles decreased greatly. This would suggest that the oxygen incorporation happens due to dangling bonds in the particle or thin film which are annealed out at higher temperatures. Alternatively, the heat on the surface keeps species such as oxygen or water off of the surface, and if there is minimal mixing in the inter-electrode region, these species do not interact with gas phase radicals which are heading for the surface. Thus there is minimal incorporation of oxygen into the thin films.

Measurement of the depletion of reactants in the plasma region as a function of plasma on-time may give insight as to differences in the SiH/NH ratio in the deposited films. Both the saturation rate and the time it takes to reach the saturation point can be found from in-situ depletion measurements of the reactant depletions as well as rate of replenishment. Both of these rates are likely related to the degree of mixing initiated by the showerhead design which introduces the reactants into the inter-electrode region. In one investigation,⁴ a decrease in the index of refraction of the deposited silicon nitride film with power is considered to be due to the decomposition properties for the reactants. This could be related to the belief that the decomposition fraction of silane saturates at a lower power density than ammonia,⁸ so that at higher rf powers, there is more N-H present in the film making a lower index of refraction.

Few in-situ studies of the time dependence of the reactant concentrations and molecular temperatures have been attempted because it is difficult to monitor these parameters without disruption of the plasma environment. Mass spectrometric studies appear to give the most

concentration information using quadrupole mass spectrometers, but by far most of these studies have looked at a continuous plasma.^{8,9} Sampling a plasma at specific times during the radio frequency pulse and at various delay times after the rf plasma pulse has occurred is a more difficult problem, and there are very few groups pursuing this type of study. Either the mass spectrometer itself must be pulsed off and on, or some sampling technique must be initiated which samples the plasma at regular interval in synch with the plasma pulse. Determination of the temperature of the reactants is not possible with mass spectrometry.

Optical spectroscopy of rf-PPECVD plasmas is possible. Laser-induced fluorescence, ultraviolet-visible spectroscopy and infrared spectroscopy have all been used to probe the plasma region. In the case of laser induced fluorescence, often the reactant molecules do not fluoresce, and as a result the technique is restricted to radical species generated in the plasma.¹⁰ Ultraviolet-visible spectroscopy and infrared spectroscopy suffer from the fact that long pathlengths are usually required at low pressures and it is difficult to just monitor the plasma region. In one FTIR study of rf discharges through silane,¹¹ the rotational and vibrational temperatures were found to be between 300 and 900 K. With these optical techniques it is also difficult to measure time dependencies smaller than a millisecond due to the mechanics and electronics involved in making the measurement, although recently step-scan FTIR now appears to have that capability. Thus accurate time dependent optical temperature or concentration measurements have not been accomplished in a small region of the plasma, by any of these methods.

An optical spectroscopic technique that can be used to probe medium pressure (133 Pa to 6670 Pa) is pulsed coherent anti-Stokes Raman scattering (CARS) spectroscopy.¹² Other groups have previously employed CARS to monitor the concentration of reactants in rf plasmas

containing silane, but they were not pulsed plasma nitride deposition plasmas.¹³ In CARS spectroscopy, and especially BOXCARS, the probing region is defined by the crossing of three pulsed probe laser beams at their focus and so the sampling volume is very small, essentially a single point in the inter-electrode region. Not only do the laser beams have to be overlapped spatially, they must be overlapped temporally as well. The pulse width of the laser beam from the Nd:YAG laser is approximately 6 ns which is just an instant compared to an rf pulse width of several microseconds or milliseconds. CARS studies performed on pulsed CDCl_3 and CCl_4 plasmas at ~ 300 Pa indicate that the internal temperature of the reactant molecules may become rather high in a short amount of plasma exposure time; as high as 1000°C in less than 0.1 ms of exposure to 50 Watts of 13.5 MHz rf under certain conditions.¹⁴ If the molecular temperatures of silane and ammonia reached higher than 1000°C in an rf-PPECVD of silicon nitride, then thermal breakdown could perhaps occur, and theories regarding the SiH/NH ratio, theories explaining the surface morphology of nitride nano-particles, and measurements of the saturation level of the decomposition fraction of SiH_4 and other reactants would possibly need revision.

Studies Executed

A big part of this effort involved the design, gathering of parts, assemblage, testing, and implementation of the radio frequency pulse plasma enhanced chemical vapor deposition (rf-PPECVD) reactor and the instrumentation required to monitor its operation. During the testing stages of the project, standard operating procedures were developed to help insure consistent and safe operation of the rf-PPECVD reactor and associated equipment. Throughout the implementation stages of the study, the standard operating procedure was tweaked slightly from the initial draft.

The reactant temperature and concentrations for silane were monitored by CARS spectroscopy as a function of plasma pulse width in medium pressure rf-PPECVD of silicon nitride thin films. The silicon nitride thin film and particle depositions were accomplished in a reactor designed and constructed at Idaho State University, and the CARS spectrophotometer was also reconstructed and interfaced to the radio frequency pulsed-plasma chemical vapor deposition reactor. For the particle studies, a pulsed introduction system was designed, built, and integrated with a quadrupole mass spectrometer to monitor the silane reactant depletion levels at the edge of the plasma region.

The CARS spectrophotometer allowed the depletion and temperature of the silane in the gas phase reactant flow to be monitored, and the pulsed sampling mass spectrometer measured just the silane depletion. Information about the deposited films or particles was collected by commercial instrumentation acquired during the course of this project. Film thickness was measured by light backscattering and scanning electron microscopy (SEM). The index of refraction was also determined by light backscattering. Atomic composition was determined by an X-ray attachment on the scanning electron microscope. Stresses on the silicon substrate wafers were determined by a stress gauge. The SiH/NH ratio was determined by infrared using a Fourier transform infrared (FTIR) spectrophotometer. For the silicon nitride particles, size was determined by SEM and composition by X-ray analysis.

All films deposited were silicon nitride on 125 mm diameter silicon wafer polished on both sides. The silicon wafer was placed on the grounded lower electrode which was temperature controlled. Silicon nitride particle production was enabled by using longer rf pulse widths at a lower repetition rate, and the lower electrode was replaced by a grounded screen. The reactant

gases used were silane, ammonia, and nitrogen. For all studies the frequency of the rf power was 13.6MHz at peak powers between 10 and 100 watts. The pressure was always regulated at 667 Pa (5 torr) and for the films, the pulse repetition rate was 10 Hz. A pulsing circuit was implemented which synchronized the rf pulse, the CARS pulsed probe laser beams, and the mass spectrometer's sampling pulse. A delay circuit allowed the placement of the CARS and mass spectrometer sampling pulses to be at times within the rf pulse or at various delay times after the tail end of the rf pulse.

In the case of the thin film deposition, a typical experimental run consisted of the following steps. The flows of all reactant gas were set on their mass controllers. The pressure regulator mass flow controller was set to 667 Pa. The rf pulser was initiated at the proper pulse-width. The plasma was pulsed synchronously with the CARS or mass spectrometer, and the delay circuit was set to sample at the predetermined time. The plasma was allowed to pulse for the total amount of time decided upon, typically 75 minutes, and sampling of the silane concentration by CARS or mass spectrometry was performed again. The delay time was changed to another value and silane concentration determination was performed again. This process continued until sampling at all delay times of interest was completed. This was called a cycle. Subsequently, the delay time was set back to the initial value and the cycle was completed again. Typically a total of three cycles could be completed during the total deposition time. The coated silicon wafer was taken out of the reactor, and the film thickness, index of refraction, stress due to the thin film, and FTIR spectrum for SiH/NH ratio were taken. In many cases a digital photograph of the wafer was taken and the atomic composition was determined by X-ray. Correlations of the spectroscopically determined silane depletion with the thin film parameters were then examined

for trends. Subsequent runs followed a similar pattern with changes being made in the rf pulse width, the rf peak power, the temperature of the substrate, or the pattern in the shower head which dispersed the reactants to the inter-electrode region.

By changing the different reactor parameters, and monitoring both resulting alterations in the gas phase reactants and film properties can give an idea of the relative role played by gas phase chemistry and surface processes. Changes in the film properties, such as the index of refraction, the atomic composition, or the SiH/NH ratio, as a result of alterations, for example, in the rf pulse width or peak power may be a result of direct changes in the gas phase chemical composition due to differences in the plasma, or indirect changes due to a large increase in temperature of the gaseous reactants, in the surface chemistry, or in both. Changes in the silane depletion in the plasma region reflect a change in the gas phase chemistry. If the temperature of the substrate does not affect the gas phase chemistry, then a difference in the film property as a result of a change in the substrate temperature reflects differences due to heating the deposition surface and therefore surface kinetic processes. Alterations in the film properties due to the changing the showerhead are likely due to gas phase mixing differences or flow patterns which would be reflected as differences in depletion of the reactant silane. By performing all of these various studies, the gas phase and surface phase processes can be separated from one another and analyzed for their relative importance.

For the silicon nitride particles, the experimental runs were similar except that pulsed mass spectrometry was used to get information about the silane depletion in the plasma. A typical run consisted of the following steps. Set the appropriate mass flow controllers for the desired reactant flow rates. Put pressure regulator at 667 Pa. The rf pulsing was started at the desired

pulse width. For the particles, the pulses were longer and both the pulse-on time and pulse off time were set at the appropriate values. The plasma was allowed to pulse for the total amount of time necessary to collect the particles. Pulsed sampling for mass spectrometric analysis of the concentration of silane at the edge of the inter-electrode region was synchronized to fall within the rf pulse initially. The delay time to the sampling was changed to a new value and resampled. This procedure occurred until all delay times of interest were sampled. Following a particular run, changes were made in either the rf pulse width, rf peak power, or reactant flow composition.

Changes in the particle properties, as in the case of film properties, may be a function of alterations in the gas phase chemical composition or in the nucleation and surface chemistry of the forming particle. Changes in the gas phase chemistry may be influenced by alterations in power, rf pulse width, and reactant flow composition. Surface and nucleation processes should be most influenced by power and pulse width.

These rf-PPECVD studies detailed in the body of this report give some insight into the relative contribution of the gas phase chemistry versus the surface processes that lead to the formation of silicon nitride thin films and silicon nitride particles. The combination and correlation of the optical spectrophotometric or mass spectrometric measurements with the thin film and nano-particle characterization measurements, that were constructed and/or implemented for this study were an essential part of the ability to make suggestions regarding conditions that can enhance the quality of silicon nitride coatings or make smaller more uniform particles. More importantly, the conclusions of these studies will add to a fuller understanding of why these conditions work better.

METHODOLOGY

This part of the report is broken down into five main sections. The first few sections describe the design and construction of the reactor and supporting equipment, the spectrometric instrumentation, interface of the reactor and spectrometric instrumentation, and the instrumentation used for analysis of the silicon nitride thin films and particles. The last section details the parameters that were used for the various runs carried out during the study.

Construction of the rf-PPECVD Reactor and Supporting Equipment

The Plasma Chamber

The plasma chamber is composed of five main sections: the body, the upper electrode support flange, the upper electrode, the lower electrode support flange, and the lower electrode and substrate support. The body section, composed of aluminum, is octagonally shaped on the outside and is a 203mm diameter tube on the inside. Several 75mm ports are placed symmetrically on the flat faces of the octagon. Onto two of the ports, on opposite sides of the chamber, five inch extensions and a spacers were added. Two inch laser-grade windows were sealed onto the ends of the spacers using o-rings. A tapped hole was drilled into each spacer to allow argon gas to flow across the face of the windows.

The upper electrode support flange consists of a ten inch diameter, 19mm thick circular plate with a five inch diameter hole drilled in the center. An o-ring groove in the wall of the 127mm diameter hole seals the upper electrode assembly to the upper electrode support. The upper electrode support is sealed to the body section by an o-ring in the groove drilled in the end of the body section. The lower electrode support is similarly constructed, and the lower electrode also seals by an o-ring in the groove of the 127mm hole in the lower electrode support.

The upper electrode accommodates both silicon nitride film deposition as well as production of nano-sized particles. The mechanical drawings for the electrodes are given in Appendix A of this report. An overview sketch of the plasma electrode arrangement is given in Figure 1. Essentially the electrodes consist of an upper stainless steel cap which is connected to a 75mm dia, 100 mm long ceramic thermal and electrical isolator. On the lower end of the ceramic isolator, five holes are drilled through the steel cap and ceramic isolator to allow for power connection, temperature measurement and control by circulation of air into the holes. The rf power comes into the reactor through the center hole and connects with a two-section upper-electrode head. The reactant gases flow through two 6 mm stainless steel tube which enter the chamber through two Ultra-torr feed-through connectors welded in the stainless steel cap on a diameter of 115 mm. Below the level of the steel cap, glass to metal seals convert the flow tubes into glass for thermal and electrical isolation. These glass tubes extend for 75 mm and a glass-to-metal seal once again converts the flow tube into steel for mating into the electrode head. The reactant flow that enters the electrode head is dispersed, by the small holes in the showerhead pattern on the electrode head, into the inter-electrode region where the rf plasma is struck.

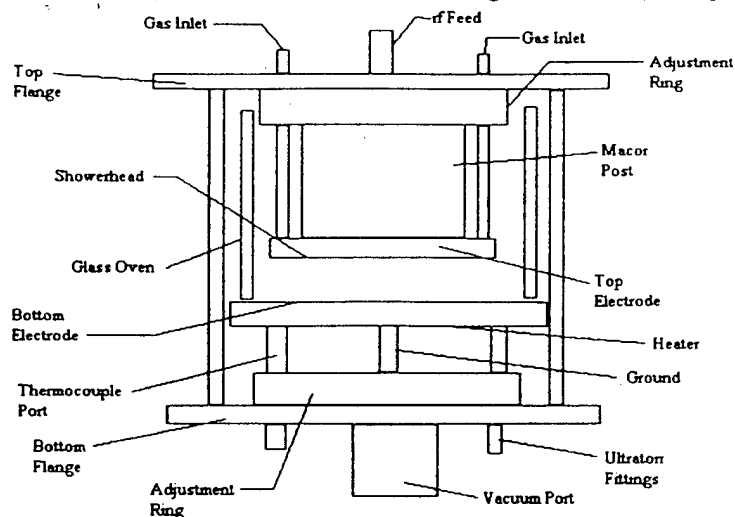


Figure 1. Overview Sketch of Plasma Electrode Arrangement.

In the first section of the upper-electrode head, gases enter through a 6.3 mm diameter port and the nitrogen and ammonia enter through a second inlet on the opposite side. The distance separating the two ports is about 75mm. A single 25 mm hole, drilled in the center of the lower plate of the first section of the upper electrode head, forces the gases to mix before they enter section two. Section 2, the showerhead section, is the dispersal section for the upper electrode. It can be separated from the first section, allowing a variety of hole patterns to be investigated. The small diameter of the holes, 0.79mm, forces more mixing to occur before the reactant gases can enter the inter-electrode plasma region. The sheer number and distribution of the holes in the showerhead causes the reactant gases to be distributed more uniformly into the plasma region.

The lower electrode, the grounding electrode, is somewhat similar to the upper electrode in that there is a stainless steel cap. The stainless cap has a vacuum port in the center which acts as the main pumping port for the rf-PPECVD reactor. The grounding electrode/substrate support plate is attached to the lower electrode steel cap by three supporting legs which contact the support plate near its 175mm diameter outer edge. The supporting legs are stainless steel tubes that are sealed at the top end which contacts the substrate support plate. The support legs are open on the bottom in order to allow probes to be inserted through them to contact the grounding electrode. A ground wire and thermocouple are inserted up two of the tubes. The value of the temperature read by the thermocouple must be corrected to account for differences in the temperature read in the support tube and the temperature at the top of the wafer. The correction was determined by experiment and is given in Table 1.

Table 1. Thermocouple Measurements vs. the Actual Temperature at the Top Center on the Lower Electrode.

Temp. Read by Thermocouple Inserted Through Supporting Leg in Substrate Support (°C)	Temperature at the Center of the Top of the Substrate Support (°C)
120	180
140	200
160	220
180	240
200	260
220	280

The differences in the temperatures are due in part to the way that the lower electrode/substrate support plate is heated.

There are actually two different circular substrate support plates for the lower electrode. The one for silicon nitride thin film depositions has a solid center that extends out to a 127 mm diameter. Below this central region is mounted a 125 mm O.D. resistive ring heater. The ring heater leads are connected to a variable ac power supply via an electrical feedthrough on one of the octagonal faces of the plasma chamber. This ring heater worked much more smoothly and uniformly than a initial design which used three cartridge heaters placed symmetrically around the support plate, and the temperature could be controlled between 60°C and 450°C. Further away from the center there is a slotted ring area to allow the gases in the inter-electrode region to escape and be pumped out of the central vacuum port in the lower electrode. A hollow cylindrical 100 mm tall glass piece, of 150 mm ID and 162 mm OD, the "glass-oven", sits on the substrate

support and surrounds the inter-electrode region where the pulsed plasma is primarily contained. The half millimeter thick, 125 mm diameter silicon wafer substrates fit on top of the substrate support and a small centering ring of 127 mm ensures that the wafer is placed correctly on the support. When the chamber is assembled, the distance between the silicon wafer substrate and the showerhead on the upper electrode is typically 22 mm, but it can be varied somewhat if necessary.

The other substrate support plate is similar, except that there is a 75mm hole in the center of the plate. The ID of the ring heater is 76mm, so the hole in the center does not disrupt the ring heater. Instead of silicon wafer, a 125mm diameter stainless steel wire screen is placed on the substrate support. This facilitates deposition of silicon nitride particles rather than thin films. Initially, a coarse grade of filter paper was placed over the 38mm diameter vacuum port to collect particles, but in practice there were sufficient particles deposited on the screen and the upper electrode that the filter paper was found to be unnecessary.

Vacuum Connections

The vacuum port on the bottom of the rf-PPECVD reactor is connected to a 38mm ball valve. The ball valve is used to help minimize the amount of nitrogen that is regulated into the vacuum pump to hold the pressure constant at the desired value, usually 667 Pa. It would be closed as much as possible during a run. Below the ball valve, an 125mm dia by 254 mm long filtering canister filled with 6 mm diameter alumina balls contacts any unreacted silane or ammonia leaving the reactor. The filter also acts as the first eliminator of particles from the gas stream so that the mechanical pump does not come into contact with them. Below the filter is a 254 mm long piece of corrugated stainless steel tubing to allow movement of the plasma chamber for centering purposes. The rest of the line all the way into the 60L/min Leybold mechanical vacuum

pump is solid stainless steel tubing of 38mm ID. Cwik Flange connectors are used to tie the the line segments and the pump together. The nitrogen flow, which is used to control the chamber pressure, is dumped into the pump directly at the inlet of the pump through a T-shaped stainless steel tube. The pump is air cooled by blowing a fan across it, and the oil is filtered by a Motor Guard oil filter while the pump is in operation. The oil is a high purity white oil made specifically for pumping corrosive and reactive gases. The oil is monitored visually at the end of each day for discoloration and/or particle content. If either of these conditions occur the oil is changed.

During a particular run, the pressure was monitored by an MKS Baratron capacitance manometer. The manometer was connected to the chamber by a 6 mm diameter corrugated tube that attached, by a Swagelock connector, to a flange on one of the octagonal faced sides of the plasma chamber. The electrical signal from the manometer transducer is fed into a Unit Corp. pressure controller which opens a mass flow controller to the right degree to allow nitrogen to flow into the vacuum pump and keep the pressure in the reactor constant. The ball valve directly below the chamber vacuum port could also be adjusted to minimize the amount of nitrogen flow needed to keep the reactor chamber pressure constant. The minimum pressure attainable with this system was roughly 20 microns.

Connection and Control of the Reactant Flow

Ultra-high purity, semiconductor grade silane and ammonia gases were obtained from Scott Specialty Gases. Initially ultrahigh purity nitrogen was also obtained from Scott, but as the studies progressed ultrahigh purity was obtained both from local vendors Air Liquide and U.S. Welding. Ultrahigh purity argon was also obtained from U.S. Welding. The silane and ammonia gases were stored in vented cabinets near the plasma chamber, along the wall. Safety valves were

incorporated into the lines between the gas cylinders and the regulators for the silane and ammonia gases. If a line after the safety valve ruptured, the high increase in flow rate would be detected and the valve would close. Additionally, the safety valves had the potential to be activated from a remote location across the room.

To get the silane and ammonia gases to the chamber, 6 mm diameter stainless steel tubing was used to first plumb the gases from the outlet of their dedicated pressure regulators to the mass flow controller manifold. Unit mass flow controllers of the correct mass flow control range and calibrated for the appropriate gas were used. Nitrogen and argon were also plumbed, using stainless steel tubing, to the manifold. The silane and ammonia lines at the input of the manifold were also connected to a valve which allowed argon or nitrogen to flow through the silane and ammonia lines as well. This served the purpose of allowing an inert gas to flush out the lines at the end of the day. The exit of the mass flow controllers from the ammonia and nitrogen were mixed in a stainless steel manifold. A single outlet from the manifold was run by stainless steel tubing to one of the stainless tubing inlets on the upper electrode of the plasma reactor. The tubes were connected together by Swagelock fittings. The outlet from the silane mass flow controller was plumbed in stainless steel to the other inlet on the upper electrode and a Swagelock fitting connected it to the stainless tubing entering the reactor. The output from the argon gas did not enter the electrode region through the electrode head. It was plumbed into both of the aluminum spacers that were placed before the laser windows.

Individual mass flow controllers were used to regulate each of the inlet gas flows. The flow rates were set manually using a Unit Corp. URS 20 control unit. Before any silane was allowed to flow, all lines were pumped out and the vacuum pump was flushed several times with

ultra-high purity nitrogen. The nitrogen flow was started first and the pressure controller was set and a plasma was struck with just the nitrogen flowing. The flow rate of the nitrogen was lowered as the ammonia flow rate was increased, and then lowered again as the silane flow was started and set to the correct value

Plasma Electronics

A Tektronix Type 191 constant amplitude sine wave generator was used as the source of the rf signal at 13.6 MHz. It was connected to a pulser box which was triggered by a Vincent Associates Model T132 Shutter Driver/Timer. The output of the pulser box was a square wave pulse, of tunable width, that had a 13.6MHz sine wave oscillating during the duration of the square pulse width. This rf pulse was sent to an ENI Model A 300 rf power amplifier for amplification to the desired peak power. The output from the power amplifier passed through a Byrd Model Model 4021 power sensor and Model 4421 wattmeter, and then into an L-type impedance matching network. The matching network was adjusted to match the impedance in the plasma with the output impedance of the power amplifier. The output from the impedance matching network was connected to the upper electrode through a wire which entered through the center hole drilled in the stainless steel cap plate and the ceramic standoff. It attached to a banana type connector plug which was soldered to the back of the upper electrode.

The Byrd wattmeter gave a direct reading of peak power of the rf pulse. The triggering of the pulser box was synchronized to the pulsing of the laser and the mass spectrometer. This was accomplished using a variable pulse width generator from Vincent Assoc. to drive the rf pulser box and two delay circuits. One of the outputs from the delay circuits triggered the flashlamps on the laser which furnished the probe beams for the CARS experiments. The other delay circuit

triggered the pulsed sampling circuitry for the mass spectrometer.

A LeCroy digitizing oscilloscope was employed to set the desired delay times for the CARS and Mass Spectrometer sampling. The output rising edge of the output from the rf pulser box triggered the scope. The output from the Q-switch of the Nd:YAG was used for the CARS timing, and the output from the signal used to open the pulsed sampler on the mass spectrometer indicated where the mass spectrum was taken. The settings were grossly checked visually as well. The value of this setup was that when the pulse width of the rf was changed, it was easy to set up the overlap.

A Standard Operating Procedure (SOP) was developed for safe and consistent integrated operation of the vacuum equipment, flow controllers, and plasma electronics. The procedure included a procedure for changing reactant gases, starting up the plasma from several conditions, shutting down the system based on the expected shutdown time and maintenance required. Great care was taken to keep some nitrogen flowing into the pump as a dilutant during a run, and to always flush the pump with nitrogen before and after a plasma study. The SOP document related to operation of the rf-PPECVD system is given in Appendix B.

Instrumentation for Spectroscopic Monitoring of Reactants in a Pulsed Plasma

Both coherent anti-Stokes Raman Spectroscopy (CARS) and mass spectroscopy (MS) were employed to monitor the reactant gas, silane, in the inter-electrode plasma region. The CARS provided information about both the temperature and the amount of silane present as a function of time. Pulsed Sampling MS provided information only on the amount of silane present during the rf pulse or at various delay times after the pulse. While the CARS sampling was almost instantaneous (6ns), the minimum practical sampling time for MS was 10 ms.

CARS Spectrophotometer

The CARS instrument has been previously described in detail,¹³ but some modifications were necessary for the present study. Briefly, the doubled output (λ_1) at 532 nm from a Continuum YG 661 Nd:YAG is split and used for two probe beams in the BOXCARS arrangement, and to pump a Pegasus dyelaser flowing Rhodamine 6G or 610 dye in methanol. The tunable dye laser output at λ_2 , along with the two λ_1 probe beams form three of the corners of a box-shaped design, and are focused in the center of the inter-electrode plasma region about 9 mm below the upper electrode. When the difference in energy corresponding to λ_1 and λ_2 , is equal to the energy of an allowed Raman vibrational transition, a relatively intense, spatially and temporally coherent beam of light at λ_3 is emitted. The energy of that beam is $E_3 = 2E_1 - E_2$, and it is more energetic than the laser light of the incoming beams. The light emitted at λ_3 propagates in a particular direction as determined by the focusing geometry of λ_1 and λ_2 . Thus the light emitted at λ_3 can be spatially discriminated from the background light of the plasma. The light at λ_3 was collected and put into a Instruments SA HR320 monochromator. The front and rear slits were 167 microns and a Hamamatsu photomultiplier tube was used as the detector.

The signal from the photomultiplier tube is collected with a EG&G Parc Boxcar Averager, Model 4121B. The analog output of the averager is collected and digitized by an A to D converter in an NEC Computer. The A to D board has a set of timers as well, and these timers are used to trigger the monochromator stepper motor box and the driver box which steps the wavelength of the dye laser output. A program steps the monochromator and the dye laser in such a way that a CARS spectrum may be take over a few hundred wavenumbers or over a small wavenumber interval.¹³ The overall layout for the CARS experiment is given in Figure 2.

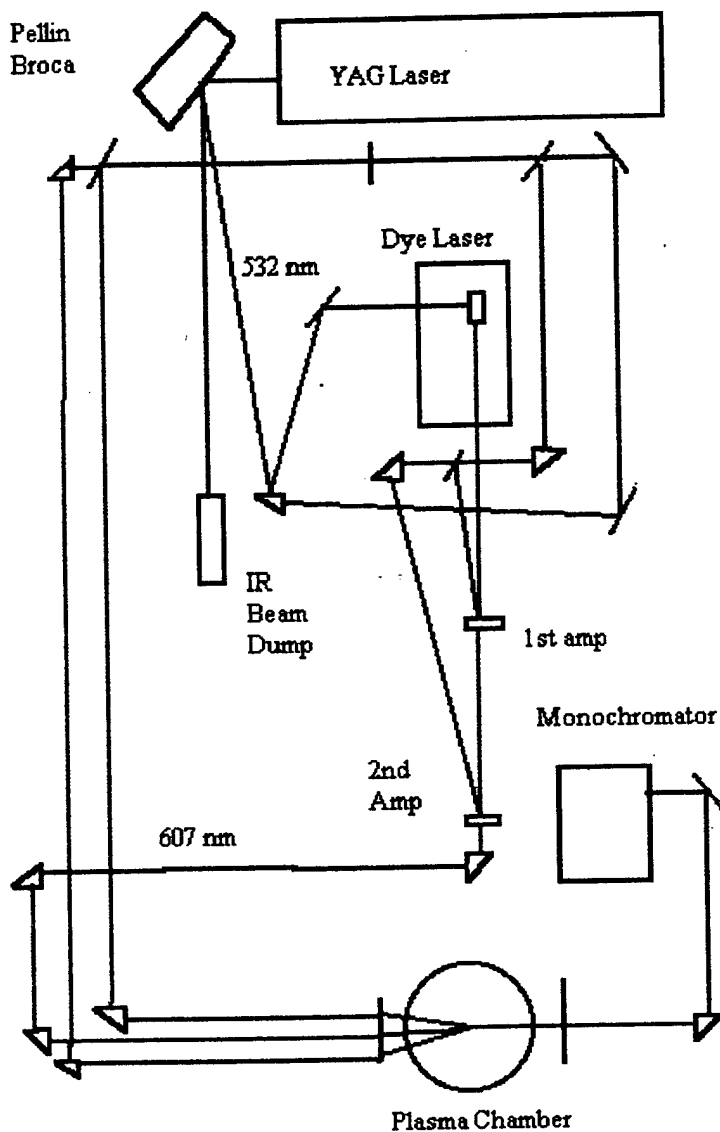


Figure 2. Overall Layout for the CARS Experiments.

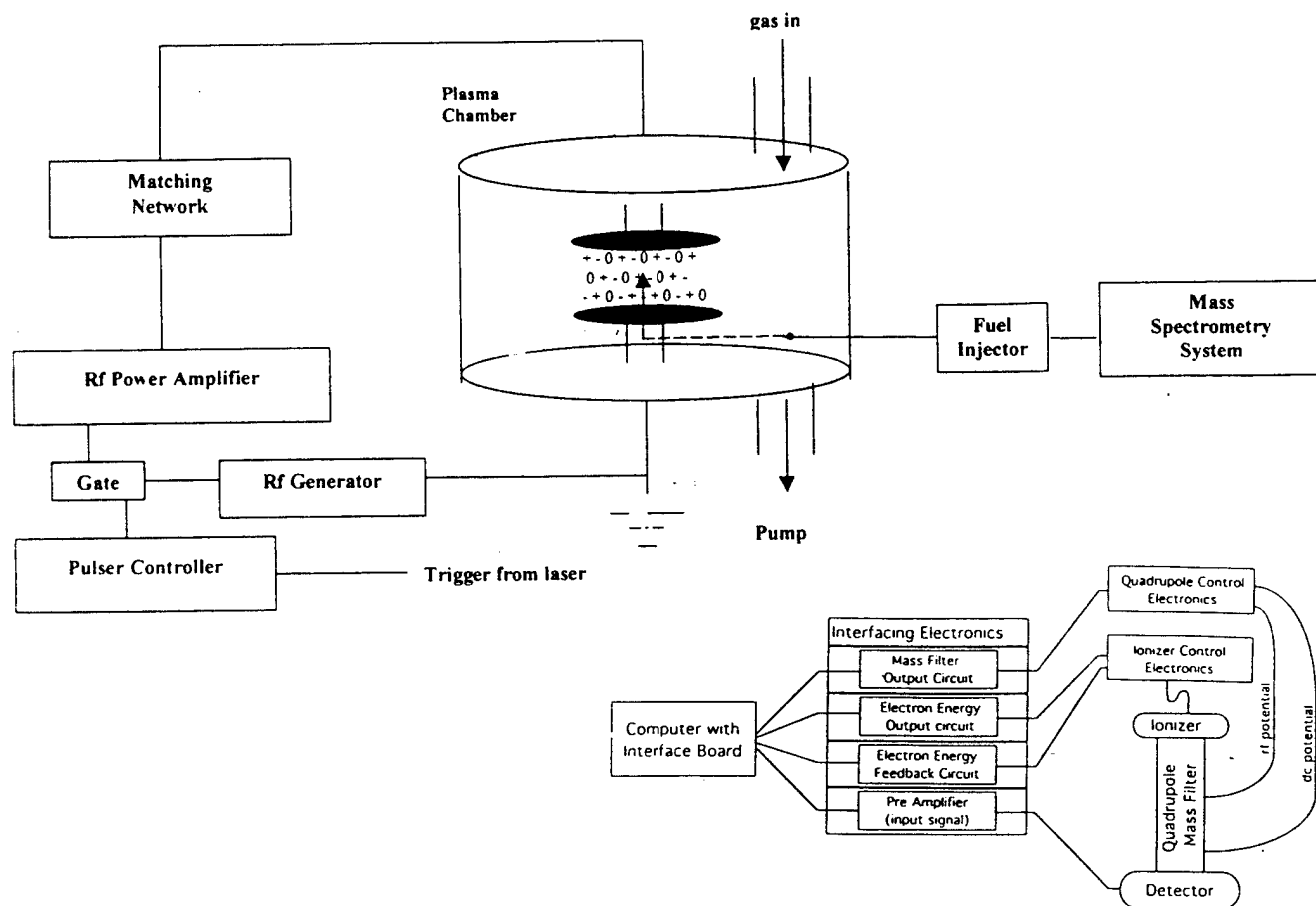
For detection of the concentration of silane gas, the dye laser was tuned to a wavelength which corresponded to the maximum in the CARS spectrum for the Q branch of the totally symmetric Si-H stretch (ν_1) at 2187 cm^{-1} . In some instances the dye laser was scanned across the Q-branch of the Si-H stretch. This was necessary to determine if the temperature of the silane reactants changed very much with plasma conditions. The validity of using a single wavelength to determine the silane depletion in the plasma is erroneous if the temperature of the reactants is

changing, since a shift in the maximum may occur or the peaks may broaden significantly. Note that CARS differs from spontaneous Raman in that for CARS the concentration is proportional to the square root of the signal intensity, and the signal is just the proportional to the intensity in spontaneous Raman.

The Pulsed Sampling Mass Spectrometer

The mass spectrometer is a quadrupole mass spectrometer consisting of an Extrel Quadrupole Power Supply (Model 011-1), an Extrel Mass Filter (Model 7324-9) with High-Q head (Model 011-5), and an Extrel Ionizer (Model 020-2). The data acquisition system involved the use of a Hewlett Packard Vectra personal computer fitted with a National Instruments Lab PC+ interface board with ten volts of detector input capability. The mass spectrometer program was developed previously for interfacing between the mass spectrometer and the computer for the purpose of data acquisition. In addition to the mass spectroscopy program, interfacing electronics were employed for external ramping of the Extrel Mass Filter. A high voltage power supply from EG&G Ortec was used to supply and external voltage to the mass filter.

The mass spectrometer chamber was pumped down to below 1×10^{-6} Pa by a Leybold turbomolecular pump in combination with an Edward roughing pump. The pressure was measured by two Varian ionization gauges. The system was baked overnight at 150°C occasionally to help maintain the vacuum. During the introduction of the plasma species into the mass spectrometer region by the pulsed sampling method, the pressure rose to a value of not more than 3×10^{-4} Pa, as measured by the ionization gauges. A block diagram of the instrument is given in Figure 3.



To allow for pulsed sampling of the plasma species, a Honda fuel injector, Model PG7-A10 was modified slightly and used as the pulsing valve. The fuel injector valve was located in the sampling line from the plasma chamber. An aluminum casing was fabricated which sealed on both ends of the valve for vacuum conditions. To sample species in the plasma, the fuel injector tip was inserted into the plasma chamber through a flange on one of the octagonal faces of the chamber, and through a hole in the glass oven which surrounded the inter-electrode rf plasma region. A 0.65m piece of 6mm stainless steel tubing connected the exit on the back of the fuel injector housing to a 3-way connector. One of the other ends in the 3 way connector led to a

valved small diffusion pump, and the other end led to a 50 μ m valved aperture. On the other side of the aperture was a small piece of ceramic tubing which led directly to the Extrel Ionizer.

Electronic timing of the fuel injector valve was accomplished by building a Pulsed Sampling Timing Circuit. This circuit used the rf pulser output, and a Model IIPU-2 delay to pulse on-and-off the 0.5 amps of current needed to open the fuel injector valve at the correctly synchronized time. The minimum pulse width needed to open the valve was about 5 ms. The fuel injector stayed open as long as the current pulse was positive. Pulses with widths longer than 2s could be used to open the fuel injector for the length of the pulse.

The methodology typically involved in using the pulsed mass spectrometer sampling system, (the fuel injector system), was as follows. Prior to using the fuel injector valve, the stainless steel line between the aperture and the fuel injector was evacuated by opening the valve to the diffusion pump. Following evacuation, such that the pressure in the mass spectrometer chamber reads below 4×10^{-6} Pa, the valve to the diffusion pump is closed. Next a toggle switch on the MS Timing Circuit is flipped and the fuel injector pulses on and off in the appropriate timing sequence. A stopwatch is used to determine the length of time that the pulsing continues and therefore the number of pulses. The number of pulses was held constant within a particular run. Characterization of the pulsed sampling mass spectrometer involved obtaining spectra and calibration curves for argon and silane.

Instrumentation for Analysis of the Silicon Nitride Thin Films and Particles

The thin films were deposited on 127 mm diameter crystalline silicon wafers from Omnisil Corp. The surface had a (1,0,0) orientation and the wafers were approximately 0.6 mm thick. The wafers were polished on both sides. The particles were collected from the stainless steel

screen used as the grounding electrode and from the surface of the upper electrode. Analysis of these depositions required the use of specialized instrumentation. For the thin films, measurements of film mass, film thickness, index of refraction, atomic composition, stress, SiH/NH ratio, and visual quality were made. Also measurements of the uniformity of thickness and index of refraction of the thin film across the entire wafer were attempted. In the case of the particles, atomic composition, size, and size uniformity were collected. These deposition parameters were measured by the instrumentation described here.

Thin film thickness was primarily determined with a Filmetrics Model F20 backscattering instrument. The backscatter signal at several frequencies is changed by the presence of a thin film on the wafer. The operator estimates the film thickness and index of refraction, and the theoretical backscatter signal is matched to the experimental one by incrementing the thickness and index. On random occasions, the thickness of the thin film was determined by a SEM to verify the backscatter results. This was accomplished by breaking the wafer and mounting it in a special holder which held it sideways. The particle sizes were measured only by scanning electron microscopy.

As mentioned above, the index of refraction was measured by the Filmetrics backscattering instrument as well. Here too, the experimental spectrum was fit to a theoretical spectrum to determine the best value for the index of refraction. Measurements on a 5mm by 5mm grid across the face of the wafer with the Filmetrics instrument allowed contour diagrams of the thin film to be made for both the thickness and index of refraction. These contour diagrams gave an indications of the uniformity of deposition and acted as a secondary check for the uniformity based on a visual inspection. Visually areas of different thickness are seen as different

colored bands on the wafer surface. A digital camera was used to record the visual description of some of the silicon wafers with thin films deposited on them.

A Leo Instruments Model 1430 SEM with an Oxford X-ray attachment was used to measure the size of the silicon nitride particles and the atomic composition of the thin films and particles. The particle size and size distribution were determined by examining several different regions of the deposited particles. In the case of an agglomerate, if the size of the particles making up the agglomerate were distinguishable, then they were reported. As mentioned previously the atomic composition was typically analyzed for silicon, nitrogen, and oxygen. Oxygen appeared to be present in almost all of the silicon nitride thin films and particles.

Film stress was determined with an Ionic Systems Inc. Stressgauge Model 30122 stress measurement system. This instrument works by measuring a deflection at the center of the wafer before and after the thin film is deposited. The thin film can stress the wafer by bowing it up or down, and therefore the deflection changes after the thin film is deposited. The stress therefore can be either compressive or tensile, and the changes in the conditions of the deposition could affect the way that the wafer deflects.

The content of hydrogen in the film in terms of the SiH/NH ratio was determined by transmission FTIR using a Perkin Elmer Paragon Model FTIR. The wafers were placed in the beam in the sample compartment, slightly turned so that the face was not exactly perpendicular to the beam. This cuts down on the fringe pattern seen due to multiple reflections caused by the films. The peak in the spectrum in region near 3350cm^{-1} is a measure of the amount of NH present in the film, and the region near 2150cm^{-1} is a relative measure of the amount of SiH in the thin film. The peak areas for these two regions were measured with Spectra Calc. In practice,

films thinner than 400 microns or so were too thin to give sufficient intensity in the SiH and NH peaks to measure their ratio.

Particulars of the Studies Accomplished in this Work

This section will be broken down into particulars for the silicon nitride thin film studies, and particulars for the particle studies. The reason for this is that different plasma parameters were held constant for these two types of studies. Some conclusions drawn from one or the other type of study, however may have ramification for the other as well.

Particulars of the Thin Film Studies

Several thin film depositions were done initially to determine a set of processing parameters for the rf-PPECVD reactor that would yield a smooth fairly uniform layer. One other stipulation was that the flow of silane had to be sufficient to get a good CARS signal, even at elevated temperatures. The initial showerhead design for delivery of the gases to the inter-electrode region did not allow for sufficient mixing of the gases to get good uniformity. One variable of the this set of parameters was then systematically changed to determine the effect of that parameter on the plasma and the resulting films. The initial set of parameters, and initial instrumentation setting, consisted of the following:

Reactor Pressure	667Pa (5torr)
Reactant Flow Rates	Silane 10sccm; Ammonia 20 sccm; Nitrogen 20 sccm
Substrate Material	Pure crystalline silicon (1,0,0) 0.6 mm thick, 127 mm dia.
Substrate Temperature	175°C
Inter-electrode spacing	22 mm
Electrode Showerhead	Radial

Upper electrode dia.	127 mm
Frequency of rf	13.6 MHz
Plasma repetition rate	10 Hz
Pulse width of rf	2ms
Peak power of rf	40 watts
Ar flow at windows	2.7 sccm
CARS sampling	Center of electrodes 9mm down from top electrode

Once the initial parameters were determined, various investigations were undertaken to determine the effects of individual reactor variables. In all, six types of investigations were pursued over the course of the proposal time.

In Study #1, CARS was used to determine if the temperature of the silane molecules in the inter-electrode region changed due to the presence of a plasma. The reactor parameters were set as describe above and the CARS spectrometer was scanned over the SiH stretch from 2176 cm^{-1} shift to 2195 cm^{-1} shift. This was done when the CARS lasers were fired when no plasma was present and at two different times relative to the 2 ms rf pulse. The CARS sampled 0.5 ms from the tail end of the rf pulse, 5 ms after the rf pulse.

In Study #2, differences in the CARS-determined silane concentration during the rf pulse and at various times after an rf pulse had completed were examined. For this and all subsequent CARS determinations of reactant concentrations, the square root of the relative intensity of the SiH peak at its maximum was used. Calculations on the distance that gases, which received an rf pulse, would move as a function of time were completed and used with the CARS information. This study gives information about the type of flow that is present in the inter-electrode region.

Reactor parameters used were the same as above with the following variations in peak power and rf pulse width: 25W, 2ms; 25W, 5ms; 25W, 10 ms, 34W, 2ms; 40W, 2ms, and 40W, 5ms. The delay times at which the CARS sampled the silane concentration were: 500 ms inside the plasma from the tail of the rf pulse, 2ms after the rf pulse, 5 ms after the rf pulse, 10 ms after the rf pulse, 40 ms after the rf pulse, and after the plasma was shut down completely for three minutes.

Even though precautions were taken to minimize deposits from occurring on the laser windows, some deposition took place. The CARS signal decreased as a function of time, so that typically the signal at the end of the run was lower than at the beginning of the run. In order to account for this, a linear decrease in signal with time was assumed, and the data were corrected based on this.

In Study #3 changes in the thin film properties with increases in peak power was examined. CARS-determined changes in the silane concentration in the plasma region, based on the square root of the peak intensity, were also performed for these studies. Correlation of the film properties and CARS spectra gave a measure of the contribution of the silane gas phase chemistry to the resulting thin film properties. The effect of varying the power was examined in alterations from the initial parameters listed here: 25W, 2ms; 34W 2ms; 40W 2ms, 30W 5ms, and 40W, 5ms. CARS measurements were made at the following delay times: in the rf pulse (0.5ms from end) and 2, 5, 10, and 40 ms after the rf pulse, but typically the silane depletion was based on the during-plasma data point.

In Study #4 changes in the properties of the thin films deposited on Si wafers as a function of rf pulse width were obtained. Here too, CARS spectra were taken simultaneously to observe any changes in the silane depletion in the gas phase for changes in the pulse width. The film

properties and depletion of silane in the plasma were measured for the following variances from the initial set of conditions: 25W, 2ms; 25W, 5ms; 25W, 10ms; 40W, 2ms; 40W, 5ms; and 40W, 10ms. Data for a continuous plasma were also collected. For the purposes of comparison, CARS measurements were made at several delay times in and out of the plasma, but depletion was based on the during-plasma data point.

In Study #5, CARS-determined silane depletions and properties of the thin films were collected as a function of differences in the showerhead design. Alteration of the showerhead was expected to affect the mixing of the gases in the inter-electrode region. CARS spectra gave information on changes in the gas mixing and how the mixing affected the concentration of silane in the inter-electrode region. Additionally, examination of the thin film properties gave an indication of how alterations in the gas phase chemistry affected the resulting silicon nitride thin films. The three showerhead designs studied were square pattern, radial or spoke pattern, and asymmetric pattern. Four sets of plasma conditions, which were the initial conditions given above with changes listed, were accomplished for each of the three heads: 40 W, 2ms, all heads; 40W 5ms, all heads; 40W, 10ms, all heads; and 30W, 5 ms, all heads. Diagrams detailing each of the three showerheads are included in Appendix A.

Study #6 involved varying the substrate temperature. The initial reactor conditions were as described above except that a 30W peak power, and 5 ms plasma was used. Also this study was done using two showerheads: the radial and square shower heads. For the radial showerhead the following substrate temperatures were used: 175, 200, 220, and 260 °C, and for the square showerhead 175, 190, 200, 220, and 240 °C were used. Changes in the substrate temperature may affect the gas phase chemistry slightly, but should affect the thin film properties much more if

the properties are determined largely from surface chemical processes. CARS spectra of the plasma measured the silane depletion and thin film properties were measured in this study for all the different temperature conditions.

Particulars of the Particle Studies

Here also, an initial set of parameters had to be experimentally determined such that a good yield of silicon nitride particles were obtained. During these initial studies it was found that the particles changed composition as a function of the time that they are exposed to air. Particularly, the % of oxygen in the particles seemed to change to a large degree. Thus in all studies for the particles, measurements of the atomic composition are not repeatable at this point, however in many cases they will be reported, since the silicon percentage did not appear to change greatly with time, apparently as oxygen became more incorporated in to the particles. That is, the oxygen incorporation into the particles seemed to affect the atomic composition of nitrogen much more than it affected the atomic composition of silicon.

For the particle studies, the initial set of parameters, and initial instrumentation setting, consisted of the following:

Reactor Pressure	667Pa (5torr)
Reactant Flow Rates	Silane 10sccm; Ammonia 20 sccm; Nitrogen 20 sccm
Substrate Material	Stainless Steel Screen
Substrate Temperature	26°C
Inter-electrode spacing	22 mm
Electrode Showerhead	Radial
Upper electrode dia.	127 mm

Frequency of rf	13.6 MHz
Time between rf pulses	2s
Pulse-on time of rf	200 ms
Pulse-off time of rf	1 s
Peak power of rf	40 watts
Ar flow at windows	2.7 sccm
MS sampling	Edge of electrode
MS sampling width	200 ms

Once the initial parameters were determined, two overall groups of investigations were undertaken for the particle studies. One group delimited the quality of the information available from the pulsed sampling mass spectrometry technique developed in the lab, and the second group studied the effects of altering individual reactor variables on the particles formed. From these two groups of particle studies, five additional types of investigations (numbered 7-11) were pursued over the course of the proposal time. Thus between the thin film studies and the particle studies there were at total of twelve types.

With regard to Study #7, CARS spectroscopy was supposed to be used to measure the time dependence of silane depletion in the plasma region. However, due to the long rf pulse widths required for the particles to deposit, the laser firing could not be easily be coordinated with the rf pulse. Also, the laser windows had some deposit on them which disrupted the CARS process. Thus pulsed sampling mass spectrometry (PSMS) was attempted. The pulsed sampling for the mass spectrometer was a novel and new approach to the sampling of a pulsed plasma at specific times within the rf pulse and outside of the rf pulse. In light of this, the first studies on

particles reflected the ability of the pulsed sampling to quantify the relative amount of silane present at the inter-electrode region as a function of the sampling time relative to the rf pulse. Evaluation of the ability of the PSMS to be calibrated was accomplished by calculating the area under the argon mass peak at 40 amu as a function of flow rate of argon into the chamber for 0, 2.5, 5.0, 7.5, and 10.0 sccm of argon. The collection conditions were similar to those given above under initial conditions with no plasma present and the only other gas flowing was nitrogen. Here the argon entered the chamber through the silane line and the showerhead or argon entered at the laser windows. A calibration curve for silane was also attempted. Here the sum of the area under the peaks at 29-31 amu was used as the silane signal. Typical PSMS spectra are given in Figure 4 taken both in and out of the plasma. Again flows of 0, 2.5, 5.0, 7.5, and 10.0 sccm of silane were used. Also the signal amplifier was changed to see it affects on the calibration curves.

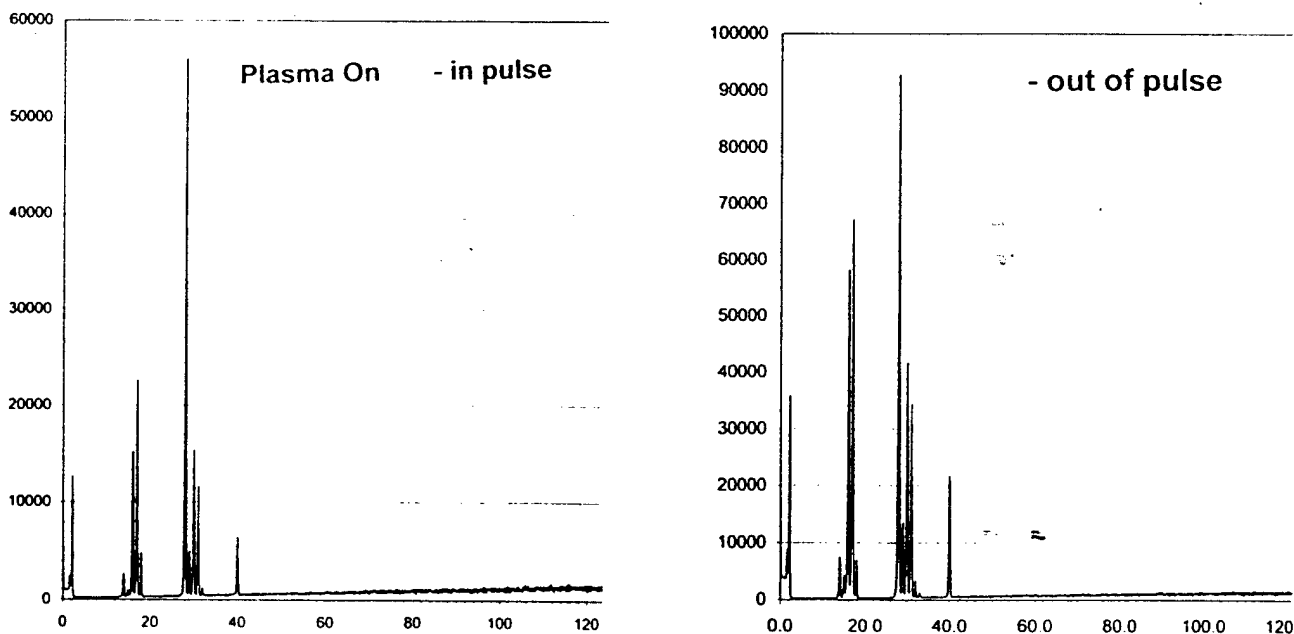


Figure 4. Typical Pulsed Sampling Mass Spectroscopy Spectra Taken Before the Plasma and During a Pulsed Plasma.

In study #8 a comparison of results obtained with pulsed mass spectrometry to results obtained with CARS was made. The depletion of silane was measured by pulsed-sampling mass spectroscopy and CARS for a 10Hz pulsed plasma with rf pulse-widths of 2ms, 5ms, 10ms, and a continuous plasma at 25 watts peak power. Here the MS pulsed sampling time (the fuel injector) was set at 10 ms. Two pieces of CARS data were taken. One was taken 500 ms from the tail of the pulse and the other was an average of values taken over a 10 ms time frame measured from the beginning of the pulse. For the continuous plasma case and the initial 100% readings taken in the absence of a plasma, the CARS measurement and pulsed sampling MS measurements were an average over several pulses taken at arbitrary times.

In study #9 the second group of studies was started. Here the silane depletion was determined by adding the areas of the 29-31 amu peaks in the mass spectrum. Studies were accomplished both in a continuous plasma at 20W, 40W, 60W, and 80W, and in pulsed plasmas. The results from the use of the pulsed sampling MS to sample the silane in the continuous plasmas can be compared with results from other groups.

For the pulsed plasmas, an investigation of the influence of rf power on the particle parameters such as size and composition and the depletion of silane in the inter-electrode region was undertaken. The mass spectral sampling of the pulsed plasmas used a fuel injector pulse width of 0.1 s. Several conditions were used which included the following. For pulse-on, pulse-off times of 2.0 seconds each, the power variance was 30W, 40W, and 50W. Additionally for pulse-on, pulse-off times of 0.2s and 2.0s respectively, powers of 20 W and 40 watts were investigated.

The effect of the pulse width was investigated for study #10. The pulse width could

change both the species present in the plasma and to a lesser extent, the nucleation and surface reactions of the particles being formed. A longer pulse width might change the surface mobility if the surface temperature changes. The power was held constant at 40W and the plasma off-time was held constant at 2.0 seconds. The plasma pulse on-time varied as 0.2 ms, 0.5 ms, 1.0 ms, and 2.0 ms. The mass spectral sampling occurred 200 ms from the front of the plasma pulse, inside the plasma pulse and 1 s or 500 ms before the plasma pulse, outside of the plasma. The other parameters were as listed in the initial parameters list given above.

The final study, #11 considered the influence of the composition of the reactant flow on the particles and silane depletion in the inter-electrode region. Here the composition of the gas phase species should be affected greatly in some cases, and the resulting change in particles should then reflect whether or not a great change gas phase species can change the resulting particle features. For these studies the power was held a 40 watts peak power, the rf was pulsed on for 2.0s and pulsed off for 2.0s as well. The pulsed sampling width for the MS was 200 ms in all cases but one, where the value was 100 ms. The silane depletion at the edge of the inter-electrode region was determined 500 ms after the rf pulse was initiated (inside the plasma pulse) and 500 ms before the plasma pulse (outside the plasma pulse) in all cases.

RESULTS

Thin Film Studies #1 - #6

Study #1 - Temperature of Silane Molecules in the Plasma Region

A possible complication to the interpretation of the square root of the intensity of the silane CARS peak being related only to the amount of silane present in the plasma region is the rotational temperature of the silane in the plasma. If the rotational and vibrational temperatures of

the silane were significantly changing with plasma pulse on-time, then both concentration and temperature contributions to differences in the peak height would have to be adequately addressed. Additionally, very large changes in the temperature of the plasma could affect the plasma and deposition chemical processes. Representative scans over the ν_1 , SiH, symmetric stretching band of silane are presented in Figure 5. These are of a 5ms 30W peak power plasma with other reactor conditions set at the initial conditions given in the Methodology Section. If the temperature were changing significantly, the peak would broaden and shift. Note that there is a depletion in signal with increasing pulse width, but the peak maximum remains at the same wavenumber shift. Calculations based on the paper "Silane Thermometry in Radio-frequency Discharge Plasmas by CARS Spectroscopy",¹⁷ indicate that a 200-300 K increase in the rotational temperature would shift the peak maximum by more than one cm^{-1} . Since the peaks inside the plasma, outside the plasma, and in the absence of a plasma remained at essentially the same position, no significant change in the temperature of the silane in the plasma was found. CARS spectra taken at other plasma powers and pulse widths gave similar results.

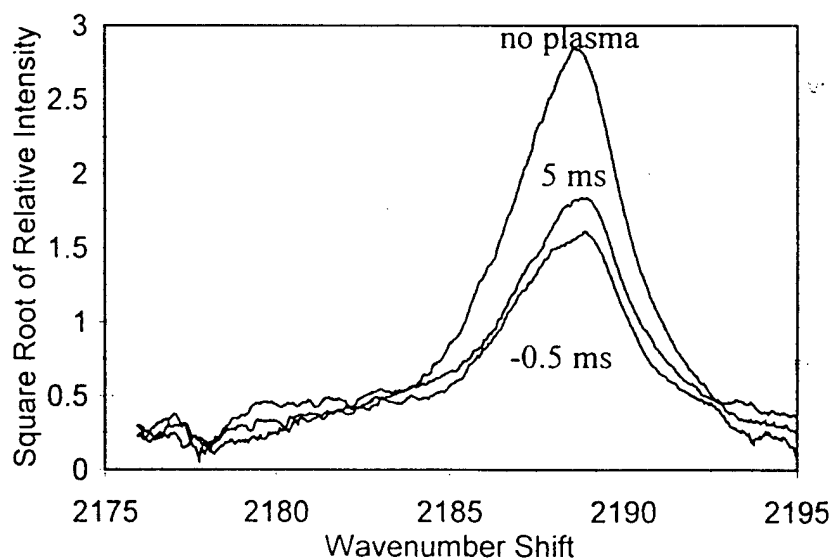


Figure 5. CARS Spectra of ν_1 of SiH_4 , Preplasma and at Various Delay Times.

Since the temperature of the silane is not increasing significantly, differences in the SiH/NH ratio of the deposited films are not likely a result of bulk gas phase temperature changes. Also thermal breakdown of the silane, at least at the flow rates and powers investigated, does not contribute to the species present in the plasma region or at the surface of the substrate.

Study #2 - CARS Determined Silane Depletion as a Function of Delay after the rf Pulse

One aspect of rf-PPECVD and PECVD that is difficult to monitor, is the path of the flow pattern taken by the reactants as they are introduced to the region between the electrodes. The flow geometry is important, as it describes the mixing that occurs between the reactants streaming out of the individual holes in the showerhead, and it is also related to the amount of time that the reactants spend in the plasma region. If the speed of the reactants leaving the showerhead has a velocity primarily in the forward direction, then the reactants will propagate largely in the direction of the substrate, at least in the upper half of the inter-electrode region. Calculations given in Appendix C, based on the ideal gas law, show that for a total flow of 53sccm, the speed of the flow exiting the holes is 1.4 mm/ms. The CARS sampling region is 9mm below the upper shower head electrode, and at that speed, a reactant molecule would move more than 15 mm in only 10 ms, well beyond the CARS probe region. That is a molecule leaving the hole, whose velocity is entirely in the forward direction, would require 6.5 ms to travel 9mm in the direction of the other electrode, and a total time of about 15 ms to travel the entire 22 mm to the opposite electrode. If the speed were divided among other velocity components, then the time would be longer. The depletion signal observed by the CARS measurements is then a function of the velocity component in the forward direction.

The CARS-determined silane concentrations as a function of power at the delay times

noted are given in Figure 6 for a 25 watt Plasma, and in Figure 7 for plasmas at several different peak powers and pulse widths. Note that for the 2ms rf pulse width, at all powers, the concentration of the silane continues to decrease for 2 ms after the completion of the rf pulse. For the longer rf pulse widths, the concentration of silane increased for all the delay intervals including 2ms after the end of the pulse.

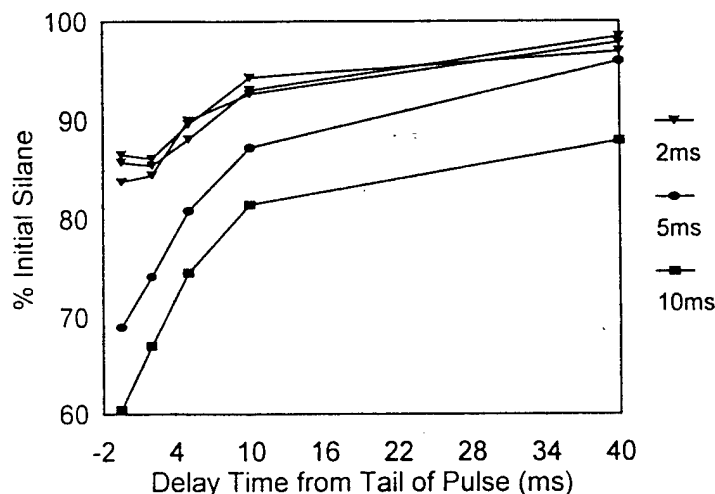


Figure 6. CARS Determined Silane Depletions for rf Pulse Widths at Specific Delay Times after the Pulse.

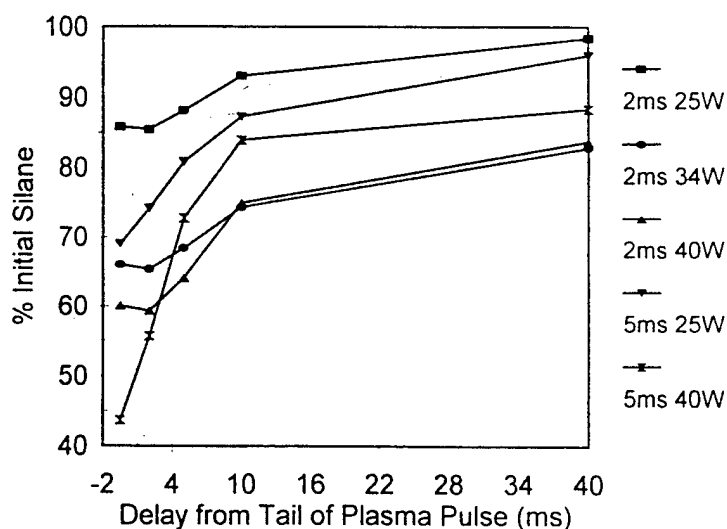


Figure 7. CARS Determined Silane Concentrations as a Function of Power at Specific Delays for 2 and 5 ms Pulse Widths.

Also for the studies performed with 25W peak power, the depletion at 0.5 ms inside of the tail end of the plasma increased from 14% depletion for the 2ms rf pulse, to 31% depletion for the 5 ms pulsed plasma, but only to 41% for the 10 ms pulsed plasma. Measurements on a continuous 25W plasma gave around 60% depletion of silane.

These results can be explained by the fact that the reactant gas velocity is primarily in the forward direction as in a segregated flow situation. As seen in figure 8, for the 2 ms rf pulse width case, the silane reactant "plug", initially between the electrodes when the plasma is pulsed on, does not move past the point where the CARS beams focus. In fact, the extra 0.5 ms of plasma on time, causes the silane to be depleted more than the measured value at 0.5 ms before the end of the rf pulse. This is seen as a lowering in the silane concentration even 2ms after the pulse. At the 2ms delay time, the top of the plug, which was initially in the inter-electrode region, would have moved a total of 6mm, and thus the plug that was exposed to a total plasma time of 2 ms would be probed by the CARS lasers. However, if there were no mixing at all, then at a delay of 10ms, the silane concentration should have returned to 0% depletion, and it does not.

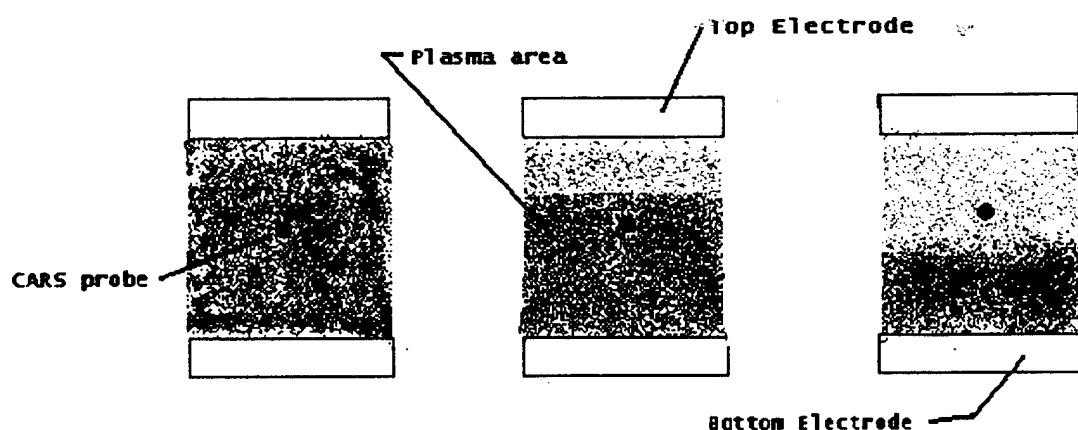


Figure 8. Schematic of Reactant Flow and Depletion as a Function of rf Pulse Width.

In the 5 ms pulse width case, the silane reactant plug initially between the electrodes, again does not move completely out of the CARS beam probe during the pulse-on time, but at a total of 7 ms, 5 ms of pulse-on time and 2ms delay, the initial plug has moved out of the CARS beam probing region. Lastly, for the 10 ms pulse width plasma, the initial plug has moved out past the CARS probe region, as the time it takes to reach the probe position is only about 6.5 ms. So effectively, the concentration of the silane probed by the plasma should be for a 6.5 ms exposure. Taking the ratio $6.5/5$ x the depletion for the 5ms exposure, the exposure depletion is approximately 42% which is about what was measured.

It is interesting that the 10ms pulsed plasma returns only to 87% of the initial silane value rather than the >95% return for the 2 and 5ms, 25W plasmas. This could be a result of the production of high vapor pressure products, such as H_2 , which are difficult to pump out of the reaction chamber. The fact that the 2ms pulsed plasmas at all the different powers investigated gave a decrease in the concentration 2 ms after the rf pulse had ended, whereas for the 5 ms pulse width plasmas at both powers investigated, there is simply a steady increase in the concentration of silane after the plasma was turned off, supports the idea of a segregated flow.

Study #3 - The Influence of rf Power on Thin Film Properties and Silane Depletion

For the pulsed plasmas with a rf pulse-width of 2 ms, the % depletion of the silane as measured 0.5ms from the end of the rf pulse, at the 9mm mark below the upper electrode, increased with increasing power. For the thin films, as the power increased there was generally a decrease in the SiH/NH ratio although the 25 watt plasma gave a lower ratio than the 34 watt plasma. The trend in the stress was similar for the 2ms pulse width, but opposite for the 5ms pulsed plasmas. The values are given in Table 2.

TABLE 2. Thin Film Parameters and Silane Depletion as a Function of rf Peak Power

Peak Power(W)	Pulse Width(ms)	% Silane Depletion	SiH/NH Ratio	Stress (dynes/cm ²)	Atomic % Si N O			Depostn. (nm/min)	Index n
25	2	14	4.8	1223 Compr.	75	18	7	2.4	2.1
34	2	34	5.8	1340 Compr.	54	34	12	2.8	2.1
40	2	40	4.6	98 Compr.	42	37	21	2.9	2.1
30	5	-	8.6	335 Tensile	49	31	20	5.6	2.0
40	5	56	6.1	1422 Compr.	46	29	25	8.3	2.0

The data indicate that at moderately low power, the film content is rich in hydrogen with more hydrogen attached to the silane than the nitrogen, and at the high power relatively less hydrogen is attached to the silane than at the lower powers. Part of this trend can be explained by a change in the silicon content of the films. The percentage of silicon in the film decreases with increasing power for all cases examined. If there is proportionally less silicon and more nitrogen in the films, then the number of NH bonds should increase relative to the number of SiH bonds. This is also reflected in the index of refraction which decreases very slightly with higher power.

However, the decrease in silicon content is not expected based on the CARS measurements of the silane depletion. According to these results, more silane has broken down in the gas phase and is available for incorporation into the thin films. This contradiction suggests that either the gas phase chemistry does not play a significant role in the formation of the thin films, or that the ammonia has similarly been depleted or perhaps depleted more. Evidence for the latter case is derived from the fact that the deposition rate increased with increasing power. More silane was broken down and available for reaction, and so more ammonia or some oxygen containing

compound must have been available as well.

Study #4 - The Influence of rf Pulse Width on the Thin Film Properties and Silane Depletion

The experiments that determined the effect of pulse width were performed at 2,5 and 10 ms pulse widths and in a continuous plasma at a peak power of 25 and 40 watts. The % depletion of silane was determined by the CARS measured depletion at a time of 0.5 ms from the tail end of the pulse. The thin film parameters and depletions are given in Table 3. For the deposition rate there are two values. One value is obtained by taking the film thickness and dividing by the total time (overall). The other value is obtained by dividing by only the total plasma on-time instead of the total time.

TABLE 3. Thin Film Properties and Silane Depletion as a Function of rf Pulsewidth

Pulse Width (ms)	Peak Pwr (W)	% Silane Depletion	SiH/NH Ratio	Stress (dynes/cm ²)	Atomic % Si N O			Depostn(nm/min) overall	on time
2	25	14	4.8	1223 Compr.	¹ 75	18	7	2.4	120
5	25	31	5.0	253 Compr.	57	30	13	5.8	120
10	25	41	5.3	425 Tensile	69	23	8	13	130
continuous	25	65	4.1	366 Compr.	29	41	30	74	74
2	40	35	4.6	98 Compr.	-	-	-	3.0	145
5	40	58	6.1	1422 Compr.	46	29	25	10.1	202
10	40	62	² 6.5	² 1526 Compr.	43	² 18	² 39	18.5	185

¹ for very thin films, the X-ray may be contaminated by bulk Si

² average of two different runs

Here the amount of silane present in the plasma region decreased with increasing pulse width.

Increasing the pulse width from 2 to 5 ms approximately doubled the observed silane depletion in the 25 watt case. However, the CARS-determined silane depletion increased by only about 30% when the pulse width was increased from 5ms to 10 ms.

The increase in CARS measured silane depletion with pulse width for the 2 and 5 ms pulse width is in good agreement with the rate of deposition as determined by the thickness measurements. The rate of deposition and total mass deposited increased nearly three times while the total silane was depleted by more than a factor of two in going from the 2 to 5 ms pulse width. The rate of deposition nearly doubled in going from a 5 to 10 ms pulse width, but the silane depletion changed only by a small factor of the expected rate. Dividing the deposited thickness by the total time that the plasma was on shows that there is generally a slight increase in deposition per "on time" with pulse width; however the continuous plasma yielded a deposition per on time lower than any of the pulsed plasma cases, just slightly above one-half of the deposition rate per on time observed for the 25W 10 ms plasma.

The Si H to NH ratio increased with increasing pulse width, but then decreased for the continuous plasma. The ratio for the continuous plasma was below that of any of the pulsed cases with the same peak power. The percentage of silicon in the thin films fluctuates with increasing pulse width. First it decreases and then increases. The stress also seems to oscillate with increasing pulse width.

Taken together, the stress, the atomic composition, the FTIR, and deposition rate suggest that changing the rf pulsed duration caused a difference in the film properties and in the silane depletion. For the continuous plasma, the depletion reached about 65%, and the film contained the lowest amount of SiH bonds relative to NH bonds. Based on the linear increase in depletion

rate with pulse width going from 2 to 5 ms, 65% and 100% depletion should have occurred a 10 ms pulse width, but as explained above it does not and should not because the CARS beams probe a region which corresponds to just a 6.5 ms pulse time. One conclusion still, is that the nature of the reactive species is changing since the gases below the CARS region are coming closer to the substrate and mixing with gases reflected off of the substrate surface while the plasma pulse is still on. With the wide variance in the trends in the thin film properties with increasing pulse width, it is difficult to interpret the results from this information.

Study #5 - Changes in the Thin Film Properties and Silane Depletion with Showerhead Pattern

The shower head pattern on the upper electrode was changed for several powers and pulse widths. The silane depletion in the plasma was measured with the CARS spectrometer 0.5 ms before the tail end of the pulse. The thin films deposited on the silicon substrate for the various shower heads and conditions were analyzed to determine their properties. The properties and silane depletions are given in Table 4.

Table 4. Thin Film Parameters as a Function of Showerhead Type at 175°C for 10Hz Pulsed Plasma and 75 Minute Deposition Time






Peak Pwr	Pulse W (ms)	Shower head	Film Wt.(g)	Depostn. ($\mu\text{g/s}$)	Stress dynes/cm ²	Thickness Cntr (μm)	Atomic %			SiH/NH Ratio	Silane Depln.	n
							Si	N	O			
30	5	Asym	0.0072	1.6	1636 Compr.	0.421	54	29	17	6.3?	24%	2.0
30	5	Square	0.0092	2.0	2098 Compr.	0.423	57	27	19	9.5	26	2.1
30	5	Radial	*0.102	1.4			49	31	20	8.6	-	2.0
40	2	Asym.	0.0032	0.71	1909 Compr.	0.169	-	-	-	7.9	12	2.1
40	2	Square	0.0042	0.93	1808 Compr.	0.227	-	-	-	7.4	16	2.0
40	2	Square	0.0046	1.0	1682 Compr.	0.253	-	-	-	5.5	-	2.0
40	2	Radial	0.0045	1.0	98 Compr.	0.220	-	-	-	4.6	35	2.1
40	5	Asym.	0.0126	2.8	104 Compr.	0.664	51	20	29	9.5	25	2.1
40	5	Square	0.0107	2.4	1886 Compr.	0.619	46	27	27	10.0	38	2.0
40	5	Radial	0.0123	2.7	1422 Compr.	0.670?	46	29	25	6.1	56	2.0
40	10	Asym.	0.0255	5.7	416 Compr.	1.20	48	12	40	8.9	42	2.0
40	10	Square	0.0257	5.7	1076 Compr.	1.38	47	23	30	7.3	56	2.0
40	10	Radial	0.0252	5.6	1503 Compr.	1.39	43	20	37	7.0	60	2.1
40	10	Radial	0.0170	3.8	1555 Compr.	1.35	43	16	41	6.1?	-	2.0

*Deposition Time Estimated as 120 min.

Two results that stand out are the thickness and deposition rate. Note that at a particular peak power and pulse width, the deposition rate is fairly uniform as is the thickness at the center of the Si substrate. The fact that the center thickness is independent of showerhead type is unexpected, especially based on the visual properties of the thin films. In the case of the

asymmetric shower head, for all but the 2ms rf pulse width case, the films show a heavy colored banding on the silicon substrate. See Figures 9a and 9b for the digital photographs of the Si substrates with the silicon nitride thin films deposited on them.

Wafer Summary

					
ID	ISU0069	ISU0071	ISU0061	ISU0082	ISU0084
Date	04/17/01	04/20/01	3/1/01	08/16/01	8/24/01
Power (watts), pulse Wid. (ms)	30, 5	30, 5	30, 5	30, 5	30, 5
Head Type	Asymmetric	Radial	Radial	Radial	Radial
Temp Range, top TC (°C)	112-117, 54	196-199, 82	118-122, 60	138-141, 72	157-162, 98
Thickness: Center (μm)	0.4211	0.5051	0.6112	0.5352	0.5100
Weight of Film (g)	0.0072	0.0101	0.0102	0.0095	0.0094
Stress (dynes/cm ²)	1636 (compress.)	3313 (tensile)	355 (tensile)	95 (tensile)	781 (tensile)
X-ray: Si, N, O (at %)	54, 29, 17	62, 36, 1	49, 31, 20	55, 40, 5	
IR: SiH/NH peak area ratio	6.3	12.0	8.6	7.2	8.0
Index of Refraction (center)	2.0	2.3	2.0	1.9	2.0
%H as Si-H	82	90	86	84	85













					
ID	ISU0070	ISU0062	ISU0078	ISU0079	ISU0080
Date	04/19/01	03/13/01	07/20/01	07/24/01	07/31/01
Power (watts), pulse Wid. (ms)	30, 5	30, 5	30, 5	30, 5	30, 5
Head Type	Square	Square	Square	Square	Square
Temp Range, top TC (°C)	112-118, 54	127-136, 74	139-142, 65	160-162, 73	179-181, 85
Thickness: Center (μm)	0.423	0.893	0.501	0.587	0.566
Weight of Film (g)	0.0092	0.0176	0.0091	0.0095	0.0099
Stress (dynes/cm ²)	2098 (compress.)	508 (tensile)	300 (compress.)	137 (compress.)	1385 (tensile)
X-ray: Si, N, O (at %)	54, 27, 19	43, 38, 19	54, 38, 8	57, 37, 6	57, 41, 2
IR: SiH/NH peak area ratio	9.5	6.6	6.6	8.9	11.6
Index of Refraction (center)	2.1	2.1	2.0	2.0	2.0
%H as Si-H	87	83	82	86	89

Figure 9a. Visual Summary of Silicon Nitride Thin Films Deposited on Si Wafers.

							
ID	ISU0067	ISU0077	ISU0063	ISU0074	ISU0066	ISU0073	ISU0064
Date	4/5/01	7/12/01	3/19/01	5/18/01	3/22/01	5/12/01	03/19/01
Power (watts), pulse Wid. (ms)	40, 2	40, 2	40, 2	40, 2	40, 5	40, 5	40, 5
Head Type	Asymetric	Radial	Square	Square	Asymmetric	Radial	Square
Temp Range, top TC (°C)	112-114, 55	119-121, 50	122-124, 50	113-116, 52	114-118, 55	113-116, 50	118-120, 57
Thickness, Center (µm)	0.169	0.220	0.227	0.253	0.664	0.760	0.619
Weight of Film (g)	0.0032	0.0045	0.0042	0.0046	0.0126	0.0123	0.0107
Stress (dynes/cm ²)	1909 (compress.)	98 (compress.)	1808 (compress.)	1682 (compress.)	104 (compress.)	1422 (compress.)	1886 (compress.)
X-ray Si, N, O (at %)	—	—	—	—	51, 20, 29	46, 29, 25	46, 27, 27
IR SiH/NH peak area ratio	7.9	4.6	7.4	5.0	9.5	6.1	10.0
Index of Refraction (center)	2.1	2.1	2.0	2.0	2.1	2.0	2.1
%H as Si-H	85	77	84	78	87	81	88







						
ID	ISU0068	ISU0076	ISU0075	ISU0081	ISU0065	ISU0083
Date	04/12/01	07/10/01	06/07/01	08/07/01	03/21/01	08/17/01
Power (watts), pulse Wid. (ms)	40, 10	40, 10	40, 10	40, 10	40, 10	40, 10
Head Type	Asymmetric	Radial	Radial	Radial	Square	Square
Temp Range, top TC (°C)	112-115, 52	119-121, 57	110-118, 50	116-120, 55	114-118, 62	118-123, 65
Thickness, Center (µm)	1.196	1.400	1.385	1.350	2.518	1.378
Weight of Film (g)	0.0255	0.0249	0.0252	0.217	0.0404	0.0257
Stress (dynes/cm ²)	116 (compress.)	193 (tensile)	1503 (compress.)	1555 (compress.)	—	1076 (compress.)
X-ray Si, N, O (at %)	48, 12, 40	49, 18, 33	43, 20, 37	43, 16, 41	48, 30, 22	47, 23, 30
IR SiH/NH peak area ratio	8.9	8.9	7.0	6.1	7.1	7.3
Index of Refraction (center)	2.0	2.2	2.1	2.0	2.0	2.0
%H as Si-H	86	86	83	81	81	81

Figure 9b Visual Summary of Silicon Nitride Thin Films Deposited on Si Wafers.

The colored bands on the visual photographs do reflect the thickness contours. This can be seen by comparison to the thickness contours shown in Figures 10a - 10c. The contours were created by measuring thicknesses on a 0.5 cm by 0.5 cm grid all across the surface of selected

wafers using the Filmetrics backscattering instrument. Note that the notch in the Si substrate is centered on the grid in the contour diagram at (0, 12.5).

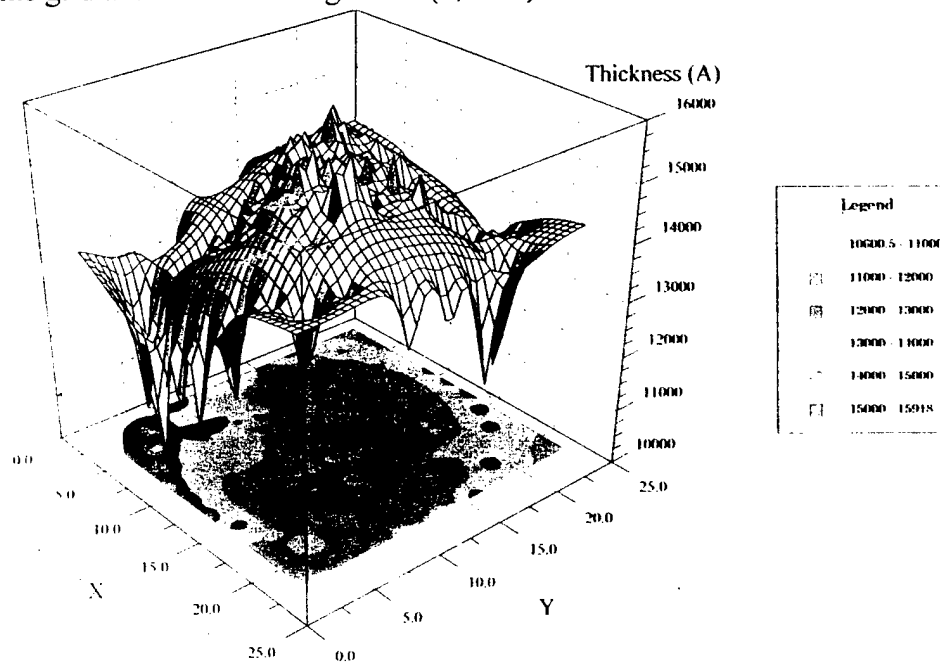


Figure 10a. Contour Diagram of Thin Film Thickness Deposited from the Square Showerhead at 40W and 10 ms rf Pulse.

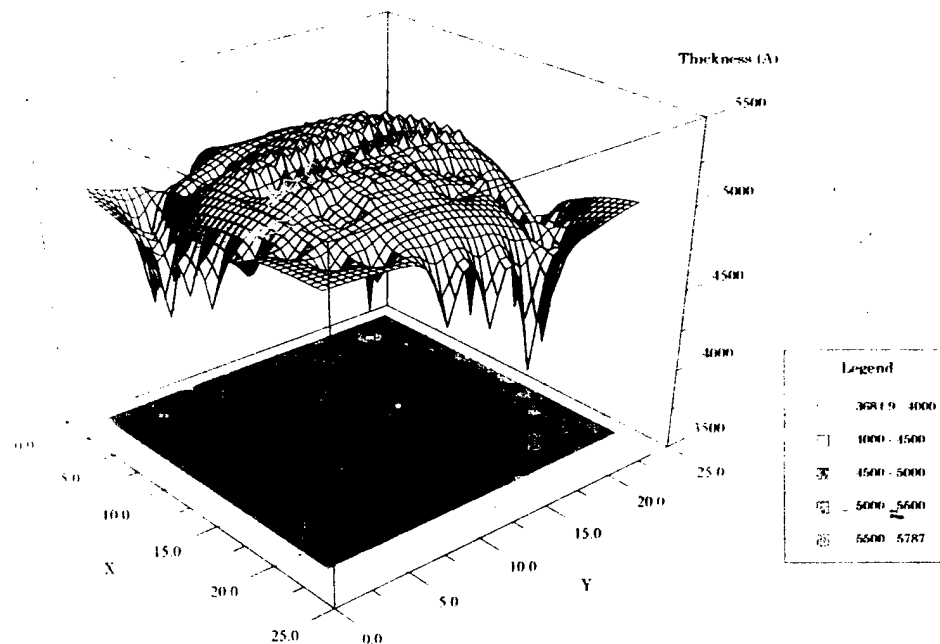


Figure 10b. Contour Diagram of Thin Film Thickness Deposited from the Radial Showerhead at 30W and 5 ms rf Pulse.

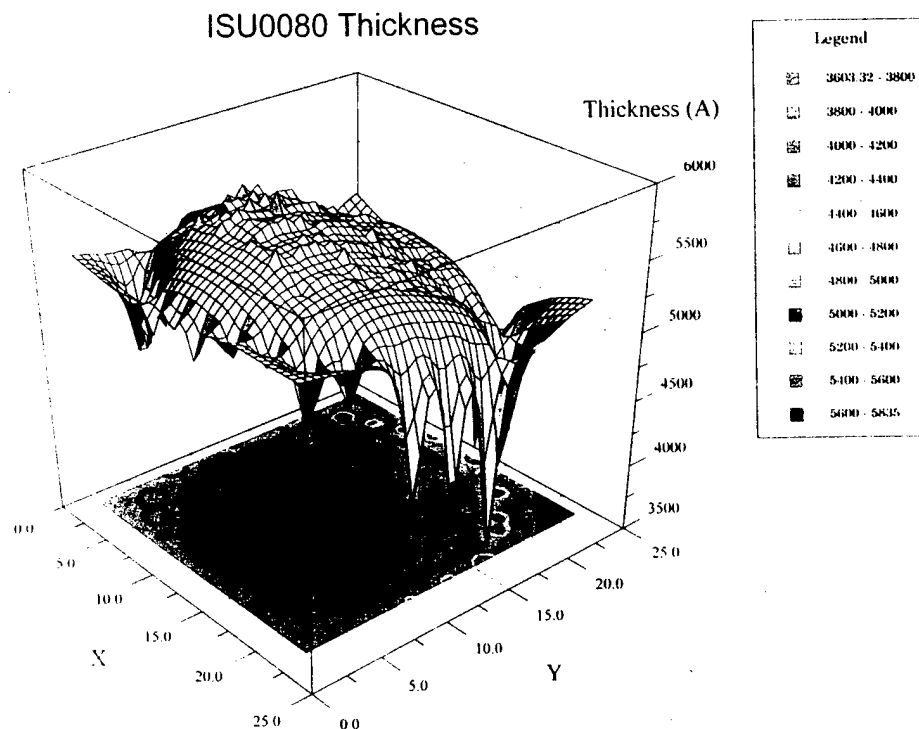


Figure 10c Contour Diagram of Thin Film Thickness Deposited from the Square Showerhead at 30 W and 5 ms rf Pulse.

The silane depletion is interesting. The depletion from the asymmetric head is always the lowest and the radial head always gives the highest depletion, based on the data given. This is likely a result of velocity components in directions other than the forward direction. The asymmetric head has 412 holes some of which are fairly close to one another. This could cause significant mixing as the flow leaves the head. This could allow gases from outside the plasma region to enter into the inter-electrode region at times after the plasma pulse has started. This would effectively dilute the plasma depleted silane with fresh silane, which probably would result in a difference in the gas phase chemistry, and the distribution across the substrate surface would be more non-uniform. For the square head, 591 holes, and the radial head, 241 holes, the spacing between holes is uniformly distributed and mixing is less likely.

It is also interesting to see that for the square head and radial heads, it appears that if the % depletion of silane is less than 40%, the wafers are visually fairly uniform. Above the 40% mark the wafers become very banded indicating a high variance in the thickness. The asymmetric head bucks the trend, as the thin film deposited with the asymmetric head was very banded even when the silane depletion measured by CARS was only 24%. As mentioned previously, this could be due to the increased mixing in the asymmetric head causing swirling flow patterns which might cause non-uniform depositions on the wafer surface. The deposition rate and the silicon content of the films don't change significantly, just the thickness pattern on the surface.

Overall, this study indicates that the flow pattern resulting from the use of a particular head can affect the uniformity of the thickness on the wafer surface. Additionally, it suggests that the silane depletion also affects the uniformity. Reasons for this might be that the thickness of the film becomes so large that the flow is affected, or the silicon % becomes so low that the films have different friction properties and are more affected by turbulence in the flows. In any case it appears that the gas phase chemistry is affecting the deposition properties.

Study # 6 - Influence of Substrate Temperature on Silane Depletion and Thin Film Properties

The role of the temperature of the silicon substrate in the deposition of the thin films of silicon nitride was explored in this part of the study. Both square and radial showerheads were used to introduce the gases into the rf-PPECVD reactor. In all runs the initial parameters besides substrate temperature were used, and the power was set at 30W peak power for a 5 ms rf pulse. The temperature of the lower electrode was changed by changing the current supplied to the resistive ring heater incorporated into the lower electrode. The temperature of the upper electrode was not maintained at a particular level, but was kept below 100°C. The silane

depletion value was obtained at 0.5 ms from the tail end of the 5ms rf pulse. Information on the film properties and silane depletion for the temperature changes is given in Table 5.

Table 5. Thin Film Parameters and Silane Depletion as a Function of Substrate Temperature for 5 ms rf pulse at 30 Watts Peak Power

Shower head	Wafer No.	Temp. °C	Film Wt.(g)	Depostn. (µg/s)	Stress Dynes/cm ²	Thick. Cntr. (µm)	Atomic %			SiH/NH ratio	Silane Depln.	n
Square	70	175	0.0092	2.0	2098 Compr.	0.423	54	27	19	9.5	15 %	2.1
Square	78	200	0.0091	2.0	300 Compr.	0.501	54	38	8	6.6	37	2.0
Square	79	220	0.0095	2.1	137 Compr.	0.587	57	37	6	8.9	-	2.0
Square	80	240	0.0099	2.2	1385 Tensile	0.566	57	41	2	11.6	36	2.0
*Radial	61	175	0.0102	1.4	broken	0.611	49	31	20	8.6	38	2.0
Radial	82	200	0.0095	2.1	95 Tensile	0.535	55	40	5	7.2	38	1.9
Radial	84	220	0.0094	2.1	781 Tensile	0.510	55	41	4	8.0	39	2.0
Radial	71	260	0.0101	2.2	3213 Tensile	0.505	62	36	1	12.0	37	2.3

* The film deposition time was estimated at 2 hr. The rest were 75 min. This Si wafer was broken.

From the information given in this table, three results stand out. The amount of oxygen, which is present in the thin films, decreases greatly with increasing temperature. Based on the small change in film weight and the small change in the Si atomic % (at least for the square shower head), it appears that the oxygen was incorporated into the films instead of the nitrogen. In the case of the square shower head, the stress changed from 2100 dynes/cm² (compressive) to 1385 dynes/cm² (tensile) when the temperature increased from 166 to 230°C. For the radial head deposited films, the most tensile value, 3213 dynes/cm² occurred at the highest value of the temp., 248°C. This may be related to the change in atomic composition mentioned previously.

Another interesting trend in the film parameters occurred in the case of the SiH/NH ratio as determined by the area of the vibrational transition peaks corresponding to these moieties in the FTIR spectrum. The ratio was relatively high at the lowest deposition temperatures, as the temperature was increased only 20°C, the ratio decreased to its lowest value. Subsequent increases in the temperature resulted in an increase in the SiH/NH ratio with the highest value occurring at the highest substrate temperature. A possible explanation for the initial drop in the ratio, with a subsequent increase may be due to the fact that much more nitrogen and much less oxygen is incorporated into the films for the first 20°C increase, thus increasing the amount of NH present. However, as the temperature is increased further, reactions on the surface result in less NH and more SiH being present in the final film.

During the depositions at the various temperatures, CARS was used to monitor the depletion of silane in the plasma region. At the higher temperatures, the CARS signal was more difficult to monitor due to a decrease in the amount of reactants present in the chamber at the higher temperatures as the pressure and volume are held constant. An ideal gas law calculation gives a 15% decrease in the moles of gas present in the chamber at 250°C from the moles present at 170°C. Representative CARS determined silane depletions for both showerhead types at several substrate temperatures given in the table show that the silane depletion in the plasma region is independent of the substrate temperature. With a single exception (square head, 175°C), the silane was depleted by between 36 and 39%. Furthermore as seen in Figure 11, the silane depletion at all delay times after the rf pulse was very similar at all substrate temperatures again with primarily that same single exception.

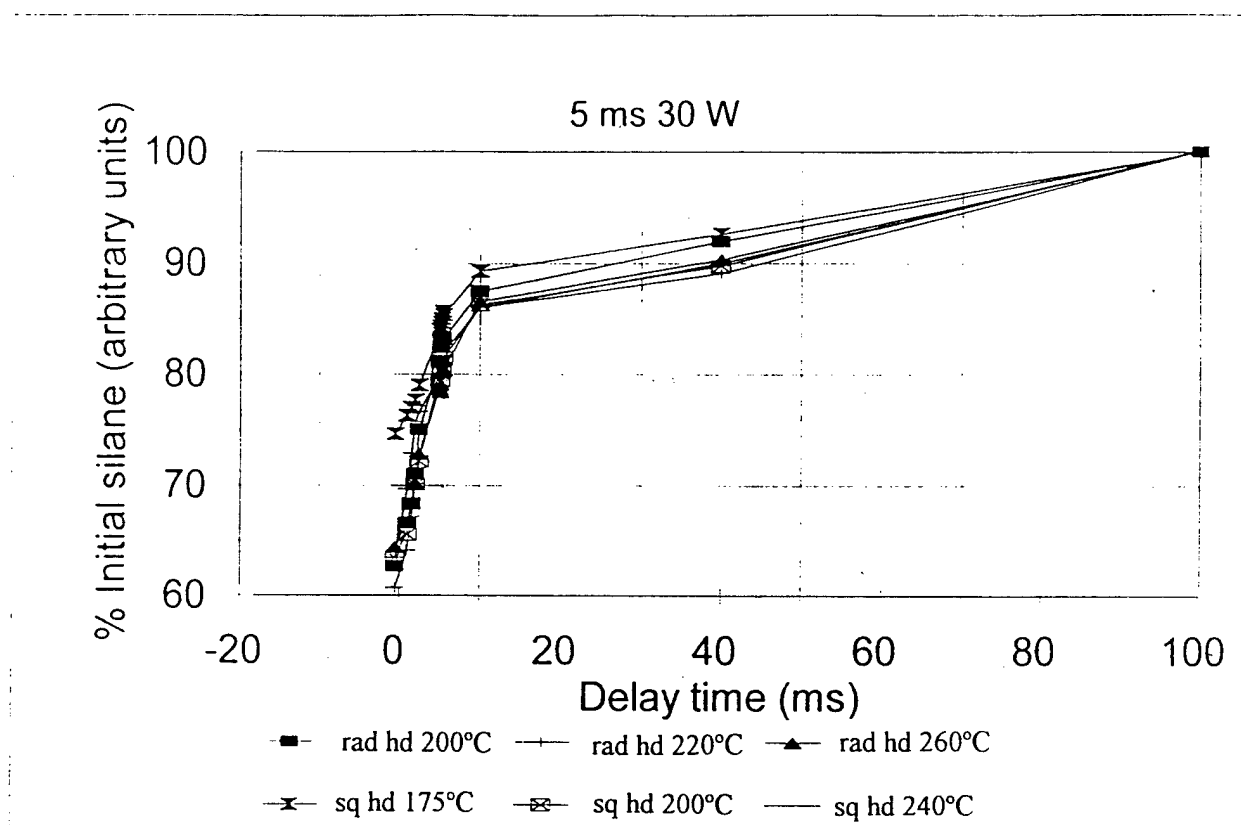


Figure 11 CARS Determined Depletion of Silane as a Function of Temperature at Several Delay Times after the Pulse

The digital photographs of the thin films deposited at these higher temperatures are also given in Figures 9a and 9b. The films deposited with the square shower head were more uniform than with the radial head, but for both shower heads, the thickness uniformity initially decreased with increasing temperature, but at 200°C, the uniformity improved. For the square head the thin film thickness uniformity was also good at 240°C. The uniformity of the thin film deposited from the radial head was much worse at 260°C.

In the previous study at 175°C it appeared that uniform films were deposited if the silane depletion was held below 40%, at least for the radial and square heads. That is apparently not the case here, suggesting that the uniformity is due to both surface and gas phase properties. The temperature mostly affected the surface chemistry, (the oxygen content of the films decreased) while the silane depletion remained the same.

Particle Studies #7 - #11

Study #7 - Studies Related to the Calibration of the Pulsed Sampling Mass Spectrometry

This part of the project involved verifying whether or not the pulsed sampling methodology, developed to sample the plasma at various delay times relative to the rf pulse, would work. One measure of this involved determining if a calibration curve could be made from the using the pulsed sampling mass spectrometer. Initially argon was used for the calibration gas. The argon entered the rf-PPECVD reactor through two entrance lines which were tested separately. The argon entered through the port near the laser windows and through the showerhead via the flow line which is typically used for silane. The calibration curves are given in Figure 12. Note that a different calibration curve is obtained depending on which port the argon enters. This is expected based on the placement of the fuel injector valve at the edge of the inter-electrode region. Argon which comes from the showerhead directly reaches the sampling valve, but entrance through the ports near the laser windows means that the argon can be pumped away before interacting with the sampling valve.

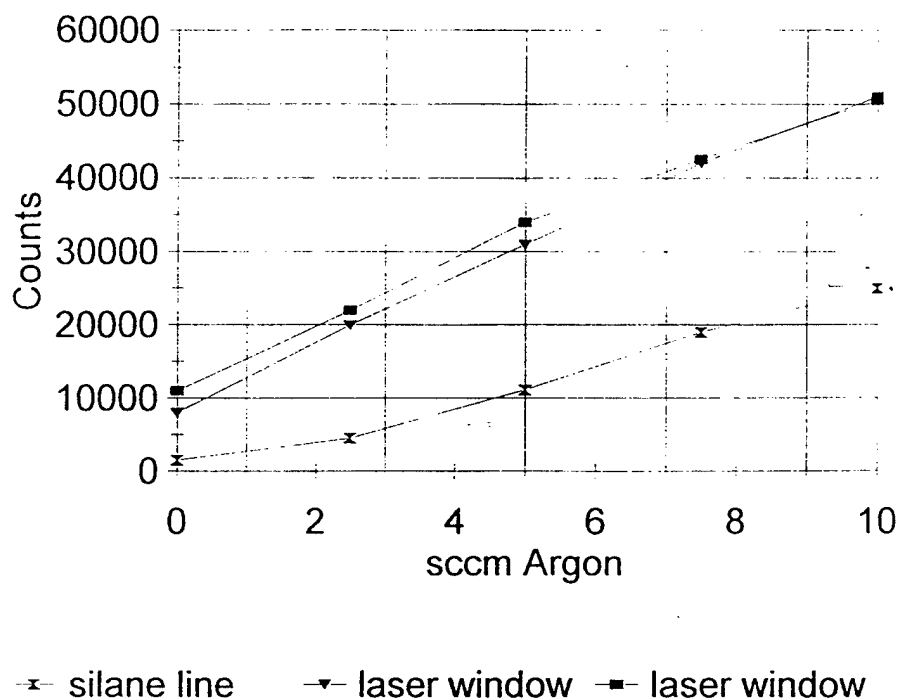


Figure 12. Argon Calibration Curves Obtained from Pulsed Sampling Mass Spectrometry

A similar experiment was attempted with silane. Silane is extremely reactive with oxygen and water, and its calibration represents the ability of the sampling method to be used with highly reactive gases. Also the effect of the signal amplifier was tested here as well. The results are presented in Figure 13. Note that there appears to be an anomaly at a flow of 7.5 sccm in all cases, but generally less counts at the mass spectrometer were observed for a lower flow of silane. The effect of changing the signal amplifier is seen as a change in the magnitude of the signal for all flows, but the slope of the calibration curve remained fairly constant. It is difficult to completely rid transfer lines and chamber walls of oxygen and water, and this figure indicates that for the level of leakage present in the pulsed sampling mass spectrometry system, a calibration is possible if some precautions are taken.

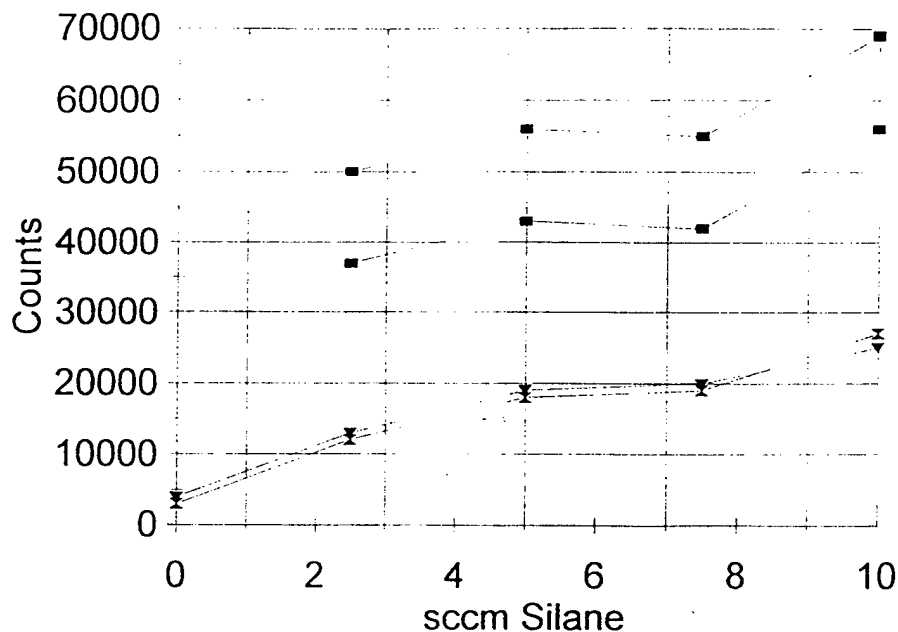


Figure 13. Silane Calibration Curves Obtained from Pulsed Sampling Mass Spectrometry with Variation in the Signal Amplifier.

Study #8 - Comparison of the Silane Level in the Inter-electrode Region Measured by CARS

Spectroscopy and Pulsed Sampling Mass Spectrometry

Studies here also involved verification that pulsed sampling MS gave results which were close to values measured by other ways. The problems with using CARS for the particle studies was problems with pulsing the laser at repetition rates less than 5 Hz and due to problems with particles coating out on the laser windows. However, for shorter pulse widths and 10Hz repetition rates CARS works well. Thus the PSMS and CARS measured silane levels can be compared in a 25 watt peak power plasma for pulse widths on the order of a few milliseconds.

One consideration that must be accounted for is that the pulsed sampling on the mass spectrometer must be longer than 5 ms in duration and probably more like 10 ms. The CARS

samples in just 6 ns. Thus CARS samples instantaneously compared to pulsed sampling mass spectrometry. In order to compare the mass spectrometric results to CARS spectroscopic results, an average between a sample taken during the pulse and one taken 10 ms later should be used. This average value is a better value to use to compare the CARS measured silane depletion to the silane depletions measured with PSMS.

Several 25 watt pulsed plasmas, with the normal initial parameters and pulse widths of 2, 5, and 10 ms and a 25 watt continuous plasma were used for the comparison. The fuel injector sampling valve for the mass spectrometer had a pulse width of 10 ms. The results of the comparison are given in Table 6.

Table 6. Comparison of CARS Measured and Pulsed Sampling MS Measured Silane Depletions in a 25 W Peak Power Pulsed Plasma

rf Pulse Width(ms)	CARS Determined % Silane Depltn. in Pulse	CARS Determined Averaged % Silane Depltn.	Pulsed MS Determined % Silane Depltn.
2	17	15	5
5	30	17	19
10	41	22	26
continuous	58	60	60

The results are not in complete agreement. The worst case occurred for the 2 ms rf pulse width. The continuous plasma results were in very good agreement. Some disagreement was expected since the CARS method probes the silane concentration in the center of the inter-electrode region, and the PSMS method probes the region at the edge of the inter-electrode region at a slightly lower position.

Study #9 - Effect of rf Power on the Silane Depletion and on the Particle Properties

The effect of increasing the rf power on the silane depletion in the inter-electrode region for a continuous plasma has been well documented. A study like this then serves as another measure to test the validity of the pulsed sampling mass spectrometer instrument. The results of this study are given in Figure 14 for the flow rates and conditions other than pulse width and power given as initial reactor conditions.

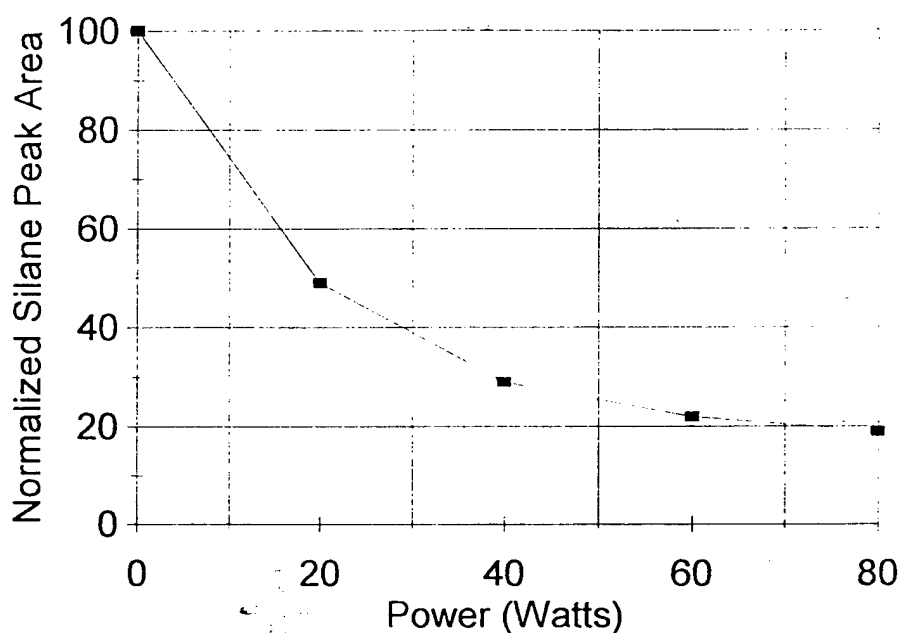


Figure 14. Pulsed Sampling MS Determined Silane Depletion as a Function of Continuous rf Power.

Note that the silane level decreases with increasing rf power as expected. The largest rate of depletion occurs for the first 20 watts of power and the rate of silane depletion with increasing power becomes less at higher powers. The silane likely reaches some equilibrium value at high rf power where the silane recombination processes happen on the same time scale as the break down

process. These depletion results are in good agreements with those reported by Smith et al.²

Based on the above results and the results of Studies 7-9, pulsed sampling MS was used to determine the silane depletions in a pulsed rf plasma used to make silicon nitride micro and nano particles. The first set of studies examined the effect of rf power on the silane depletion and the resulting particles in a pulsed rf plasma. The conditions were essentially the initial conditions given in the Methodology section for flow rate, showerhead type, rf frequency, etc. except that the power was varied for two different rf pulsing scenarios. The results are given in Table 7.

Table 7. Effect of rf Power on Silane Depletion and Silicon Nitride Particle Size and Composition.

Pwr. (W)	Pulse-on Time (s)	Pulse-off Time (s)	Atomic %			Particle Size (μm)	MS Pulse Width (s)	% Silane Depletion	
			Si	N	O			200ms in	500ms before
30	2.0	2.0	43	12	45	0.2	0.1	33	22
40	2.0	2.0	46	21	34	0.2-0.4	0.1	61	51
50	2.0	2.0	25	8	67	0.2-0.4	0.1	64	53
20	0.2	2.0	46	26	28	0.15	0.1	30	15
40	0.2	2.0	44	54	15	0.1-0.2	0.1	55	30

All particle sizes reported here are based on a survey of several regions of the particles collected from the rf-PPECVD reactor after deposition had occurred. In most cases there were larger species present, collections of smaller particles stuck together such that they made a larger agglomerate. The agglomerates were often as large as a micron in diameter, but they always appeared to be made up of the smaller spherically shaped particles. The sizes reported in the table are the sizes of the smaller particles not the agglomerates. Samples of SEM micrographs of the particles are given in Figures 15a and 15b.



Figure 15a. SEM Micrograph of Silicon Nitride Particles Showing Agglomerates.

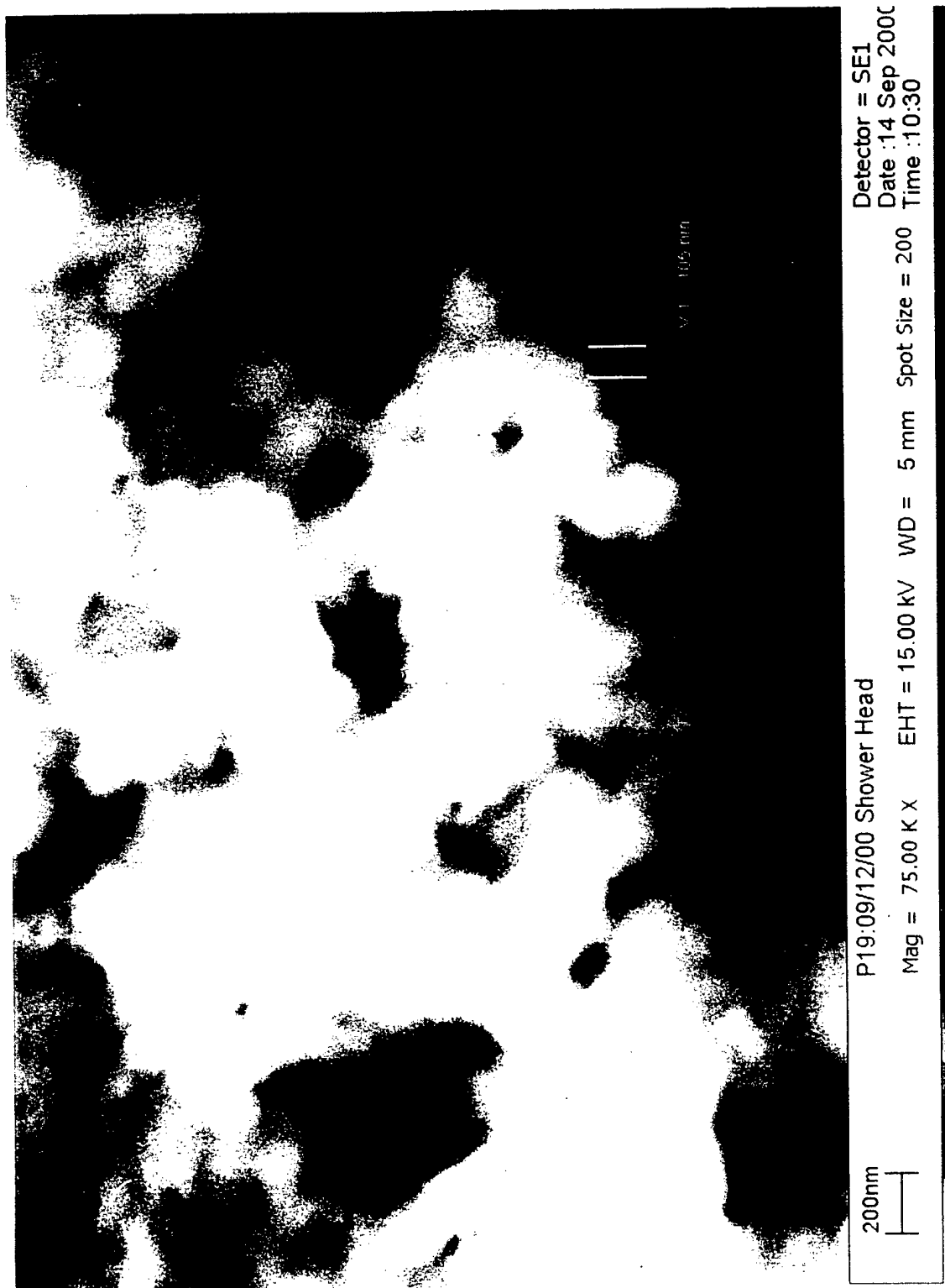


Figure 15b SEM Micrograph of Silicon Nitride Particles Showing Cases without Significant Agglomeration

As mentioned in the Methodology section, the atomic composition of the particles appeared to change with time or length of exposure to air. This was not the case for the thin films. The values reported in the table reflect varying times of exposure to air and therefore are difficult to interpret. If one assumes that the oxygen is incorporated into the particles at the expense of nitrogen incorporation, then the % silicon should not be affected by length of exposure to air. This appears to be the case for the examples listed in Table 7.

Examining the particle size information, in Table 7, there seems to be a direct relationship between the peak power and the size of the particles. That is, the smallest particles were created at lower peak powers. Again this particle size is based on the diameter of the smallest particles which, in some cases, were packed together to form a larger agglomerate. This result may be due to an increase in the temperature of the species which make up the particles at higher temperature, allowing the species to overcome a surface activation barrier, come together, and form larger particles at a higher temperature. Alternately, there are likely higher amounts and more types of reactive species present at a higher power, several of which lead to the formation of larger particles.

The depletion results support this last suggestion since the depletion of the silane reactant gas increased both in the rf-pulse and outside of the rf-pulse with increasing power. Note that the mass spectrometer was able to measure a difference in the reactant depletion during the rf pulse as opposed to when it was off. A greater depletion is observed at higher powers in the pulsed rf plasmas. A larger depletion is observed 200 ms inside of the pulse than 500 ms before the next pulse. A larger range of particle sizes is observed in the higher powered pulsed plasmas.

Study #10 - Influence of rf Pulse Width on Silane Depletion and Particle Properties

The information collected on the effect of rf pulse width (see Table 8) is still largely preliminary. It purports to show the effect of pulse width on the silane depletion and the particle size. However, there was a difficulty in picking the sampling times. They were different and the MS pulse width also varied in one case. Thus it is difficult to draw conclusions from the silane depletion values listed.

Table 8. The Importance of rf Pulse Width on Silane Depletion and Silicon Nitride Particle Size.

Pwr. (W)	Pulse-on Time (s)	Pulse-off Time (s)	MS Pulse Width (s)	Sampling Time (s) in pulse	Sampling Time (s) before pulse	% Silane Depletion in pulse	% Silane Depletion before pulse	Particle Size(μm)
40	0.2	2.0	0.1	0.2	1.0	55	38	0.1-0.2
40	0.5	2.0	0.1	0.2	1.0	50	30	0.1-0.2
40	1.0	2.0	0.2	0.2	0.5	42	22	-
40	2.0	2.0	0.1	0.5	0.5	61	51	0.2-0.4

The particle size, on the other hand, should not be affected by the mass spectrum parameters, and from the limited information presented, it appears that the particle size also increased slightly with increasing pulse width. The reasons for this may be similar to the reasons given for the increase in particle size noted for an increase in power. The smaller particles may become more heated or there are more and different types of species present at longer pulse widths which allow the formation of larger particles.

Study # 11 - Influence of the Composition of Silane and Ammonia in the Reactant Flow on Silane Depletion and Silicon Nitride Particle Properties

The results from studies of the effect of reactant flow composition on the silane depletion, particle size, and atomic composition are detailed in Table 9. The initial reactor parameters were

used except as follows. The peak power was 40 watts, the temperature was not regulated for all of the studies given in the table, and the overall flow also varied somewhat. Again as in the previous tables of this section, the particle size is based on the smallest particles which in many cases were part of a larger agglomerate.

Table 9. Effect of Silane and Ammonia Flow on Silane Depletion in the Plasma and Silicon Nitride Particle Size and Composition in a 40W Pulsed Plasma Pulsed on and off for 2s.

Reactant Flow Compos.(%)			Particle Size (mm)	Atomic %			MS Pulse Width (s)	Silane Depletion 500ms	
Silane	Ammonia	Nitrogen		Si	N	O		in rf-pulse	before pulse
20	20	60	0.2 - 0.4 ^a	46	21	34	0.1	61%	51%
6	44	50	<0.2 ^a	35	21	40	0.2	53%	49%
33	0	77	0.1 - 0.2 ^a	78	16	6	0.2	85%	81%
20	0	80	0.1 - 0.2 ^a	60	33	7	0.2	70%	65%
2	0	98	< 0.1	28	50	22	0.2	90%	80%

^a means individual particle sizes, often as part of a much larger agglomerate

The most striking result of this part of the investigation is that the particle size decreased with a decrease in the percent silane present in the reactant flow. Apparently, dilution of the silicon-containing building blocks forces a reduction in the size of the particles which can be formed. Also, in the case of a reactant flow containing just 2% silane, no agglomerates were observed. All of the particles observed were less than 100 nm in size (see Figure 15b). This should be contrasted with the particles formed at 33% silane where there were many large agglomerates formed.

There appeared to be a mixed trend in the silane depletion results as determined by the pulsed mass spectrometry method. At the higher flow rates of silane there was a fairly high

depletion of silane, then at lower flows, a smaller percentage of the silane reactant gas was depleted. However, for reactant flows with a very small composition of silane, for example 2%, the highest depletion of silane was observed.

Although this data is preliminary, possible explanations for these trends can be offered. The change in the silane depletion with silane composition in the reactant may have to do with the electron distribution in the plasma. In order for the silane to react with the nitrogen to form silicon nitride species, the nitrogen must be activated or atomized. This requires a high energy electron if there are no nitrogen species other than molecular nitrogen. Ammonia on the other hand will form fragmented radicals at lower energies, and silane can use low energy electrons as well as high energy electrons. Also at high concentrations, combination process start to become important.

When there is nothing but a low amount of silane and molecular nitrogen present, there are a sufficient number of high energy electrons to activate enough nitrogen to react with all the silane. At a higher composition of silane, the silane competes with the nitrogen for these electrons and so not enough nitrogen is activated. At even higher concentrations of silane combination processes, where silane radicals bump into other silane radicals forming disilane or other more complicated stable species, can occur. This event depletes the silane present in the inter-electrode region.

CONCLUSIONS

A rf-PPECVD reactor was constructed, tested, and implemented in the study of thin film and particle depositions of silicon nitride. Coherent Anti-Stokes Raman Spectroscopy and pulsed sampling mass spectrometry were used to monitor the silane depletion in the plasma region during

and after the rf pulse occurrence. The temperature of the silane molecules was also monitored by CARS. This information was correlated with film and particle properties such as atomic composition and thickness or size to gain indirect information about the relative role played by gas phase and surface interactions in the uniformity and composition of the resulting thin films and particles. Much of the information, gained from the studies attempted, pointed to a contribution from both the gas phase and surface processes.

In particular the silane depletion in the gas phase increased with power. From the results this did not seem to be solidly related to the film properties other than the % of silane present in the films and particles. The higher the power the higher the silane depletion, and the lower the concentration of silicon in the particle or film. Both gas phase reactions and surface reactions could cause this to occur. If the silane loses more hydrogens at higher powers, and the ammonia starts to breakdown as well, then more hydrogens could be broken off the silane and bonding to nitrogen or oxygen from water could occur. This should be reflected in the SiH/NH ratio it should get smaller with higher power. Based on most the data it does, but not in all cases. The film changes are likely due to a concerted process that happen both in the gas phase and on the surface. It is difficult to separate these two contributions from each phase. The studies where the power changed or the pulse width changed do not give a clean cut answer as to whether the gas phase or surface chemistry is more important.

For the thin films a related study that gives more direct information about the surface processes is the study where the substrate temperature was changed. Based on the information in the table, the silane depletion remained roughly the same at all temperatures, so if there is a change in the film properties, it is almost exclusively due to a change in the surface processes.

The study revealed that as the temperature was increased there was a slight change in the percentage of silicon in the films largely due to the fact that the oxygen level decreased and the nitrogen levels increased and decreased. The SiH to NH ratio also generally increased suggesting that less NH or more SiH was incorporated at higher temperatures. The stress values were also interesting since they became more tensile with increasing temperature. All of these effects are related to the surface processes rather than the gas phase process. Since the thin film property changes here are so different than the film properties resulting from an increase in the pulse width or power, one must conclude that both surface and gas phase reactions contribute to the resulting alterations in the films for those process changes.

At the other extreme, a change in the gas delivery shower head should affect the gas flow and not the surface processes as much. The results show that the asymmetric head has the lowest silane depletion at the same pulse width and power as the square and radial heads. The asymmetric head likely changes the gas phase depletion by altering the degree of mixing. The radial head has the highest depletion. This is somewhat reflected in the atomic composition of the thin films, as the radial has the lowest silane content and the asymmetric generally has the highest. Also generally the radial head has the lowest SiH to NH ratio. The fact that the head type has any affect at all on the thin films means that gas phase chemistry affects the resulting films. Based on this study the affect appears to be smaller than the effects of changes in the substrate chemistry.

For the square and radial heads, the silane depletion amount is directly related to the film uniformity for the films at 175°C. For depletion of about 40% and below, the films were uniformly deposited. However, when conditions caused the depletion to be above that amount, the films became more nonuniform and looked more like the films deposited from the asymmetric

showerhead. It would be interesting to try other reactant compositions to see if the CARS determined depletions could predict regions where the films would be uniform for these conditions

One of the more novel accomplishments of this work was the construction, testing, and use of the pulsed sampling mass spectrometer system. The calibration studies, continuous plasma studies, and CARS comparison studies indicate that PSMS can be used to monitor a pulsed plasma deposition. Also, in some of the studies, pulsed sampling mass spectroscopic measurements were taken during the rf pulse and before the rf pulse. The sampling done during the rf pulse always had a lower composition of silane, than the samples taken outside of the pulse.

The particle studies looked at the effect of power pulse width and reactant flow composition on particle parameters. From the power studies it appears that at low powers the particles are smaller. The silane is more depleted at higher powers but there is not much more silicon incorporated into the particles. The higher powers cause silane, ammonia, and nitrogen radicals to all form leading to a different chemistry than at the low powers where predominantly silane and some ammonia are formed. The availability of these other species leads to larger particles and a larger distribution of particle sizes.

The change in particle size with the percentage of silane in the reactant supports the idea that the chemistry in the plasma affects the particle size. The smallest particles with the most uniform size distribution are those created from reactant flows with a very small percentage of silane present in them. This silane was 90% depleted and is likely to be more completely reacted since it has an excess of reactant surrounding it. When more silicon containing species are present in the plasma region, recombination processes can occur. Thus a silyl radical may collide with a

silane molecule and form a disilyl radical before colliding with a nitrogen species from ammonia or nitrogen. Apparently the particles formed from particles containing the disilyl radical and larger silyl radicals nucleate and grow in a different way than the ones containing only the silyl radicals. The ones from larger radicals are themselves larger and contain relatively more silicon. The evidence for this is indirect since no radicals could be directly observed.

Conclusive results regarding the relative role of gas phase chemistry and surface chemistry on the formation of silicon nitride thin films and particles was not possible from these studies. Information about the ammonia depletion and measurement of some products would give a much more complete picture. Nonetheless, these studies suggest that both gas phase and surface phase processes affect the resulting properties.

EXECUTIVE SUMMARY

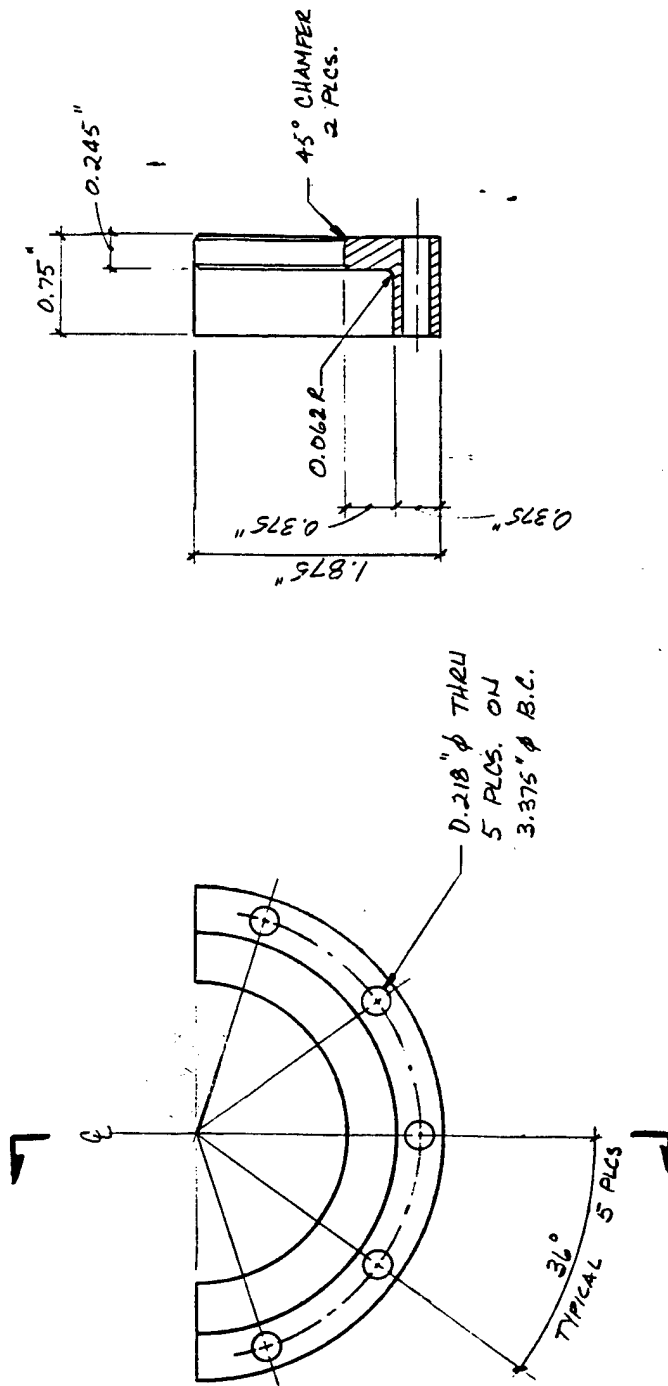
Much of the work given in this Final Technical Report were previously reported in a Master's Research Paper or in a journal article. Two Master of Science students completed their degree during the three years that this work was funded. One student is continuing her studies toward a Ph.D. in applied Science and Engineering and the other is working as a Process Engineer at American Microsystems Inc., a local computer chip manufacturer. Since the Research Papers that these students used to complete their degree are available from the Chemistry Department at Idaho State University, they are not included in an appendix. The paper that was written and published is available from *Applied Spectroscopy*, in the July 2001 issue. A second paper has been written as is currently being submitted to a journal. A copy of the manuscript that is close to being submitted is included in Appendix D. Supporting data is included in Appendix E.

APPENDICIES

Appendix A. Drawings of the Plasma Chamber.

MATERIAL LIST				
PART No.	QTY	DESCRIPTION	MANUFACTURER PART No.	MATERIAL
1	1	CERAMIC POST		MACOR
2	2	TOP COLLAR		SST
3	2	BOTTOM COLLAR		SST
4	1	CERAMIC TOP		ALUMINA SILICATE
5	1	CERAMIC RING		ALUMINA SILICATE
6	4	SUPPORT		ALUMINUM
7	1	PLATEN		SST
8	1	OVEN		GLASS
9	1	OVEN SUPPORT		ALUMINUM
10	6	SUPPORT GUIDE		ALUMINUM
11	1	TOP FLANGE		SST
12	5	HALF COUPLING		SST
13	AR	1/4" COPPER TUBING		COPPER
14	2	POSITIONING RING		SST
15	5	ULTRA TORR ADAPTOR	SWAGelok SS-6-UT-A-8BT	SST
16	1	TOP FLANGE ASSY.		
17	1	RADIAL SHOWER HEAD		ALUMINUM
18	1	SQUARE SHOWER HEAD		ALUMINUM
19	1	ASYMETRIC SHOWER HEAD		ALUMINUM
20	1	SPIRAL SHOWER HEAD		ALUMINUM
21	1	SUPPORT ASSEMBLY		
22	1	O-RING	GREENE-TWEED 9146-SS630	
23	5	O-RING	PARKER 2-013	KALREZ
24	1	O-RING	PARKER 2-037	KALREZ

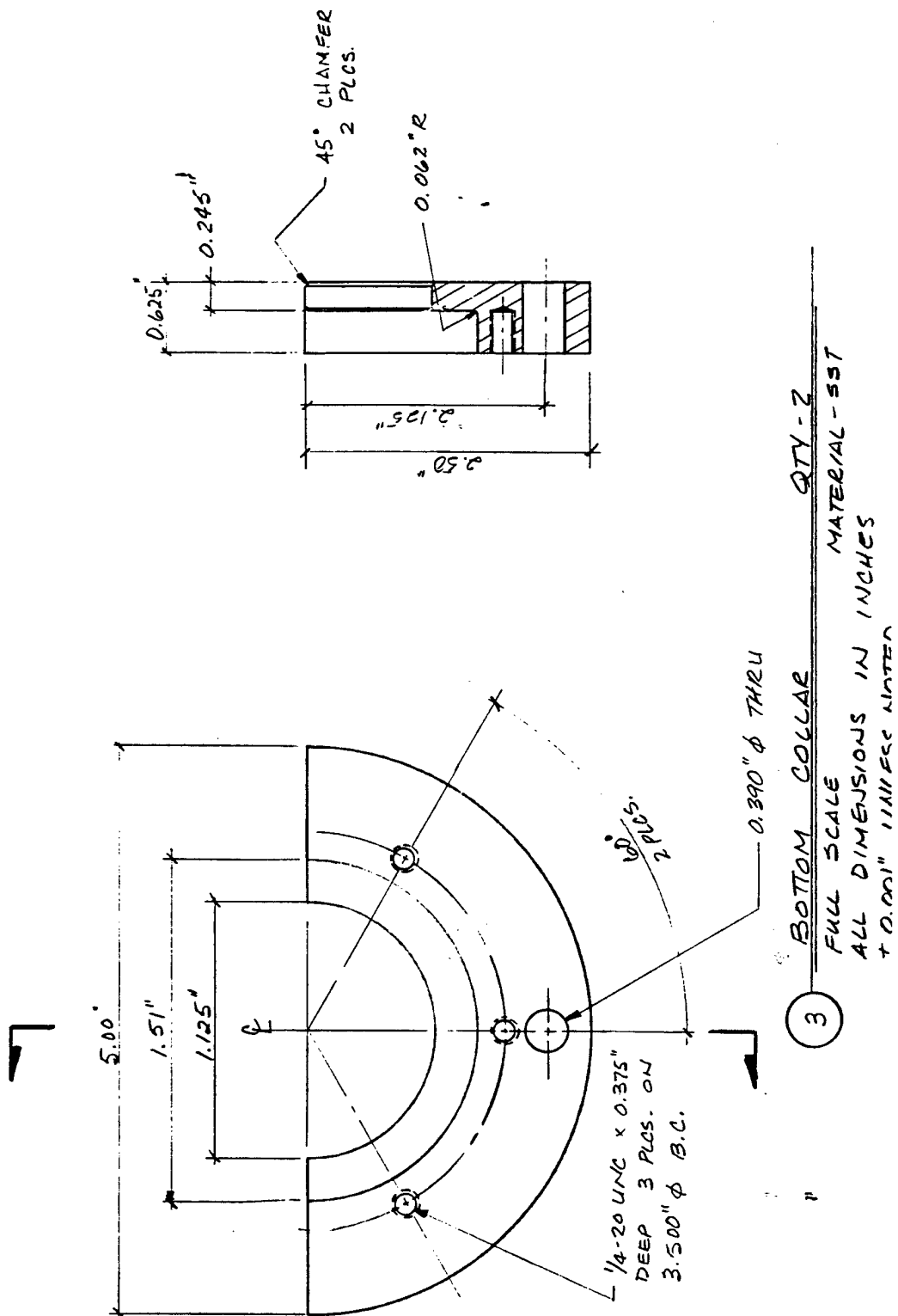
MATERIAL LIST CONT.				
PART No	QTY.	DESCRIPTION	MANUFACTURER PART No.	MATERIAL
25	2	O-RING		
26	1	BOTTOM FLANGE		SST
27	1	BOTTOM FLANGE ASSY		
28	10	SOCKET HEAD CAP SCREW 1/4-20 UNC x 1/2"		SST
29	4	SOCKET HEAD CAP SCREW #6-32 UNC x 1/2"		SST
30	4	PAN HEAD SCREW #4-32 UNC x 3/8"		SST
31	4	SOCKET HEAD CAP SCREW #6-32 UNC x 3/4"		SST
32	4	HEX NUT #6-32 UNC		SST
32	AR	CERAMIC STAND	MCMASTER-CARR	ALUMINA SILICATE
33	3	GLASS-TO-METAL TUBE	GREAT GLASS	
34	2	GLASS-TO-METAL TUBE	GREAT GLASS	
35	6	SOCKET HEAD CAP SCREW #10-24 UNC x 1"		SST
36	1	POST TOP		SST
37	4	SOCKET HEAD CAP SCREW 1/4-20 UNC x		SST
38	1	PLATEN ASSEMBLY		
39	1	RF PLUG		

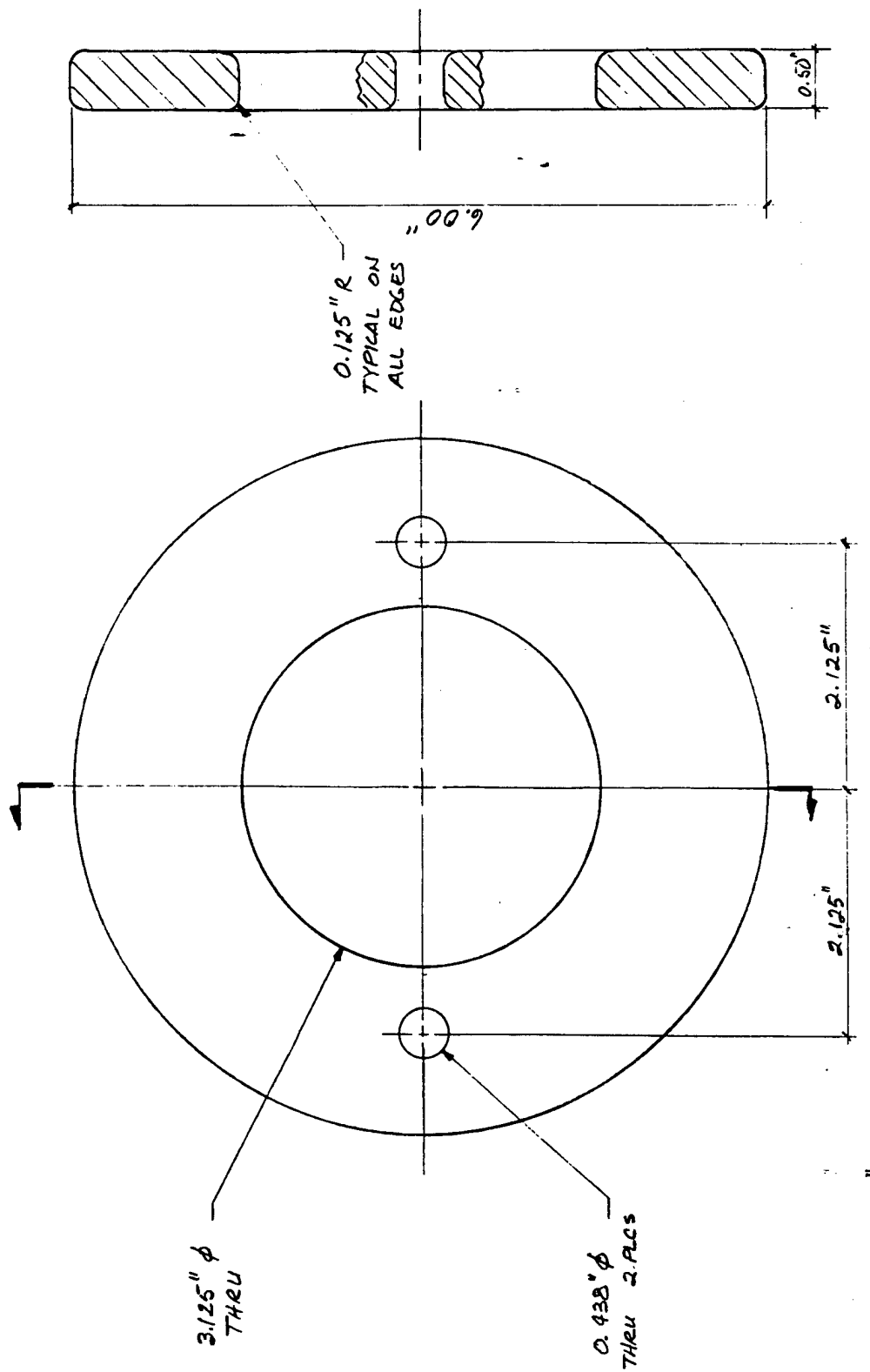


TOP COLLAR QTY: 2

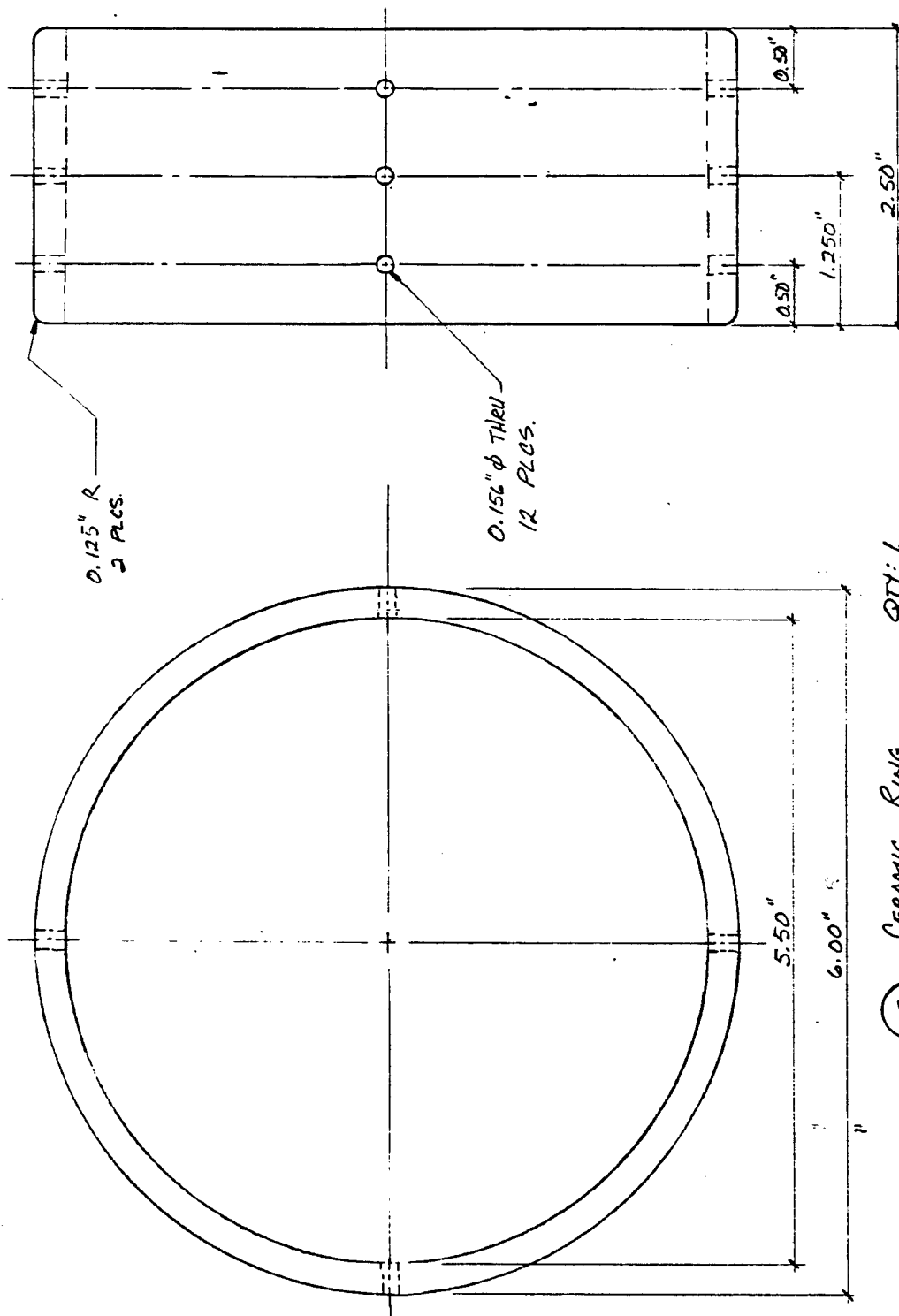
2

FULL SCALE
ALL DIMENSIONS IN INCHES
± 0.001" UNLESS NOTED
MATERIAL - SST

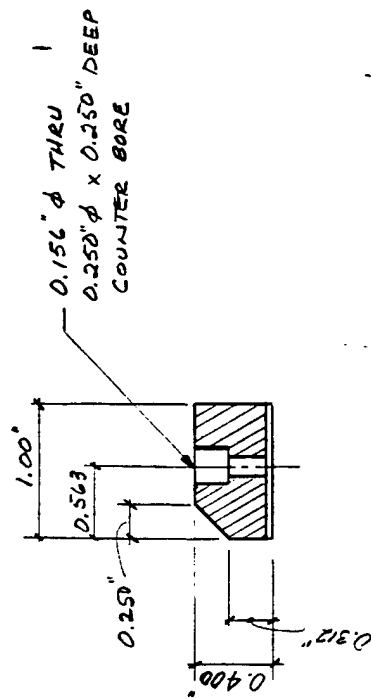
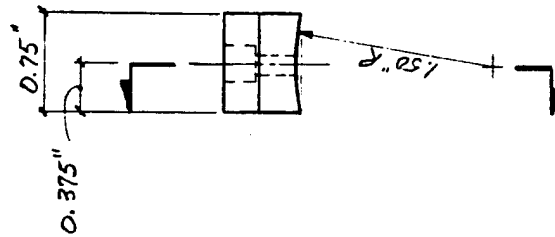




4 CERAMIC TOP QTY: 1
 FULL SCALE ALL DIMENSIONS IN INCHES
 1/8" = 1" UNLESS NOTED OTHERWISE



5 CERAMIC RING QTY: 1
 FULL SCALE ALL DIMENSIONS IN INCHES
 ± 0.001" UNLESS NOTED MATERIAL - ALUMINA SILICATE



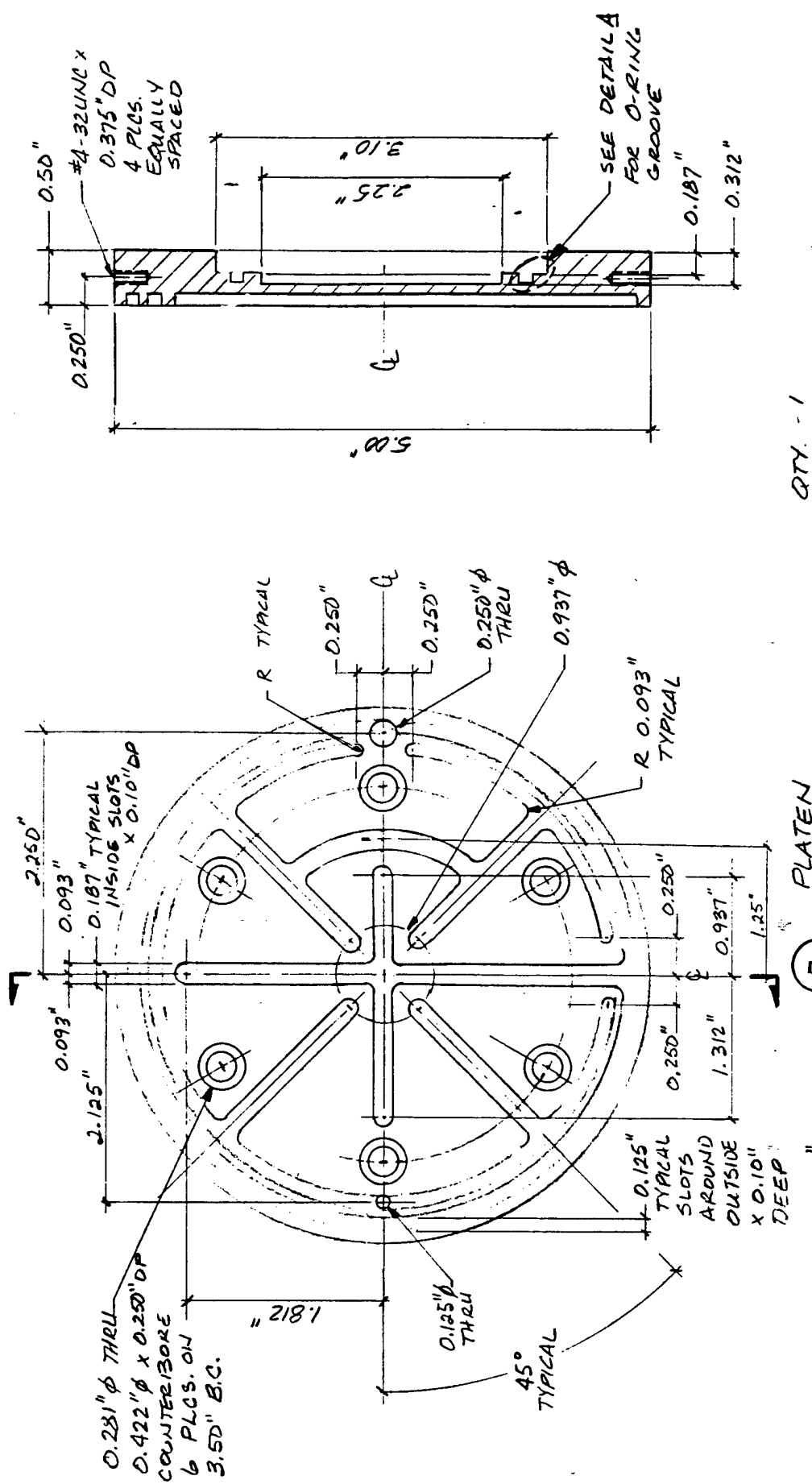
6 SUPPORT QTY : 4

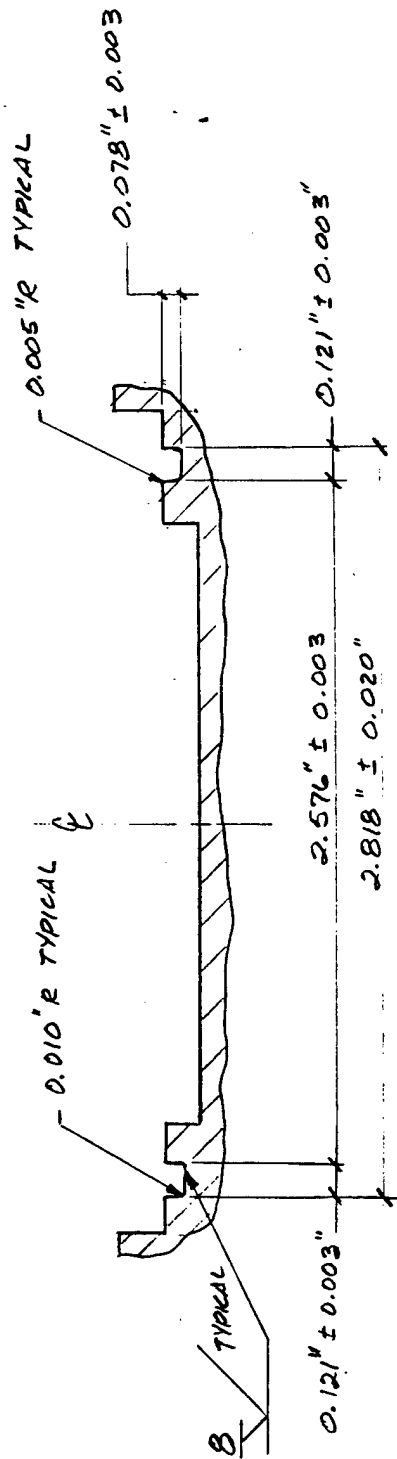
FULL SCALE

ALL DIMENSION IN INCHES

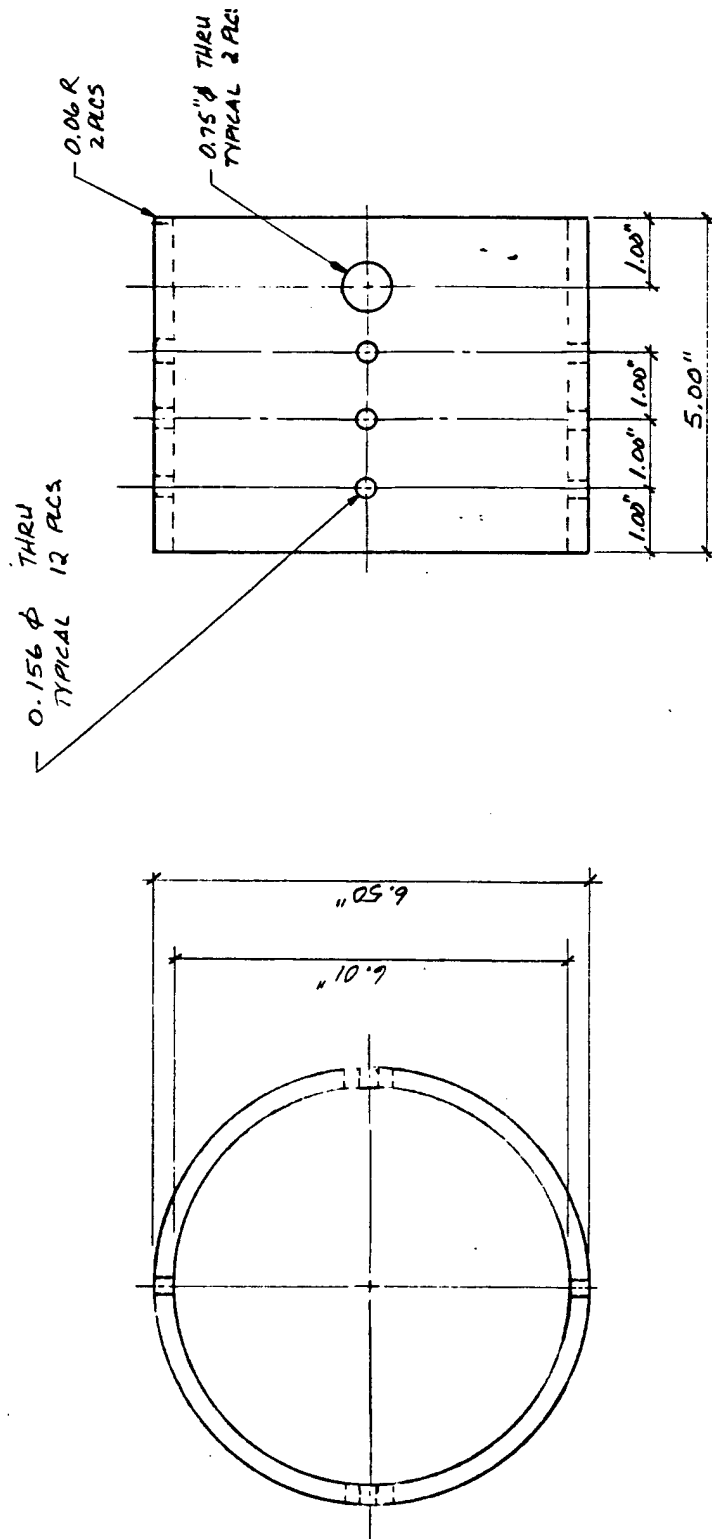
± 0.001 " UNLESS NOTED

MATERIAL - ALUMINUM

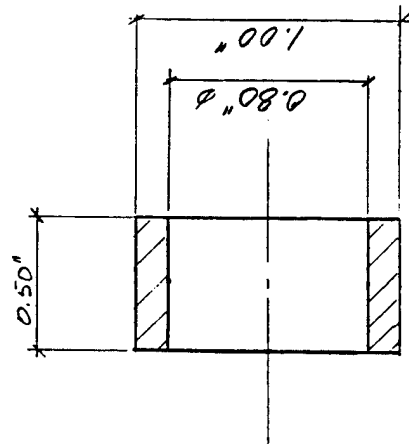




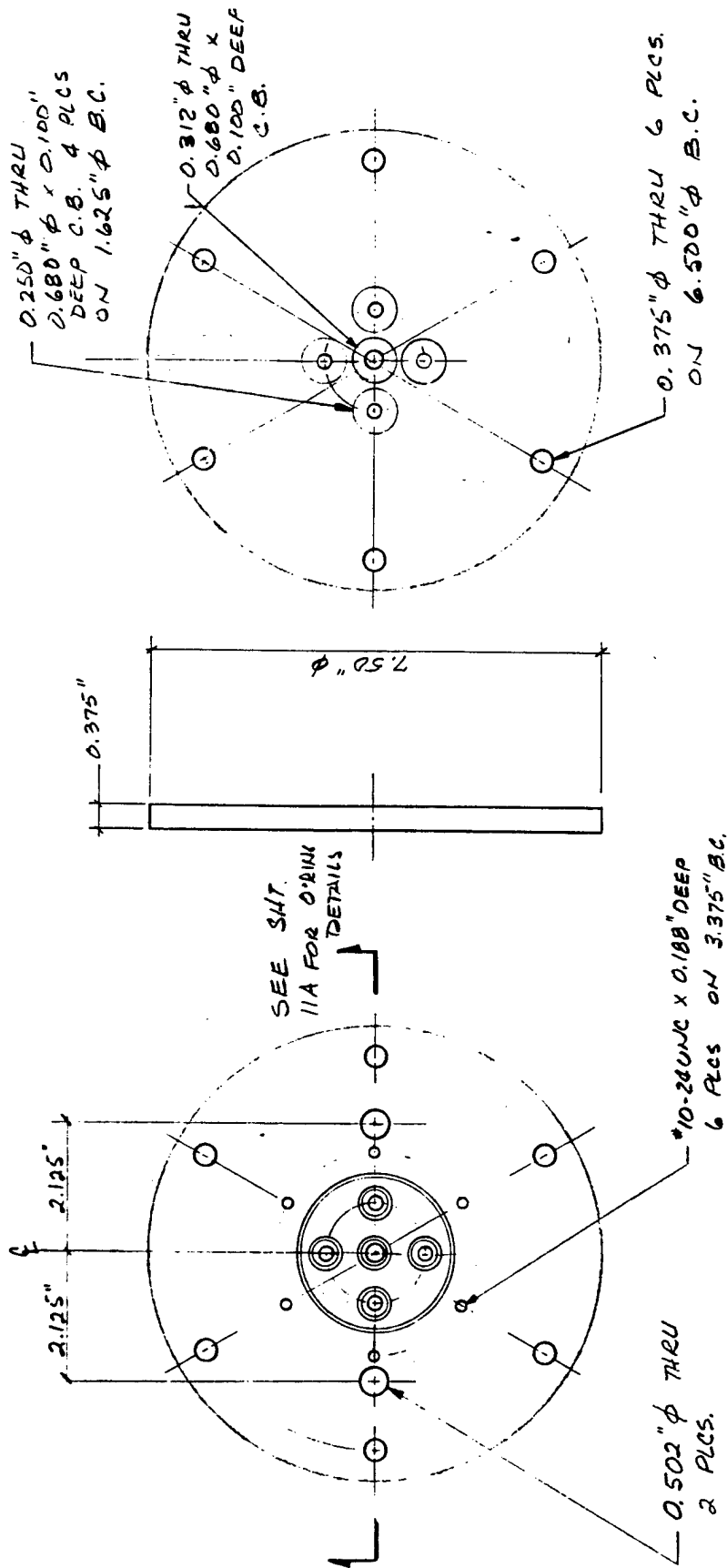
DETAIL A O-RING GROOVE
 $\frac{1}{2}" = 1"$



8 OVEN QTY: 1
 HALF SCALE
 ALL DIMENSIONS IN INCHES
 ± 0.001 " UNLESS NOTED
 MATERIAL - GLASS



10	SUPPORT GUIDE	QTY - 6	MATERIAL - ALUMINUM
	FULL SCALE		
	ALL DIMENSIONS IN INCHES		
	± 0.001" UNLESS NOTED		



11

TOP FLANGE

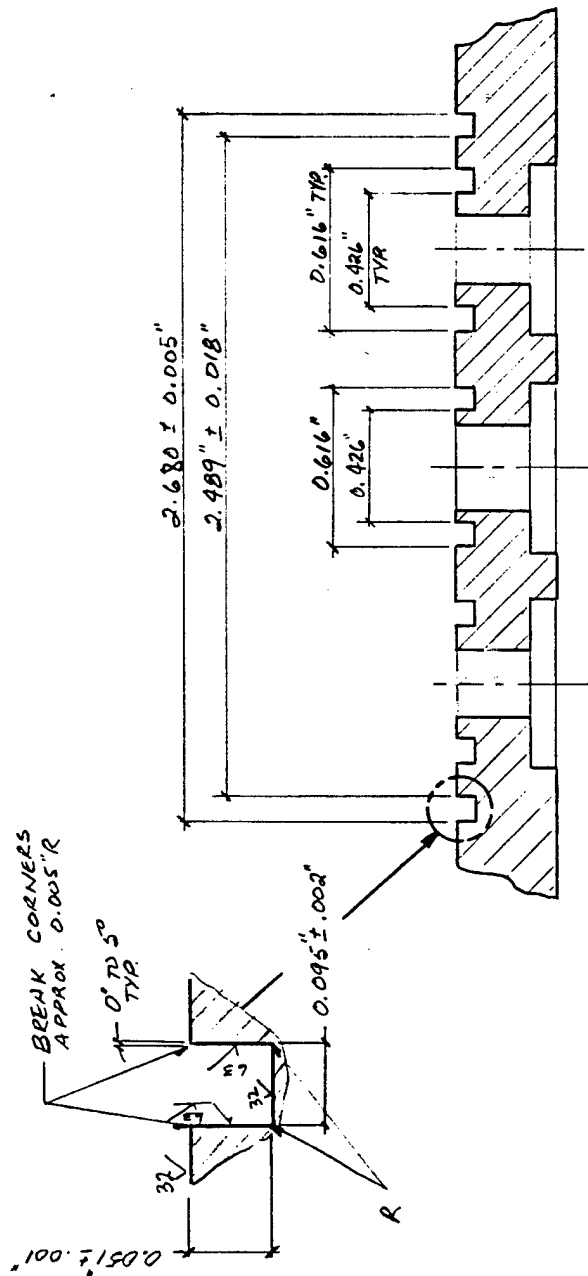
QTY - 1

HALF SCALE

MATERIAL - SST

ALL DIMENSION IN INCHES

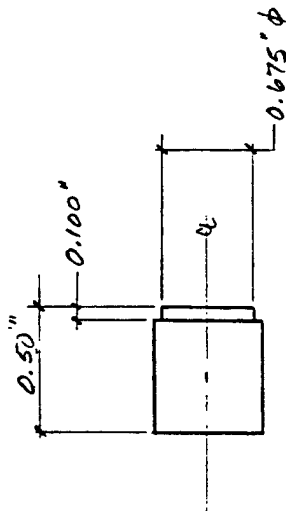
$\pm 0.001"$ UNLESS NOTED



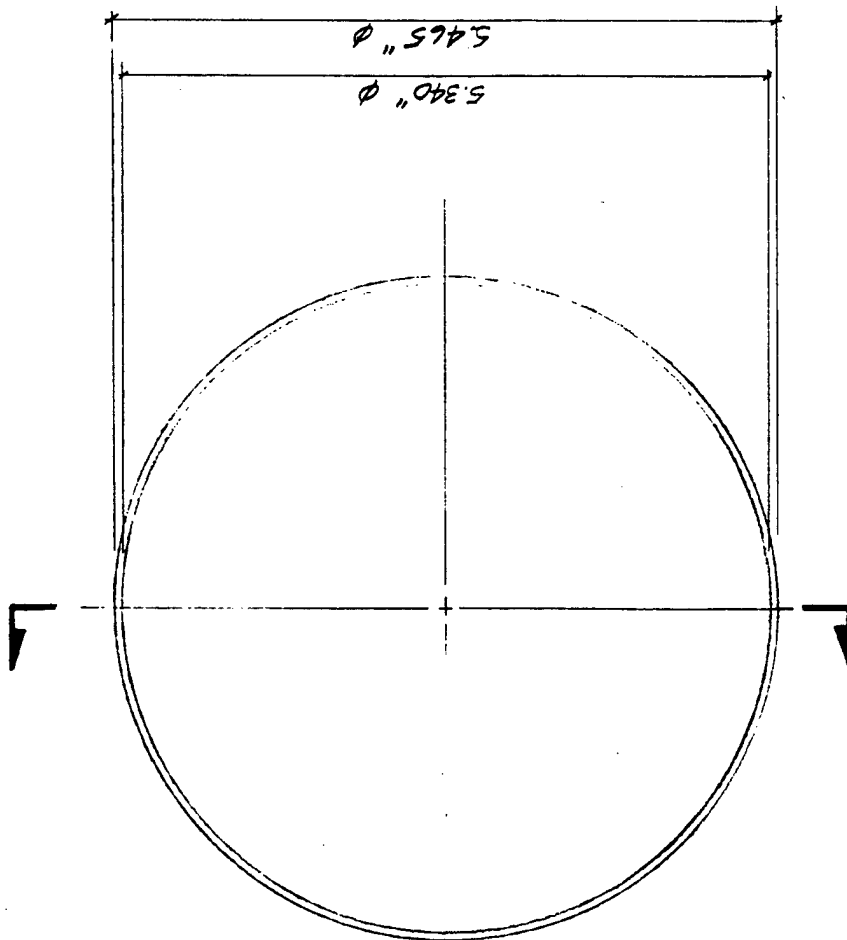
11A O-RING DETAILS TOP FLANGE

SCALE: $\frac{1}{2}" = 1"$

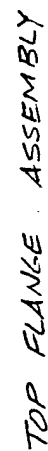
ALL DIMENSIONS IN INCHES



12	HALF COUPLING	QTY - 5
	FULL SCALE	MATERIAL - SST 1/4" SCH. 40
	ALL DIMENSIONS IN INCHES	
	±0.001" UNLESS NOTED	

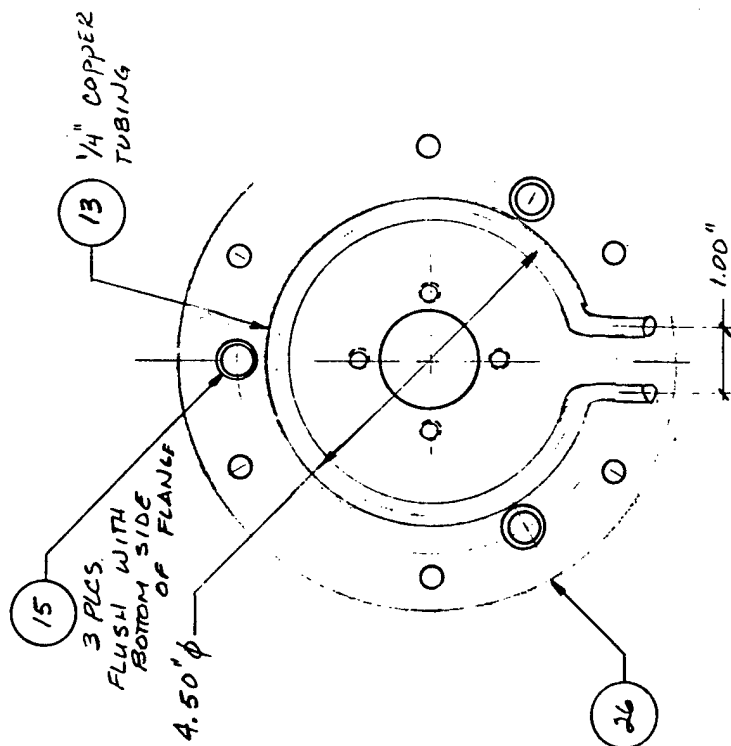


14 POSITIONING RING QTY-2
 NOT TO SCALE MATERIAL-SST
 ALL DIMENSIONS IN INCHES
 $\pm 0.001"$ UNLESS NOTED



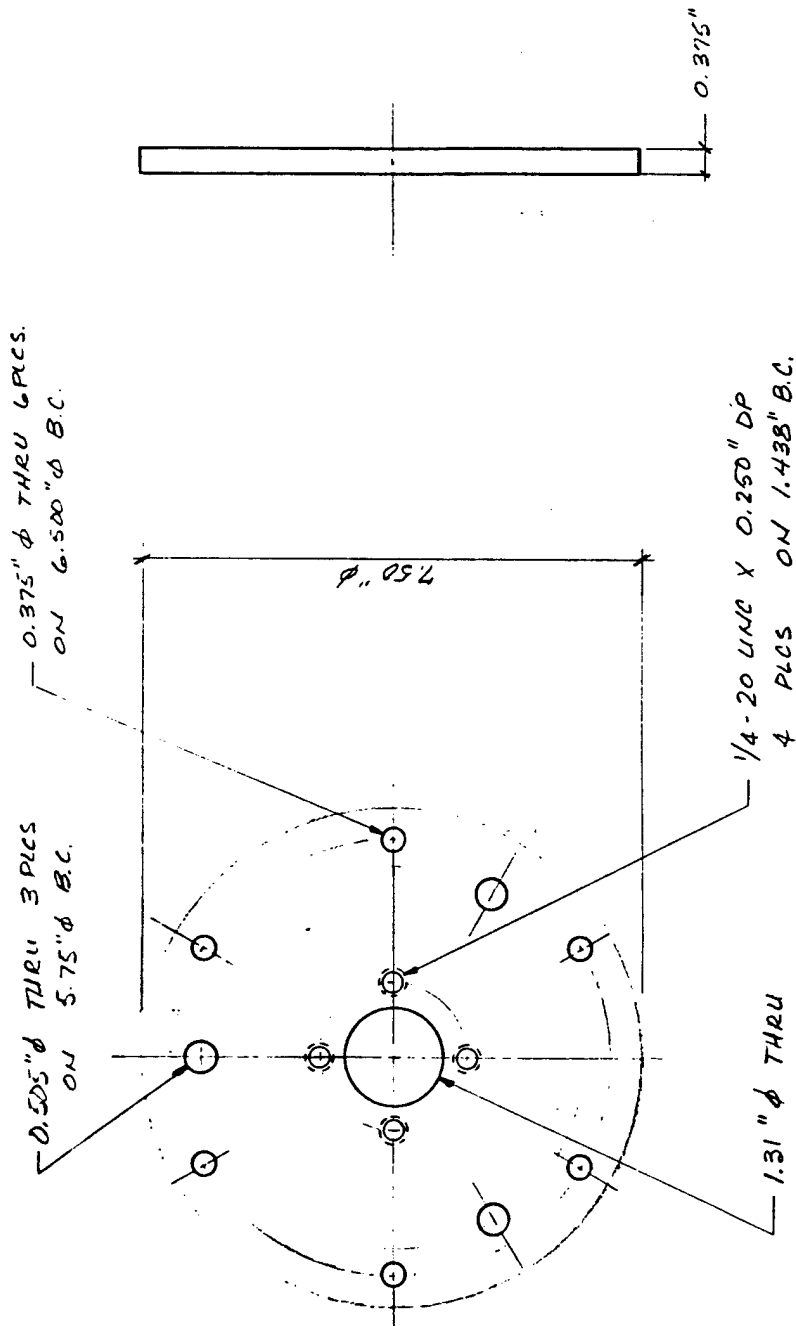
3/4 SCALE

$\pm 0.01"$ UNLESS NOTED

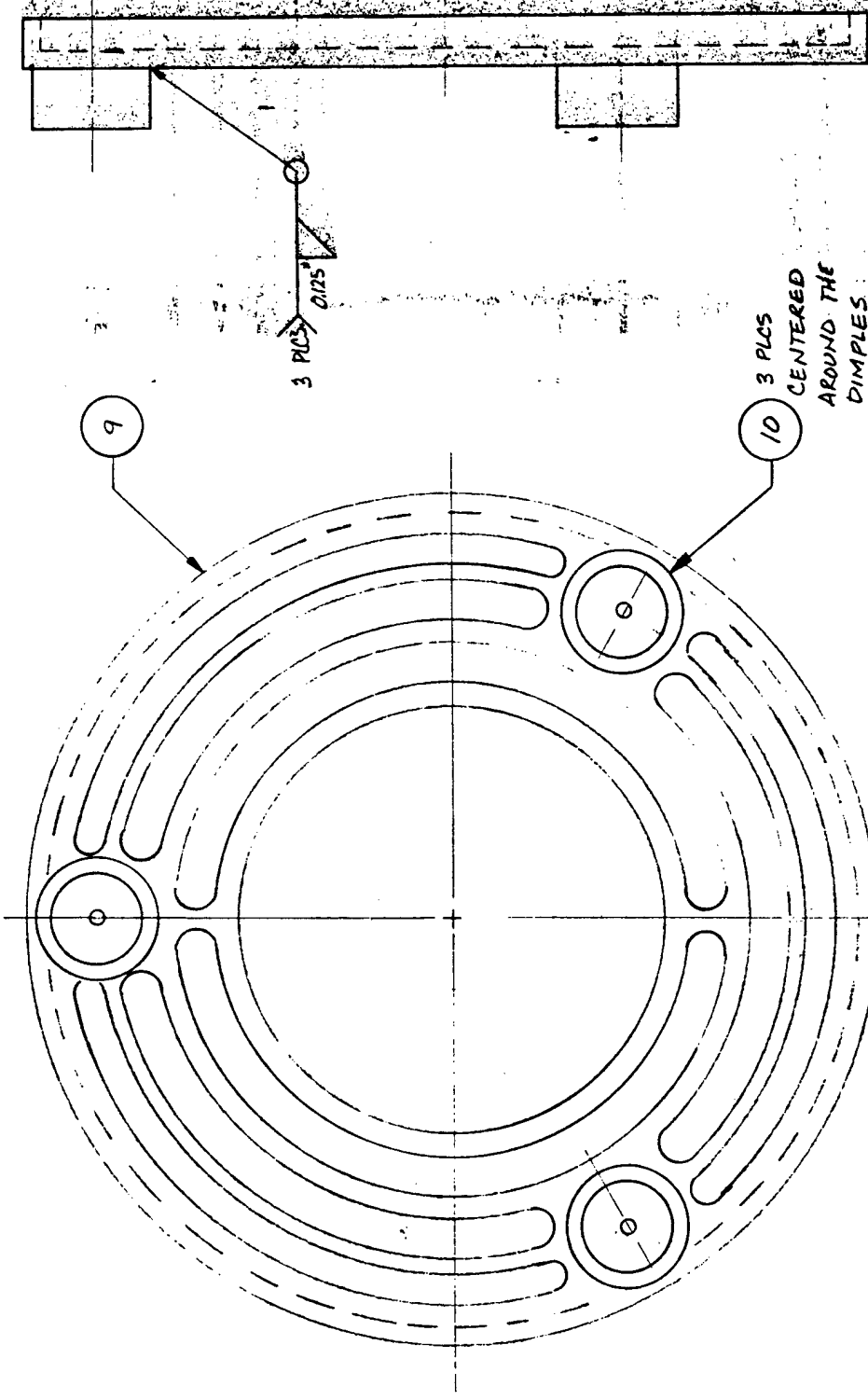


27 BOTTOM FLANGE ASSEMBLY

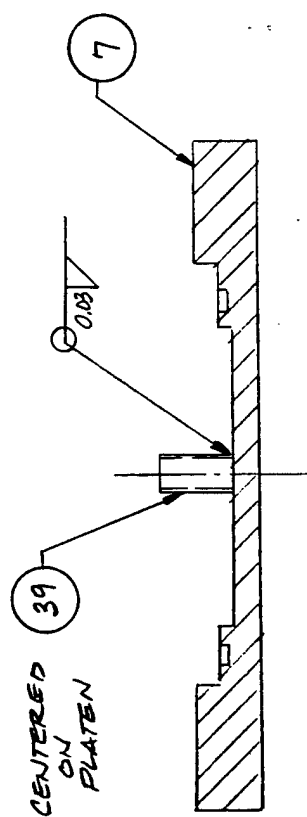
HALF SCALE
ALL DIMENSION IN INCHES
 $\pm 0.05"$ UNLESS NOTED



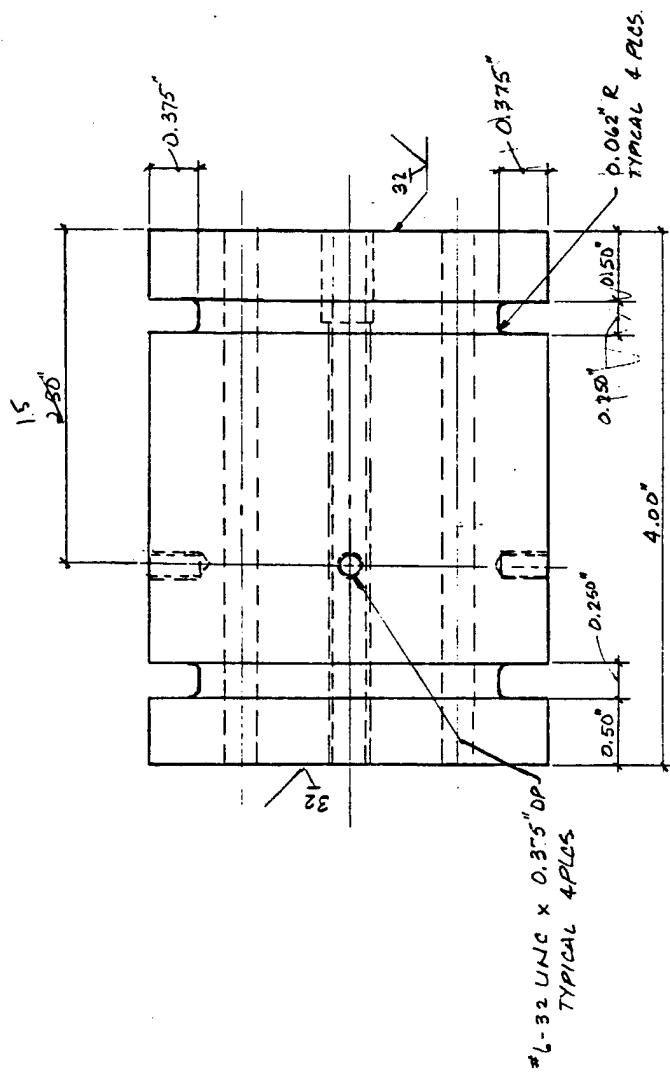
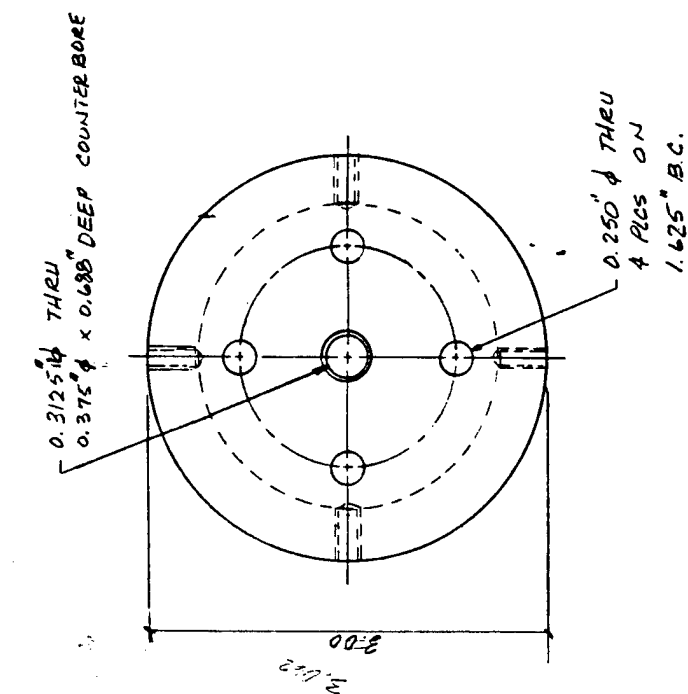
26 BOTTOM FLANGE QTY - 1
SCALE - HALF MATERIAL - SST
ALL DIMENSIONS IN INCHES
± 0.001" UNLESS NOTED



21 SUPPORT ASSEMBLY



38 PLATEN ASSEMBLY
FULL SCALE

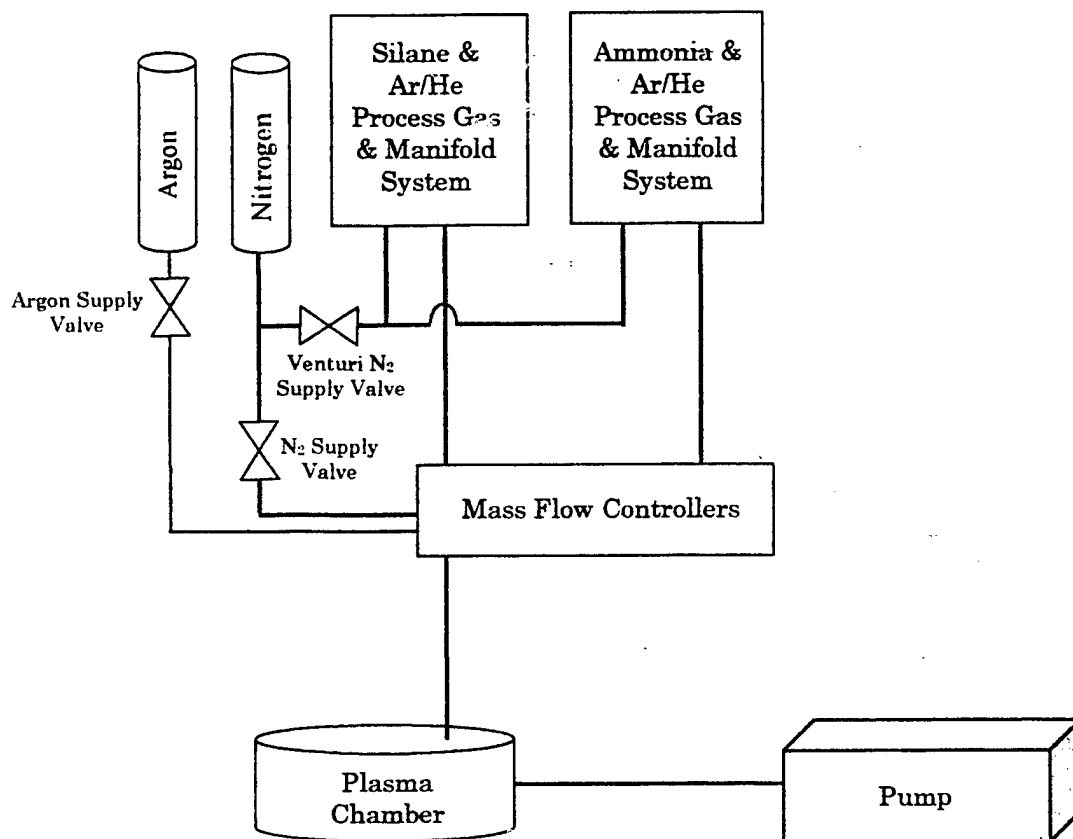


1 CERAMIC FBST QTY:1

FULL SCALE
ALL DIMENSIONS IN INCHES
± 0.001" UNLESS NOTED
MATERIAL - MACOR

**Appendix B. Standard Operating Procedure for the Pulsed Plasma Enhanced Chemical
Vapor Deposition System**

SYSTEM BLOCK DIAGRAM



Gas System Procedures

1. GENERAL SAFETY REQUIREMENTS

- 1.1 All people who change gas bottles must be familiar with the physical, chemical and health hazard characteristics of the gases they are responsible for changing.
- 1.2 Any gas bottle that has been dropped must be reported to R. Rodriguez.
- 1.3 Visually inspect the new gas bottle. Do not attempt to connect any gas bottle that indicates signs of damage.
- 1.4 Do not change the silane gas bottle alone.
- 1.5 Have all the safety equipment within easy reach and be sure that it is ready for use before starting the bottle change procedure.
- 1.6 Ensure all gas bottles that are not in use have the cylinder valve protection cap in place.
- 1.7 All gas cylinders (new and used) must be secured in place during transport, use and storage.
- 1.8 Use the proper gas bottle change procedure for the system you are working on.
- 1.9 Manifold valves are closed when handles are positioned perpendicular to the gas line, and open when handles are positioned parallel to the gas line.
- 1.10 Cylinder valve is closed when handwheel is positioned fully clockwise, and open when handwheel is positioned fully counterclockwise. Never use a pipe wrench, pliers, or any other tool on a cylinder valve handwheel.
- 1.11 Observe correct direction of CGA nut rotation. Left hand threads are common on CGA nuts; they are differentiated from right hand threads by the presence of notches on the hex corners.
- 1.12 Open-end wrenches, adjustable open-end wrenches, flare nut wrenches and DISS wrenches are suitable for use with compressed gas fittings. NEVER USE PIPE WRENCHES OR PLIERS.
- 1.13 If a DISS fitting is loosened, always replace the gasket before tightening the nut. A torque wrench should be used to tighten the fitting to 35 ft/lbs torque.

2. EQUIPMENT AND MATERIAL

- 2.1 Proper gloves (fire proof gloves for Silane).
- 2.2 Full air bottle and hood.
- 2.3 Cordless phone.
- 2.4 Full bottle of gas to be changed.
- 2.5 Flashlight, mirror and Snoop for leak detection.
- 2.6 Gas cart (where needed).
- 2.7 Suitable wrenches for the gas system to be worked on. In instances where a nut or fitting are not provided on a CGA extension, use a pair of vice grip pliers to .

prevent twisting of the pig tail.

ABBREVIATIONS AND DEFINITIONS

- 3.1 CGA/DISS – A gas fitting type. CGA stands for “Compressed Gas Association”.
- 3.2 F-MFPC – Mass flow controller feed valve to control nitrogen flow into the pressure controller.
- 3.3 GSM – Gas safety monitor, a device to continuously monitor a gas sensor and automatically shut off process gas flow when flow limit is exceeded.
- 3.4 GSM-V1 – Pneumatic valve controlled by gas safety monitor (GSM) that allows process gas into the system.
- 3.5 HPI – High pressure isolation valve.
- 3.6 HPV – High pressure vent valve.
- 3.7 LPI – Low pressure isolation valve.
- 3.8 LPV – Low pressure vent valve.
- 3.9 MF – Mass flow controller feed valves. P-MF indicates a purge gas valve. F-MF indicates a main feed valve to the mass controller unit.
- 3.10 NH₃-T – Transfer valve used to control gas leaving the ammonia process gas manifold system.
- 3.11 PGI – Purge gas inlet valves. Includes PGI-1, PGI-2, and PGI-3.
- 3.12 Regulator adjust knob – Knob located on a regulator to control gas delivery pressure.
- 3.13 SiH₄-T – Transfer valve used to control gas leaving the silane process gas manifold system.
- 3.14 Supply valves – Three small valves (Venturi N₂, N₂, and argon) located next to the argon and nitrogen regulators that control the gas supply into the system.
- 3.15 VGS – Vacuum generator supply valve.
- 3.16 VVG – Vacuum vent gauge valve.

MANUAL CYLINDER CHANGE PROCEDURES FOR SILANE, AMMONIA AND THE PURGE GAS CYLINDERS IN THE PROCESS GAS SYSTEMS

Sub-sections of Section 4 are steps of the cylinder change procedure. The sub-sections are generally performed in sequence. If they are not, the user is cautioned to be aware of the necessary valve positions before doing any work.

- 4.1 PROCESS GAS MANIFOLD ISOLATION AND CYLINDER SHUTOFF.
 - 4.1.1 Open enclosure window to gain access to process gas manifold controls.
 - 4.1.2 Verify (and change if needed) that all process gas manifold valves for the cylinder to be changed are in the “short-term” shutdown position as listed in section 7. This includes isolating manifold from process equipment by closing the low pressure isolation (LPI) valve and closing the process gas

cylinder valve.

- 4.1.3 Set the Gas Safety Monitor (GSM-1) SERVICE/PURGE rocker switch to "purge".

4.2 CYLINDER VALVE SHUTOFF TEST

- 4.2.1 Check the N₂ for the venturi system that supplies the vacuum at the VGS, and the argon for the purge gas inlet (PGI). Open the small Venturi N₂, N₂, and argon supply valves. Be sure there is sufficient and correct delivery pressure for each gas inlet. The N₂ should be adjusted to 80 – 100 psi and the argon should be adjusted to 100 psi.
- 4.2.2 Verify the process gas cylinder valve is closed, the GSM controlled pneumatic valve GSM-V1 is open, the high pressure inlet (HPI) is open, the high pressure vent valve (HPV) is closed, and the transfer valve (NH₃-T or SiH₄-T) is open.
- 4.2.3 Verify that both the N₂ inlet and the gauge valves located on the venturi panel are open. The venturi vacuum gauge should read maximum vacuum level: -20 to -25 in. The N₂ delivery pressure can be adjusted to do this. (Vacuum increases as the N₂ delivery pressure increases.).
- 4.2.4 Turn on the vacuum generator by opening the vacuum generator supply (VGS) valve. Open the vacuum vent gauge valve (VVG) and check for maximum vacuum (-20 to -25 in.). Use this maximum vacuum level as a reference during the purging cycle.
- 4.2.5 Make sure the process gas delivery pressure shown on the regulator is no more than 20 psi. Adjust if necessary.
- 4.2.6 Evacuate the manifold by opening the low pressure vent valve (LPV) and then VERY SLOWLY opening the low pressure inlet valve (LPI).
- 4.2.7 After 20 seconds, check the venturi vacuum gauge for base vacuum. If this has not happened, leave valves open until base vacuum is reached. Close the LPV and the LPI.
- 4.2.8 Turn off the vacuum generator by closing the vacuum generator supply valve (VGS).
- 4.2.9 Begin the cylinder valve leak check by observing both regulator gauge readings.
- 4.2.10 Wait 2 minutes, then observe both regulator gauge readings.
- 4.2.11 Should the pressure indicated by either regulator gauge increase, the cylinder valve leaks or it is not completely closed. To reseal the cylinder valve, open the cylinder valve one turn, then close the valve tightly. Once the valve has been opened you must repeat steps 4.2.4 through 4.2.9. Should pressure indicated by either regulator gauge continue to increase, the cylinder valve may be defective. Tag the bottle as defective and notify R. Rodriguez.
- 4.2.12 Should both gauges indicate stable pressure, the cylinder valve is properly closed.

- 4.2.13 Open the low pressure isolation valve (LPI). Pressurize the manifold with purge gas by opening the purge gas cylinder valve and the purge gas inlet (PGI) valves (PGI-1, PGI-2, PGI-3).
- 4.2.14 After 8 seconds, close the purge gas inlet valve 1 (PGI-1).
- 4.2.15 Turn on the vacuum generator by opening the vacuum generator supply valve (VGS).
- 4.2.16 Vent the low-pressure side of the manifold by opening the low pressure vent valve (LPV).
- 4.2.17 After 8 seconds, close the low pressure vent valve (LPV).
- 4.2.18 Adjust the regulator to minimum setting. (turn counter clockwise).
- 4.2.19 Isolate the regulator from the gas cylinder by closing the high pressure isolation valve (HPI).

4.3 PURGING PRIOR TO SPENT CYLINDER DISCONNECTION (PREPURGE)

- 4.3.1 Verify the process gas cylinder valve is closed and the GSM controlled pneumatic valve GSM-V1 is open.
- 4.3.2 Activate vacuum by opening the vacuum generator supply valve (VGS).
- 4.3.3 Evacuate the manifold by opening the high pressure vent valve (HPV).
- 4.3.4 After 8 seconds, close the high pressure vent valve (HPV).
- 4.3.5 Pressurize the manifold with purge gas by opening the purge gas inlet valve 1 (PGI-1). (At this time, all 3 PGI valves should be opened.)
- 4.3.6 After 8 seconds, close the purge gas inlet valve 1 (PGI-1).
- 4.3.7 Repeat steps 4.3.3 through 4.3.6 for a total of 20 cycles.
- 4.3.8 Turn off the vacuum generator by closing the vacuum generator supply valve (VGS).
- 4.3.9 Pressurize the manifold with purge gas by opening the purge gas inlet valve 1 (PGI-1).

4.4 SPENT CYLINDER DISCONNECTION AND REMOVAL FROM ENCLOSURE.

- 4.4.1 Put fire-resistant gloves on.
- 4.4.2 Open the enclosure door.
- 4.4.3 With a suitable wrench/wrenches loosen the CGA/DISS nut.
IMPORTANT! Observe correct direction of CGA nut rotation. Left hand threads are common on CGA nuts; they are differentiated from right hand threads by the presence of notches on the hex corners.
- 4.4.4 Open-end wrenches, adjustable open-end wrenches, flare nut wrenches and DISS wrenches are suitable for use with compressed gas fittings.
NEVER USE PIPE WRENCHES OR PLIERS.
- 4.4.5 Completely unscrew nut and withdraw nipple from cylinder valve.
Decrease the pressure on the purge gas inlet regulator (PGI) to 20 psi.
- 4.4.6 Install the cylinder valve outlet cap or plug on cylinder; tighten securely.

- Observe the correct direction of rotation.
- 4.4.7 Install cylinder valve protective cap on cylinder.
 - 4.4.8 Unfasten safety strap and chain; remove spent cylinder from cabinet.
 - 4.4.9 Move the cylinder to storage area; properly secure with safety strap or chain.
 - 4.4.10 Label spent cylinder with a "SPENT" label so it will not be confused with a full cylinder. Attach label to bottle and sign and date the label.

4.5 FULL CYLINDER INSTALLATION AND CONNECTION

- 4.5.1 Verify the following valve positions:

High pressure inlet	HPI	closed
Purge gas inlet valves 1 – 3	PGI-1 thru 3	open
pressure inlet	LPI	closed
Gas safety monitor valve	GSM-V1	open
Silane or ammonia transfer valve	SiH ₄ -T	closed
(depending on cylinder to be changed)	or NH ₃ -T	closed
High pressure vent valve	HPV	closed
Low pressure vent valve	LPV	closed
Silane or ammonia mass flow inlet	SiH ₄ -MF3	closed
(depending on cylinder to be changed)		or NH ₃
closed		
vacuum vent generator valve	VVG	closed
vacuum generator supply valve	VGS	closed

- 4.5.2 Verify purge gas delivery pressure is 20 psi.
- 4.5.3 Obtain a full cylinder; position inside enclosure.
- 4.5.4 Loosely position safety chain or strap around cylinder.
- 4.5.5 Remove cylinder valve protective cap.
- 4.5.6 Rotate cylinder to align valve outlet with CGA/DISS nipple.
- 4.5.7 Tighten safety chain and strap to securely hold cylinder.
- 4.5.8 Hand tighten cylinder handwheel. Remove cylinder valve outlet cap or plug. Observe correct direction of rotation.
- 4.5.9 Install a new CGA/DISS gasket at the connection, if required.
- 4.5.10 Clean and check the nipple and cylinder valve outlet. Align CGA/DISS nipple with cylinder valve outlet insert fitting, then hand tighten nut while holding the assembly together. Observe correct direction of the nut rotation.
- 4.5.11 Support the nipple with a suitable tool and securely tighten the nut on the DISS fitting with the torque wrench.
- 4.5.12 Close the purge gas inlet valve 1(PGI-1).
- 4.5.13 Comment from Terry: -adjust purge gas delivery pressure to 100 psi. Is this correct?

4.6 CGA CONNECTION LEAK TEST

4.6.1 Make sure the nitrogen supply to the Venturi vacuum system is on and flowing. Verify delivery pressure is 80 psi. Verify that both the N₂ inlet and the gauge valves located on the venturi panel are open. The venturi vacuum gauge should read -20 to 25 inches.

4.6.2 Verify (and adjust if necessary) the state of the following valves:

High pressure isolation	HPI	open
Low pressure isolation	LPI	open
Gas safety monitor valve	GSM-V1	open
Silane or ammonia transfer valve	SiH ₄ -T	open
(depending on cylinder to be changed) or NH ₃ -T		open
High pressure vent valve	HPV	closed
Low pressure vent valve	LPV	closed
Purge gas inlet valve 1	PGI-1	closed
Purge gas inlet valves 2 and 3	PGI-2, PGI-3	open
Silane or ammonia mass flow inlet	SiH ₄ -MF3	closed
(depending on cylinder to be changed)		or NH ₃
closed		
vacuum vent generator valve	VVG	closed
vacuum generator supply valve	VGS	closed

4.6.3 Press "open valve" on Gas Safety Monitor (GSM-100) if indicator light on unit shows valve is closed.

4.6.4 Activate vacuum by opening the vacuum generator supply valve (VGS). Open the vacuum vent gauge valve (VVG) and check for maximum vacuum (-20 to -25 in.) and adjust N₂ delivery pressure as necessary.

4.6.5 Evacuate the manifold by opening the high pressure vent valve (HPV) and low pressure vent valve (LPV).

4.6.6 After 10 seconds, close the high pressure vent valve (HPV) and low pressure vent valve (LPV).

4.6.7 Deactivate vacuum generator by closing the vacuum generator supply valve (VGS).

4.6.8 Pressurize the manifold by opening the purge gas inlet valve 1 (PGI-1).

4.6.9 Test the connection for leakage using a suitable method, such as a helium mass spectrometer, thermal conductivity or bubble fluid leak detector. If snoop is used, wash off the fitting with Electowash.

4.6.10 Close the PGI-1 valve.

4.6.11 If no leak is detected, go to step 4.6.23

4.6.12 If a leak is detected, support the nipple with a suitable wrench and tighten the nut. **CAUTION!** Do not use excessive torque that could damage the fitting.

- 4.6.13 Repeat steps 4.6.8 – 4.6.10 once.
- 4.6.14 If leak persists, open the HPV valve.
- 4.6.15 After 4 seconds, close the HPV valve.
- 4.6.16 Support the nipple with a suitable wrench to prevent rotation and loosen the nut.
- 4.6.17 Partially unscrew the nut.
- 4.6.18 Carefully align the nipple with the cylinder valve outlet then hand tighten the nut while holding the nipple in alignment. NOTE! If a DISS fitting is loosened, always replace the gasket before tightening the nut.
- 4.6.19 Support the nipple and securely tighten the nut.
- 4.6.20 Repeat steps 4.6.2 through 4.6.11.
- 4.6.21 If leakage persists, consider other possible causes such as an improperly installed or omitted gasket, or scratched gasket.
- 4.6.22 If leak cannot be stopped, obtain necessary assistance to determine cause.
- 4.6.23 Release and close enclosure door.
- 4.6.24 Unless steps in sub-section 4.7 are to be performed immediately, deactivate venturi system by closing both valves on the panel.

4.7 PURGING AFTER FULL CYLINDER CONNECTION (POST PURGE).

- 4.7.1 Open enclosure window.
- 4.7.2 Verify the state of the valves as in step 4.6.2.
- 4.7.3 Adjust regulator to maximum setting by turning pressure-adjusting screw clockwise.
- 4.7.4 Verify that both the N₂ inlet and the gauge valves located on the venturi panel are open and the N₂ cylinder deliver pressure is 80 psi. The venturi vacuum gauge should read -20 to -25 in.
- 4.7.5 Activate vacuum by opening vacuum generator valve (VGS).
- 4.7.6 Evacuate manifold by opening the high pressure vent valve (HPV) and low pressure vent valve (LPV).
- 4.7.7 After 10 seconds, close high pressure vent valve (HPV), low pressure vent valve (LPV), and vacuum generator supply valve (VGS).
- 4.7.8 Pressurize manifold with purge gas by opening the purge gas inlet valve 1 (PGI-1).
- 4.7.9 After 5 seconds, close the purge gas inlet valve 1 (PGI-1).
- 4.7.10 Repeat sequence of steps 4.7.5 through 4.7.9 nineteen times for a total of 20 cycles.
- 4.7.11 Evacuate low-pressure side of the manifold by opening the low pressure vent valve (LPV).
- 4.7.12 Evacuate the high pressure side of the manifold by opening the high pressure vent valve (HPV).
- 4.7.13 After 15 seconds, close the high pressure vent valve (HPV), then close the low pressure vent valve (LPV).
- 4.7.14 Verify that the high pressure isolation valve (HPI) is open, the low

pressure isolation valve (LPI) is closed, and the purge gas inlet -1 (PGI-1) is closed.

- 4.7.15 Observe regulator pressure gauges, each should indicate minimum attainable pressure.
- 4.7.16 Turn off vacuum generator by closing the vacuum generator supply valve (VGS). Close the inlet and gauge valves on the venturi panel.

4.8 PURGE GAS INLET VALVE SHUT OFF TEST

- 4.8.1 Observe both regulator gauge readings.
- 4.8.2 Wait 2 minutes, then again observe both regulator gauges.
- 4.8.3 Should pressure indicated by either regulator gauge increase, purge gas inlet valve or cylinder valve is not completely closed. Tighten valves as necessary being careful not to over tighten.
- 4.8.4 Should both gauges indicate stable pressure, purge gas inlet and cylinder valves are properly closed.
- 4.8.5 Adjust the regulator to minimum setting by unscrewing the pressure adjusting screw on the regulator counterclockwise.
- 4.8.6 Close the high pressure isolation valve (HPI).

4.9 PROCESS GAS CYLINDER START-UP

4.9.1 Valve check:

High pressure isolation	HPI	closed
Low pressure isolation	LPI	closed
Gas safety monitor valve	GSM-V1	open
Silane or ammonia transfer valve	SiH ₄ -T	open
(depending on cylinder to be changed) or NH ₃ -T		open
High pressure vent valve	HPV	closed
Low pressure vent valve	LPV	closed
Purge gas inlet valves 1 - 3	PGI-1 thru 3	closed
Silane or ammonia mass flow inlet	SiH ₄ -MF3	closed
(depending on cylinder to be changed)		or NH ₃
closed		
vacuum vent generator valve	VVG	closed
vacuum generator supply valve	VGS	closed
Mass flow purge gas valve:		
nitrogen for ammonia	N ₂ -P-MF1	closed
nitrogen and argon for silane	N ₂ -P-MF3	closed
	Ar-P-MF3	closed

- 4.9.2 Slowly and carefully open the process gas cylinder valve.
- 4.9.3 Open high-pressure isolation valve (HPI) enabling process gas to enter the manifold. Regulator delivery pressure may indicate slight pressure

increase.

- 4.9.4 If regulator cylinder pressure indicates normal full cylinder pressure, go to step 4.9.8.
- 4.9.5 If the regulator cylinder pressure gauge indicates abnormally low pressure, verify that a full cylinder has been installed by examining the cylinder tag. If an empty cylinder has been erroneously installed, obtain a known full cylinder and repeat steps 4.1.1 through 4.9.4.
- 4.9.6 If a cold cylinder of a liquefied gas (such as dichlorosilane, ammonia, or hydrogen chloride) has been installed, allow the cylinder to warm up before checking for correct pressure.
- 4.9.7 If the cause of a low cylinder problem cannot be determined, obtain assistance to determine cause before proceeding.
- 4.9.8 Adjust regulator to provide specified delivery pressure: 10 psi or as indicated in Daily Work Plan. Note that regulator outlet pressure will increase slightly as cylinder contents are depleted.
- 4.9.9 Open low-pressure isolation valve (LPI), enabling process gas to enter process equipment piping if the processing run is to begin immediately following cylinder replacement.
- 4.9.10 Verify that regulator is functioning properly using the procedure in section 4.10.
- 4.9.11 Re-adjust regulator, as required, to maintain specified delivery pressure.
- 4.9.12 Verify that all valves are in the correct operating positions using the list in section 7. Close enclosure window.
- 4.9.13 Position service/purge switch on the Gas Safety Monitor to "service".
- 4.9.14 Log the process gas cylinder change in the system log book.

4.10 REGULATOR FUNCTION CHECK

- 4.10.1 Look for leaks and creeps.

4.11 PURGE GAS CYLINDER CHANGE PROCEDURE

DO NOT USE THIS PROCEDURE! It is still incomplete.

Terry notes: cylinder valve, pull vacuum to bottle, monitor gauge, shut LPI, pump out monitor regulator.

- 4.11.1 Verify that the purge gas cylinder valve and associated PGI valve are closed.
- 4.11.2 Remove the gas cylinder.
- 4.11.3 Place the gas bottle in the proper cylinder storage area. Be sure to label the bottle with a used sticker. Be sure to sign and date the bottle.
- 4.11.4 Obtain a new cylinder, install the new cylinder in the cabinet, and fasten the safety chain and strap.
- 4.11.5 Remove the cylinder valve safety cap. Be sure the cylinder valve is tightly closed. Remove the cylinder valve outlet safety cap.
- 4.11.6 Align the valve outlet to the CGA/DISS fitting. Hand-tighten the

- CGA/DISS nut to the valve outlet. Then use the specified wrenches to tighten the nut.
- 4.11.7 Close the cabinet door and open the cabinet window.
 - 4.11.8 Slowly and carefully, open the cylinder valve.
 - 4.11.9 Properly leak check the CGA/DISS fitting. Perform section 4.2, then steps 4.7.4 through 4.7.9.
 - 4.11.10 Adjust the regulator if necessary.
 - 4.11.11 Close the cabinet window.
 - 4.11.12 Verify that all valves are in the correct operating positions.

5. NORMAL OPERATION OF SYSTEM

5.1 SYSTEM PREPARATION BEFORE STARTING THE PROCESS

- 5.1.1 Check that all the valves are correctly positioned from system shutdown as listed in section 7.
- 5.1.2 Turn on the pump, filter motor cooling fan, and pump.
- 5.1.3 Open all of the mass flow controllers by setting the turn-pots on URS-100 to maximum setting. Wait until flow on URS-100 reads 0. Close all turn pots.
- 5.1.4 Open the mass flow control feed main valves for all the gases: F-MF1 through F-MF5 and F-MFPC. Open all turn-pots to maximum setting. Wait until flow on URS-100 reads 0.
- 5.1.5 Close all the mass flow controllers except ammonia (#1) by setting their turn-pots to 0.
- 5.1.6 Close the mass flow control feed main valves for all the gases except ammonia: F-MF2 through F-MF5 and F-MFPC.
- 5.1.7 Verify the N₂ purge valve (N₂-P-MF1) on the ammonia mass flow line is closed.
- 5.1.8 Close the ammonia mass flow controller by setting the turn-pot #1 to 0. Close the ammonia feed valve (F-MF1).
- 5.1.9 Slowly open the ammonia cylinder valve, and the ammonia high pressure isolation valve (HPI).
- 5.1.10 Verify that the reading on the ammonia gas cylinder pressure gauge is at least 40 pounds. If less, consider changing the gas cylinder before starting the process. Check and adjust the cylinder delivery pressure 10 psi or value specified in daily work plan.
- 5.1.11 Slowly open the ammonia low pressure isolation valve (LPI), the ammonia transfer valve (NH₃-T), and the ammonia inlet valve (NH₃-MF1).

- 5.1.12 Verify that the N₂ and argon purge valves (N₂-P-MF3, and Ar-P-MF3) on the silane mass flow line are closed.
- 5.1.13 Open the silane mass flow controller by setting the URS-100 turn-pot #3 to maximum. Wait until flow on URS-100 reads 0, then close turn pot #3.
- 5.1.14 Open the silane feed valve (F-MF3), and the silane inlet valve (SiH₄-MF3).
- 5.1.15 Pump out the silane line. Wait until flow on URS-100 reads 0.
- 5.1.16 Close the silane mass flow controller by setting the turn-pot #3 on URS-100 to 0. Close the silane feed valve (F-MF3).
- 5.1.17 Slowly open the silane cylinder valve, and the silane high pressure isolation valve (HPI).
- 5.1.18 Verify that the reading on the silane gas cylinder pressure gauge is at least 40 pounds. If less, consider changing the gas cylinder before starting the process. Check and adjust the cylinder delivery pressure 10 psi or value specified in daily work plan.
- 5.1.19 Slowly open the silane low pressure isolation valve (LPI), the silane transfer valve (SiH₄-T), and the silane inlet valve (SiH₄-MF3).
- 5.1.20 Open the nitrogen mass flow controller by setting the URS-100 turn-pot #2 to maximum. Wait until flow on URS-100 reads 0, then close turn pot #2.
- 5.1.21 Open the process nitrogen mass flow feed valve F-MF2, then open nitrogen mass flow controller by setting the turn-pot #2 to maximum.
- 5.1.22 Pump out the nitrogen line.
- 5.1.23 Close the nitrogen mass flow controller by setting the turn-pot #2 on URS-100 to 0. Set the control switch on UPC-20C to "close" position.
- 5.1.24 Slowly open the nitrogen cylinder valve.
- 5.1.25 Verify that the reading on the nitrogen gas cylinder pressure gauges is at least 200 pounds. If less, consider changing the gas cylinder before starting the process. Check the delivery pressure is 40 psi and adjust if necessary. Open the process N₂ supply valve near the regulator.
- 5.1.26 Open mass flow valve to the pressure controller N₂ feed (F-MPPC).
- 5.1.27 Open the argon mass flow controllers by setting the URS-100 turn-pots #4 and #5 to maximum.
- 5.1.28 Close all the turn-pots to 0.
- 5.1.29 Open the argon mass flow feed valves F-MF4 and F-MF5.
- 5.1.30 Set the argon turn-pots #4 and #5 to maximum.
- 5.1.31 Pump out the argon line.
- 5.1.32 Close the argon mass flow controller by setting the turn-pots #4 and #5 on URS-100 to 0.
- 5.1.33 Slowly open the argon cylinder valve.
- 5.1.34 Verify that the reading on the argon gas cylinder pressure gauge is at least 200 pounds. If less, consider changing the gas cylinder before starting the process. Check the delivery pressure is 20 psi and adjust if necessary. Open the argon supply valve near the regulator.

- 5.1.35 Purge the oil in the pump by setting the control switch on the URS-20P pressure control unit to the "close" position until chamber pressure drops to 1 Torr. Set the switch to the "purge" position for 10 seconds. Repeat the "close" and "purge" cycle ten more times. Set switch to "close" position.
- 5.1.36 Set the N_2 mass flow turn-pot #2 to correct setting based on current experiment run parameters. (Usually this will be around 50.)
- 5.1.37 Set the process argon mass flow turn-pot #4 to correct setting based on current experiment run parameters. It is possible that argon will not be used for some runs.
- 5.1.38 Set argon window mass flow control turn-pot #5 to 30.
- 5.1.39 Set pressure controller to current run parameter or 1 Torr by adjusting ball valve and pressure controller URS-20P. Set control switch on URS-20P to the "control" position.
- 5.1.40 Strike up the plasma at 20 – 50 W continuous power or equivalent by turning on the RF and the RF amplifier.
- 5.1.41 Once the plasma is ignited, very slowly open the ammonia feed valve (F-MF1). Adjust the ammonia mass flow turn-pot #1 on URS-100 to correct setting for current run. (Usually around 20.)
- 5.1.42 Bring pressure up to 4 – 5 Torr (check current run parameters) using pressure controller and ball valve. Verify pressure reading matches run parameter.
- 5.1.43 Verify that there is a plasma.
- 5.1.44 Very slowly open the silane feed valve (F-MF3). Adjust silane flow at the URS-100 turn-pot #3 to correct setting for current run. (Usually around 10.)
- 5.1.45 Set pulser and the power.
- 5.1.46 Adjust L-network for maximum impedance matching.
- 5.1.47 Ensure that electrodes are at the correct temperature based on current run parameters.

5.2 SYSTEM RESET AFTER COMPLETING THE PROCESS

- 5.2.1 Close the mass flow feed valves for silane (F-MF3) and ammonia (F-MF1).
- 5.2.2 After 4 minutes, set the silane (#3) and ammonia (#1) mass flow turn-pots to 0.
- 5.2.3 After 2 minutes, set both argon turn-pots (#4 and #5) to 0, and close both mass flow feed valves (F-MF4 and F-MF5).
- 5.2.4 Turn off the plasma.
- 5.2.5 Set N_2 mass flow turn-pot to 25.
- 5.2.6 Purge the oil in the pump by setting the control switch on the URS-20P pressure control unit to the "close" position until chamber pressure drops to 1 Torr. Set the switch to the "purge" position for 20 .

- seconds. Repeat the "close" and "purge cycle ten more times. Set switch to "close" position.
- 5.2.7 Close the main vacuum valve to disconnect the main chamber.
 - 5.2.8 Wait for 10 minutes as chamber fills with nitrogen.
 - 5.2.9 Open the chamber relief valve.
 - 5.2.10 Open chamber lid and remove wafer. Put a new wafer in chamber and replace the lid.
 - 5.2.11 Close the chamber relief valve.
 - 5.2.12 Open the vacuum valve.
 - 5.2.13 Purge the oil in the pump by setting the control switch on the URS-20P pressure control unit to the "close" position until chamber pressure drops to 1 Torr. Set the switch to the "purge" position for 20 seconds. Repeat the "close" and "purge cycle ten more times. Set switch to "control" position.
 - 5.2.14 Set the N₂ turn-pot to current experiment run parameter.
 - 5.2.15 Slowly open the argon mass flow feed valves (F-MF4 and F-MF-5). Set argon turn-pots (#4 and #5) to current experiment run parameters.
 - 5.2.16 Fully open silane (#3) and ammonia (#4) turn-pots and allow system to pump for 4 minutes. Wait until flow on URS-100 reads 0, then close both (#3 & #4) turn-pots to 0.
 - 5.2.17 Open the ammonia mass flow feed valve (F-MF1) and set ammonia turn-pot (#1) to current run parameter. Open the silane mass flow feed valve (F-MF3) and set silane turn-pot (#3) to current run parameter.
 - 5.2.18 System is now ready to begin a run.

5.3 SYSTEM SHUTDOWN PROCEDURES

5.3.1 SHORT TERM SHUTDOWN/RESTART PROCEDURE

Use this procedure when system is not in use for 2 hours or less.

Shutdown Steps

- 5.3.1.1 Turn off the RF. Close the LPI, HPI, transfer (SiH₄-T and NH₃-T), and gas cylinder valves for the silane and ammonia process gases.
- 5.3.1.2 Set silane and ammonia mass flow turn-pots to 0.
- 5.3.1.3 Purge the oil in the pump by setting the control switch on the URS-20P pressure control unit to the "close" position until chamber pressure drops to 1 Torr. Set the switch to the "purge" position for 20 seconds. Repeat the "close" and "purge cycle nine more times. Set switch to "close" position.
- 5.3.1.4 Close all of the mass flow feed valves (F-MF1 through F-MF5).
- 5.3.1.5 Set nitrogen (#2) and argon (#4, #5) mass flow turn-pots to 0.
- 5.3.1.6 Close the nitrogen and argon cylinder valves.
- 5.3.1.7 Adjust curtain so it is not touching either gas cabinet.

Restart Steps

- 5.3.1.8 Slowly open the N₂ mass flow feed valve (F-MF2). Set the N₂ mass flow turn-pot #2 to correct setting based on current experiment run parameters. (Usually this will be around 50.)
- 5.3.1.9 Slowly open the argon mass flow feed valve (F-MF4). Set the process argon mass flow turn-pot #4 to correct setting based on current experiment run parameters. It is possible that argon will not be used for some runs.
- 5.3.1.10 Slowly open the window argon mass flow feed valve (F-MF5). Set argon window mass flow control turn-pot #5 to 30.
- 5.3.1.11 Purge the oil in the pump by setting the control switch on the URS-20P pressure control unit to the "close" position until chamber pressure drops to 1 Torr. Set the switch to the "purge" position for 20 seconds. Repeat the "close" and "purge" cycle nine more times. Set switch to "close" position.
- 5.3.1.12 Open the gas cylinder valves, the HPI, LPI, and transfer (SiH₄-T and NH₃-T) valves for the silane and ammonia process gases.
- 5.3.1.13 Perform steps 5.1.38 through 5.1.46 to complete the normal restart sequence.

5.3.2 LONG-TERM SHUTDOWN PROCEDURE

Use this procedure when shutting down the manifold and associated equipment for longer than 2 hours but less than 1 week.

- 5.3.2.1 Close the LPI, HPI, transfer (SiH_4 -T and NH_3 -T), silane and ammonia inlet valves (SiH_4 -MF3 and NH_3 -MF1), and gas cylinder valves for the silane and ammonia process gases.
- 5.3.2.2 Leave mass flow controllers open (turn-pots set to normal setting) and let the pump run until the flow for silane and ammonia on the URS-100 reads zero for one minute.
- 5.3.2.3 Purge the oil in the pump by setting the control switch on the URS-20P pressure control unit to the "close" position until chamber pressure drops to 1 Torr. Set the switch to the "purge" position for 20 seconds. Repeat the "close" and "purge" cycle ten times. Set switch to "close" position.
- 5.3.2.4 Open silane and ammonia mass flow turn-pots to maximum settings.
- 5.3.2.5 Set the ammonia and silane turn-pots to 0.
- 5.3.2.6 Clear the ammonia mass flow controller by opening the N_2 purge-mass flow valve (N_2 -P-MF1) in the ammonia feed section, and set the NH_3 turn-pot #1 to maximum setting. Wait for 1 minute. Close the purge valve. After the flow reaches 0, close the ammonia mass flow turn-pot.
- 5.3.2.7 Clear the silane mass flow controller by opening the N_2 purge-mass flow valve (N -P-MF3) in the silane feed section, and set the SiH_4 turn-pot #3 to maximum setting. Wait for 1 minute. Close the purge valve. After the flow reaches 0, close the silane mass flow turn-pot.
- 5.3.2.8 Close all of the mass flow controllers by setting the turn-pots on the URS-100 to 0.
- 5.3.2.9 Verify that hand valves in the mass flow cabinet are closed except the N_2 feed valve (F-MFPC) to the pressure controller.
- 5.3.2.10 Set the control switch on the URS-20P pressure control unit to the "close" position until chamber pressure drops to 1 Torr. Set the switch to the "purge" position for 20 seconds. Repeat the "close" and "purge" cycle nineteen more times for a total of twenty.
- 5.3.2.11 Shut off the pump by unplugging it.
- 5.3.2.12 Open the chamber relief valve. After 2 minutes, set URS-20 control switch to the "close" position.
- 5.3.2.13 Close the N_2 mass flow feed valve (F-MFPC) to the pressure controller.
- 5.3.2.14 Close the chamber relief valve.

- 5.3.2.15 Close all gas cylinder valves. Close the process N₂ venturi N₂, and argon supply valves.
- 5.3.2.16 Adjust curtain so it is not touching either gas cabinet.
- 5.3.2.17 Check pump fluid for color and particulate. Schedule maintenance if needed.

5.3.3 EXTENDED SHUTDOWN PROCEDURE

Use this procedure when shutting down the manifold and associated equipment for 1 week or longer.

- 5.3.3.1 Close the LPI, HPI, transfer (SiH_4 -T and NH_3 -T), and gas cylinder valves for the silane and ammonia process gases.
- 5.3.3.2 Leave mass flow controllers open (turn-pots set to normal setting) and let the pump run until the flow readings for both silane and ammonia on the URS-100 read 0 for 2 minutes.
- 5.3.3.3 Purge the oil in the pump by setting the control switch on the URS-20P pressure control unit to the "close" position until chamber pressure drops to 1 Torr. Set the switch to the "purge" position for 20 seconds. Repeat the "close" and "purge" cycle nine more times. Set switch to "close" position.
- 5.3.3.4 Open silane and ammonia mass flow turn-pots to maximum settings.
- 5.3.3.5 Clear the ammonia and silane mass flow controllers by opening the N_2 purge-mass flow valve (N_2 -P-MF1) in the ammonia feed section and the argon purge-mass flow valve (Ar -P-MF3) in the silane mass flow section for 2 minutes.
- 5.3.3.6 Close all of the mass flow controllers by setting the turn-pots on the URS-100 to 0.
- 5.3.3.7 Close the silane (SiH_4 -MF3) and ammonia (NH_3 -MF1) mass flow valves.
- 5.3.3.8 Verify that hand valves in the mass flow cabinet are closed except the N_2 feed valve to (F-MFPC) to the pressure controller.
- 5.3.3.9 Set the control switch on the URS-20P pressure control unit to the "close" position until chamber pressure drops to 1 Torr. Set the switch to the "purge" position for 20 seconds. Repeat the "close" and "purge" cycle nineteen more times for a total of twenty.
- 5.3.3.10 Shut off the pump by unplugging it.
- 5.3.3.11 Open the chamber relief valve. After 2 minutes, set URS-20 control switch to the "close" position.
- 5.3.3.12 Close the N_2 mass flow feed valve (F-MFPC) to the pressure controller.
- 5.3.3.13 Close the chamber relief valve.
- 5.3.3.14 Check pump fluid for color and particulate. Schedule maintenance if needed.
- 5.3.3.15 Close all gas cylinder valves. Close the process N_2 , venturi N_2 , and argon supply valves.
- 5.3.3.16 Adjust curtain so it is not touching either gas cabinet.

5.3.4 EMERGENCY SHUTDOWN PROCEDURE FOR A FIRE IN THE CHAMBER OR IF THE PUMP MALFUNCTIONS

Emergency steps should only be performed if they can be accomplished without injuring yourself.

- 5.3.4.1 Set the NH_3 and silane remote switches to "shut" (downward) position or push the red "shutdown" buttons on both GSM-100 units.
- 5.3.4.2 Put on the hood with the connected air supply canister and the fire-resistant gloves.
- 5.3.4.3 Close the silane cylinder valve.
- 5.3.4.4 Close the ammonia cylinder valve.
- 5.3.4.5 Close the silane and ammonia mass flow feed valves (F-MF1 and F-MF3) or pull the ribbon connectors off of the mass flow controllers.
- 5.3.4.6 Close the transfer gas valves in the process gas cabinets (SiH_4 -T and NH_3).
- 5.3.4.7 Close both low pressure isolation valves (LPI).

5.3.5 EMERGENCY SHUTDOWN PROCEDURE FOR A FIRE IN THE GAS CABINETS OR MANIFOLD

Emergency steps should only be performed if they can be accomplished without injuring yourself.

- 5.3.5.1 Set the NH_3 and silane remote switches to "shut" or the off position or push the red "shutdown" buttons on both GSM-100 units.
- 5.3.5.2 Put on the hood with the connected air supply canister and the fire-resistant gloves.
- 5.3.5.3 Close the silane cylinder valve.
- 5.3.5.4 Close the ammonia cylinder valve.
- 5.3.5.5 Close the transfer gas valves in the process gas cabinets (SiH_4 -T and NH_3).
- 5.3.5.6 Close both low pressure isolation valves (LPI).

6. GAS SAFETY MONITOR (GSM-1A) OPERATION

6.1 CONTROL SWITCHES

- 6.1.1 Service-Purge Rocker Switch
Used to select operation mode.
- 6.1.2 Shutdown

Latches the valve in the closed state and causes valve to close
Green VALVE OPEN indicator should go off.

6.1.3 Open Valve

Latches the valve in the open state and causes valve to open.
Green VALVE OPEN indicator should go on.

6.1.4 Alarm Reset/Horn Silence

Stops horn

Resets all triggered alarm circuits so normal operation can resume.

6.2 ALARM IN SERVICE MODE

GSM-1A will:

Alarm indicator RED LED flashes.

Horn is activated

Valve closes 6 seconds after receipt of signal.

USER should:

Close cylinder valve.

Press ALARM RESET/HORN silence switch.

Diagnose/repair cause of alarm.

Open cylinder valve.

Press ALARM RESET/HORN silence.

Press OPEN VALVE switch.

6.3 FIRE or GAS RELEASE

Press RED SHUTDOWN switch.

Close process cylinder valves (silane and ammonia).

Clear the area.

6.4 PURGE MODE

Purge mode YELLOW LED flashes.

Horn is not activated if there is a remote shutdown or remote valve open.

7. VALVE AND SWITCH LIST

		Normal Operate Position	Short-term Shutdown Position	Long-term Shutdown Position	Extended Shutdown Position
<u>Ammonia System</u>					
NH ₃ gas cylinder valve		open	closed	closed	closed
Argon/He purge gas cylinder valve		closed	closed	closed	closed
GSM-V1	gas safety monitor control valve 1	open	open	open	open
NH ₃ -T	ammonia process gas transfer valve	open	closed	closed	closed
HPI	high pressure isolation valve	open	closed	closed	closed
LPI	low pressure isolation valve	open	closed	closed	closed

HPV	high pressure vent valve	closed	closed	closed	closed
LPV	low pressure vent valve	closed	closed	closed	closed
PGI-1	purge gas inlet valve	closed	closed	closed	closed
PGI-2	purge gas inlet valve	closed	closed	closed	closed
PGI-3	purge gas inlet valve	closed	closed	closed	closed
VGS	vacuum generator supply valve	closed	closed	closed	closed
VVG	vacuum vent gauge valve	closed	closed	closed	closed
N ₂ -Venturi	N ₂ supply to venturi	closed	closed	closed	closed
Venturi gauge valve		closed	closed	closed	closed

Silane System

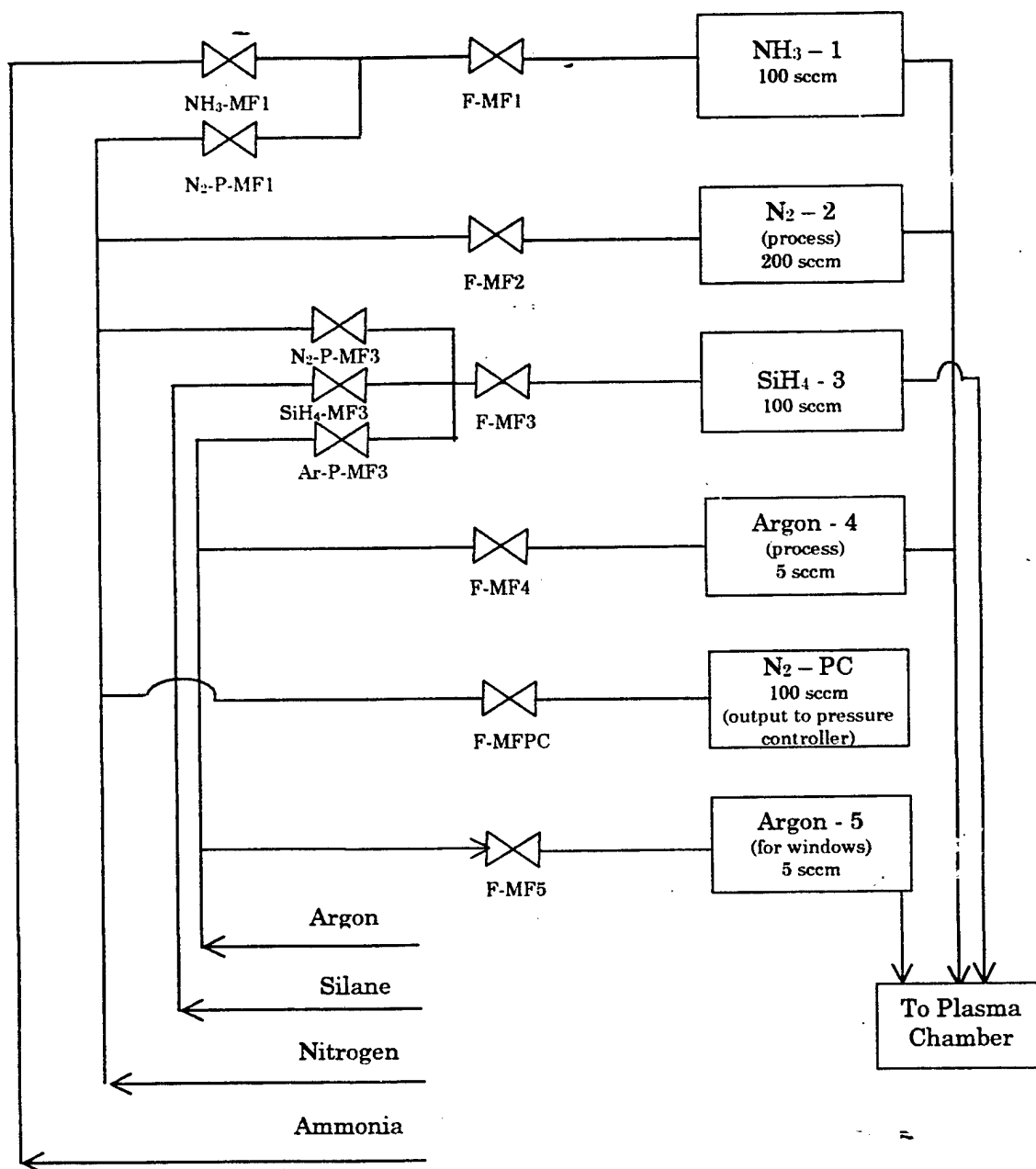
SiH ₄ gas cylinder valve		open	closed	closed	closed
Argon/He purge gas cylinder valve		closed	closed	closed	closed
GSM-V1	gas safety monitor control valve 1	open	open	open	open
SiH ₄ -T	silane process gas transfer valve	open	closed	closed	closed
HPI	high pressure isolation valve	open	closed	closed	closed
LPI	low pressure isolation valve	open	closed	closed	closed
HPV	high pressure vent valve	closed	closed	closed	closed
LPV	low pressure vent valve	closed	closed	closed	closed
PGI-1	purge gas inlet valve	closed	closed	closed	closed
PGI-2	purge gas inlet valve	closed	closed	closed	closed
PGI-3	purge gas inlet valve	closed	closed	closed	closed
VGS	vacuum generator supply valve	closed	closed	closed	closed
VVG	vacuum vent gauge valve	closed	closed	closed	closed
N ₂ -Venturi	N ₂ supply to venturi	closed	closed	closed	closed
Venturi gauge valve		closed	closed	closed	closed

Mass Flow Controller Valves

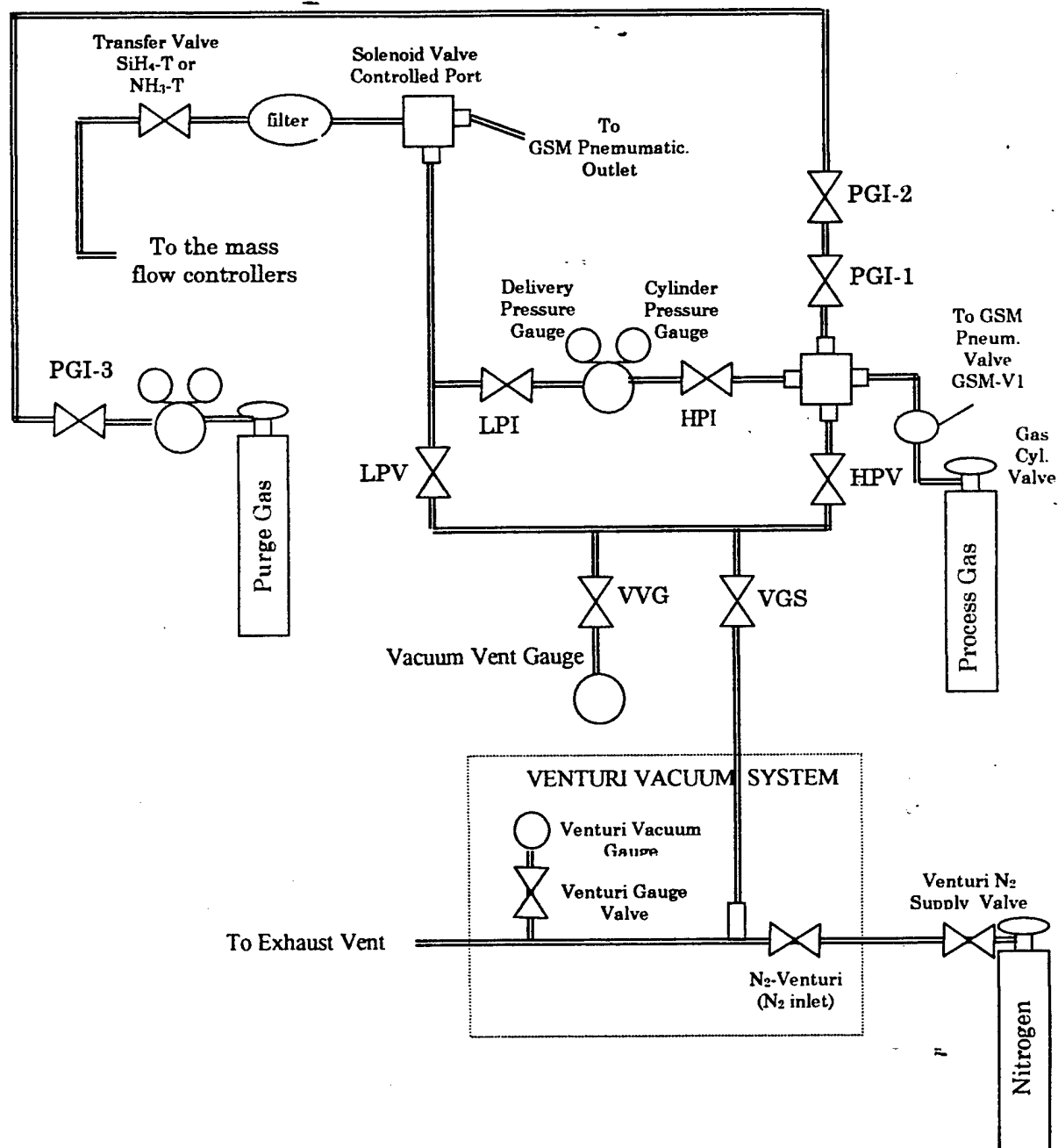
NH ₃ -MF1	ammonia inlet	open	closed	closed	closed
F-MF1	main ammonia feed	open	closed	closed	closed
N ₂ -P-MF1	nitrogen purge on ammonia line	closed	closed	closed	closed
F-MF2	main nitrogen feed	open	closed	closed	closed
F-MF3	main silane feed	open	closed	closed	closed
N ₂ -P-MF3	nitrogen purge on silane line	closed	closed	closed	closed
SiH ₄ -MF3	silane inlet	open	closed	closed	closed
Ar-P-MF3	argon purge on silane line	closed	closed	closed	closed
F-MF4	main argon feed for process	open	closed	closed	closed
F-MF5	main argon feed for window	open	closed	closed	closed
F-MFPC	mass flow to pressure ctr. N ₂ feed	open	closed	closed	closed

	Normal Operate Position	Short-term Shutdown Position	Long-term Shutdown Position	Extended Shutdown Position
<u>Other Valves and Switches</u>				
Nitrogen gas cylinder valve	open	closed	closed	closed
Process N ₂ supply valve	open	closed	closed	closed
Venturi N ₂ supply valve	closed	closed	closed	closed
Argon gas cylinder valve	open	closed	closed	closed
Argon supply valve	open	closed	closed	closed
URS-20P control switch	control	close	close	close
Remote SiH ₄ and NH ₃ emergency shutdown switches	open	open	open	open

9. MASS FLOW CONTROLLERS



10. PROCESS GAS MANIFOLD LAYOUT



**Appendix C. Calculations of the Speed of Gas Exiting the Holes in a Radial
Showerhead**

Appendix C

To calculate the velocity of the gas coming out the showerhead holes, the following assumptions were made: 1) the ideal gas law is applicable, 2) the diameter of the holes is 0.79 mm, and the temperature, 366 K, was the average of room temperature and the temperature of the substrate.

The total flow was 53 sccm at STP. Using the ideal gas law, the volumetric flow rate into 666 Pa (5 torr) can be found.

$$F_{5 \text{ torr}} = F_{\text{STP}} * 366\text{K} * 760 \text{ torr} / (5 \text{ torr} * 273\text{K}) = 9857 \text{ cm}^3/\text{min}$$

The surface area of the holes is given by $A = \pi d^2/4 = 3.14159 * 0.79^2/4 = 0.4951 \text{ mm}^2/\text{hole}$

And the total surface area is $241 \text{ holes} * 0.4951 \text{ mm}^2/\text{hole} * 1 \text{ cm}^2 / 100 \text{ mm}^2 = 1.193 \text{ cm}^2$

Taking the flow rate and dividing by the total surface area gives the velocity of the gases leaving the upper showerhead electrode:

$$9857 \text{ cm}^3/\text{min} / 1.193 \text{ cm}^2 * 1\text{min} / 60 \text{ sec} * 1 \text{ sec} / 1000 \text{ ms} * 10 \text{ mm} / 1 \text{ cm} = 1.38 \text{ mm/ms}$$

Appendix D. Manuscript of the Journal Article Currently Being Submitted.